Fall 2023

Assessment and Sourcing of Heavy Metal Contamination of Middle East Semi-Enclosed Marine Environs Via Near-Shore Sediment Analysis

Abdullah Alnasser
Southern Methodist University, asalnasser@smu.edu

ASSESSMENT AND SOURCING OF HEAVY METAL CONTAMINATION OF MIDDLE EAST SEMI-ENCLOSED MARINE ENVIRONS VIA NEAR-SHORE SEDIMENT ANALYSIS

Approved by:

Andrew Quicksall, Associate Professor, Chair

Khaled Abdelghany, Professor

Neil Tabor, Professor

Bret story, Associate Professor

Mark Boyd, Adjunct Professor

ASSESSMENT AND SOURCING OF HEAVY METAL CONTAMINATION OF MIDDLE EAST SEMI-ENCLOSED MARINE ENVIRONS VIA NEAR-SHORE SEDIMENT ANALYSIS

A Dissertation Presented to the Graduate Faculty of the

Bobby B. Lyle School of Engineering

Southern Methodist University

in

Partial Fulfillment of the Requirements

for the degree of

Doctor of Philosophy

with a

Major in Civil and Environmental Engineering

by

Abdullah Sulaiman Alnasser

B.S., Civil Engineering, Qassim University
Master of Civil and Environmental Engineering, Southern Methodist University

December 16, 2023

ACKNOWLEDGMENTS

I would like to thank special people who have been always supportive and motivative. I would have not made it through my doctoral degree without them. I greatly would like to express my sincere gratitude and appreciation to my academic advisor, Dr. Andrew Quicksall, whose knowledge, insight, and suggestions have always guided me throughout the work. I am very appreciative and thankful for your help, support, and encouragement. Your unstoppable and positive support made me stronger and more confident in academic research. I am also deeply thankful to my committee members, Dr. Niel Tabor, Dr. Khaled Abdelghany, Dr. Mark Boyd, and Dr. Brett story. Their advice, questions, and comments have absolutely enhanced this work.

I would like to greatly thank my father, Sulaiman Alnasser, who passed away years before I have started my doctoral degree, and my mother, Munirah Alnasser, there are no words to express my thanks and appreciation for making me the way I am today. I always feel like a baby whenever you came to my mind. Thank you, father, for the great memories you have made and thank you mother for the continued effort you put in every day and night to make my siblings, my wife and kids, and me happy. I hope that you both are proud of me. Enormous and Special thanks to my wife, Ashwaq Alnasser, for her unconditional support and unfailing motivation. I am really grateful to you; you have been always amazing. I certainly would never make it this far without you being all the time next to me showing patience and love. For my lovely kids, Rakan and Abdulaziz, I am really sorry for being away and maybe moody the last two years of this work! You both are the best gift I have ever received.

My sincere thanks extended to my brother, Mohammad Alnasser, and my sisters, Adlah Alnasser, Zainab Alnasser, and Norah Alnasser, who have been continuously supportive with all kinds of help during the years of my work. I am grateful for all what you have done to me; I will never forget that as I believe that I am very lucky to have a wonderful family like you and cannot imagine my life without you.

I would like to thank Qassim university for their financial support. I also would extend my sincere thanks to my lab group, Uma Lad, Kenneth Hamilton and Hope Rasmussen for their helpful discussions and thoughts. I also would like to thank my amazing friends for their great support all the time.

Alnasser, Abdullah B.S., Civil Engineering, Qassim University, 2011
Master of Civil and Environmental Engineering, Southern Methodist University, 2016

ASSESSMENT AND SOURCING OF HEAVY METAL CONTAMINATION OF MIDDLE EAST SEMI-ENCLOSED MARINE ENVIRONS VIA NEAR-SHORE SEDIMENT ANALYSIS

Advisor: Dr. Andrew Quicksall

Doctor of Philosophy conferred December 16, 2023

Dissertation completed September 13, 2023

Heavy metal contamination in the natural world is complex as many metals can be sourced anthropogenically, naturally, or via both vectors. Many heavy metals are known to be toxic, non-biodegradable, and trophic level bio-magnifiers. Therefore, it is important to monitor and study their concentrations, distributions, and processes for transport and sequestration. Near-shore marine sediments act as a sink for heavy metals in the water column due to their physiochemical properties.

In this dissertation's second chapter, thirty sediment samples from three latitudinally distinct mangrove areas from the Red Sea of Saudi Arabia (near Yanbu, Jeddah, and the Farasan Islands) were analyzed for lead concentrations and isotopic ratios. Lead is persistent in the environment and can cause health problems for humans when exposed. Lead isotopic ratios are used to determine potential sources. End member mixing models were then used to quantify source contribution. Results showed that legacy leaded gasoline and natural sources dominate the lead loading of the Jeddah and Farasn Islands environments while the industrial city of Yanbu has an additional anthropogenic lead source, likely industrial ore. Jeddah has the highest petrol impact compared to the Farasan Islands and Yanbu sites while the dominant Pb source in the Farasan

Islands is natural. This is one of very few studies in the region to report environmental Pb isotopic ratios and the first to do so for mangrove sediments.

The third chapter here assessed current and historical ecosystem risk of total heavy metal loadings on mangrove environments in the near-shore mangrove stands of the Saudi Arabian Red Sea. Concentrations of numerous metals (V, Cr, Cu, Ni, Zn, Cd, and Pb) and associated sediment parameters (sediment organic matter, carbonate, and silicate) were measured. Associated environmental risk indices were calculated for distinct mangrove regions, Yanbu, Jeddah, and the Farasan Islands, at surface and at depth. Heavy metal sources were determined and categorized as anthropogenic, natural, or both. Results showed that the Yanbu site has experienced higher stress compared to the other two sites due to its elevated metals concentrations in its lower sediments. The Yanbu location has mostly anthropogenic metals sourcing in addition to natural sources for Cr, Cu, Zn, Cd, and Pb while V and Ni have solely a natural delivery. The Farasan Islands ecosystem receives Cd from anthropogenic sources while Cu and Zn have been derived from natural and anthropogenic sources to the sediments. The rest of elements (V, Cr, Ni, and Pb) have a natural delivery to the Farasan Islands. For the Jeddah site, all measured heavy metals have been delivered to the Jeddah environment via an anthropogenic source, mostly likely wastewater discharge. The lower, older, sediments of Yanbu were the most polluted by heavy metals compared to the older, or lower, sediments of Jeddah and the Farasan Islands. Surface values suggest an amelioration of Yanbu as they show, in general, similar metal concentrations to Jeddah and the Islands. Jeddah and the Farasan Islands have a similar trend in heavy metals concentrations with respect to depth. Organic matter, carbonate, and silicate were measured, and the results showed that most of the heavy metals across the three locations have been complexed by silicates when sequestered to the sediments. This study provides a bigger picture of the current heavy metal

environmental status in mangrove sediments as the number of prior studies on mangrove sediments in the Saudi Arabian Red Sea is limited. The overall heavy metals concentrations are relatively low compared to other local and worldwide studies. However, the elevated metal concentrations in the lower sediments of Yanbu made Yanbu site as the most contaminated region in the study area. The controlling anthropogenic source (wastewater discharge) in the Jeddah environment makes the Jeddah site an environmental concern despite low concentrations compared to Yanbu. Clearly, exacerbation is possible, thus, the outcomes of this chapter could inform environmental management decision makers in the region to regulate heavy metals inputs to the Red Sea environment.

The fourth chapter of this dissertation is a meta-analysis of published work on heavy metal loadings in near-shore surface sediment data from the Arabian Gulf. Numerous studies have been published in the last two decades with little to no cross-work synthesis. As the area continues to grow, a holistic summary of these data is necessary for the research and environmental management community. Heavy metal concentrations in 2086 sediment samples from 106 sites distributed across the Arabian Gulf were collected from literature to assess the degree of contamination for the Gulf marine system as well as sourcing. These sites have been divided into three sub-regions to contrast the heave metal contamination level by region. Results showed that the Gulf has a high environmental stress from Cd, Co, Cr, Cu, Ni, Pb, Zn, Fe, V, and As with different degrees of contamination. Cr, Ni, and Fe have lower contaminations than Cd, Co, Cu, Pb and As. Zn and V have the lowest environmental pressure among all elements. Mn has been delivered to the Gulf marine environment from natural sources. The current environmental status of the Arabian Gulf basin is that of heavy pressure from the human and industrial activities which

needs urgent attention from management entities in the surrounding countries to help mitigate contamination.

The Saudi Arabian Red Sea coast and the countries adjacent to the Arabian Gulf basin have undergone major coastal economic and urban development due to population growth. This dissertation gives a current assessment of heavy metal pollution in both basins' environments. Chapter 2 suggests that the northern end of the Saudi Red Sea (Yanbu) has higher Pb concentration from three sources, natural, gasoline, and industrial ore. Meanwhile, the mid-coast and southern end of the Saudi Red Sea (Jeddah and the Farasan Islands, respectively) have a comparable amount of Pb, and both have received Pb from natural and gasoline sources with no third Pb component. However, Jeddah has the highest petrol Pb impact among the three regions. Chapter 3 illustrates that heavy metal contamination was highest in the Yanbu environment based on its lower sediments as Jeddah and the Farasan Islands have similar, and lower, metal concentrations with respect to depth. Both chapters have different methods yet show similar major observations. Yanbu has notably higher environmental risk across the study area of the Red Sea while Jeddah is the next most contaminated site and the Farasan Islands have the least environmental pressure among the three regions.

Eleven elements were analyzed in the near-shore sediments of the Arabian Gulf and only one element was naturally delivered to the Gulf basin while the rest have been anthropogenically delivered. Specifically, the Gulf basin is at very serious environmental risk from Cd, Co, Cr, Cu, Ni, Pb, Zn, Fe, V, and As which have been delivered to the Gulf marine system from anthropogenic sources. These elements have different degrees of pollution where Cd, Co, Cu, Pb and As are the highest contaminants. Cr, Ni, and Fe are the second highest pollutants while Zn and V have the lowest contamination degree. The only element found as solely natural across the Gulf ecosystem

is Mn. This dissertation provides useful records of heavy metal contamination status and sourcing in sediments from the Saudi Arabian Red Sea and the Arabian Gulf basins. Also, this work suggests spatial trends of heavy metals in both basins as well as historical changes in the Saudi Arabian Red Sea. These updated records are not only valuable for the research community, but also for the management and environmental regulation entities in the regions.

TABLE OF CONTENTS

LIST OF TABLES

LIST OF FIGURES

CHAPTER 1

INTRODUCTION

1.1 Heavy metals and sediments in marine ecosystems

Although all metals at some exposure level are considered toxic, many are necessary and play essential roles in biological systems. Fundamental elements positively contribute to body metabolism such as iron, copper, selenium, and zinc. Toxic elements negatively impact live organisms when they surpass a threshold concentration and have no value biologically, for instance, cadmium, mercury, and lead (Bosch et al., 2016). Due to the toxicity, persistence, and bioaccumulation characteristics of many heavy metals, they are often thought of as the most serious contamination threat to natural ecosystems (Anbuselvan et al., 2018). Sources of heavy metals entering marine ecosystems can be anthropogenic, such as agricultural discharges and industrial wastes, or natural, such as weathering of parent rocks and soils and atmospheric fallout (Çevik et al., 2009). Heavy metals that are derived from anthropogenic activities can be found in soil, air, and water (Idris, 2008). Water and wind can easily transport metals from their sources to coastal areas where they can deposit in sediments (Marchand et al., 2011). Organic matter, iron and manganese hydroxides, silicates, and carbonate in marine sediments are known adsorbents and/or precipitating agents for heavy metals (Da'na, 2017; Lin & Chen, 1998; Ochoa-Valenzuela et al., 2009). This is demonstrated through calcium carbonate-based remediation as

seen through Ahmad et al. (2012) who used it as a treatment method to remove heavy metals from contaminated water.

Growth of industrialization and heavy agriculture activities lead to heavy metal increase in water bodies and associated sediments and subsequently in human populations through ingestion (Rahman et al., 2019). These exposures can drive deleterious health conditions in humans specific to each metal. For instance, chromium causes different pulmonary problems such as fibrosis, tumors, and lung inflammation. High consumption of copper threatens human health by causing kidney and liver injury, while the high intake of lead can cause intelligence quotient reduction in kids (Rahman et al., 2019). If cobalt exceeds its concentration threshold in the body, it causes anaemia, asthma, and neuropathy (Paithankar et al., 2021). High exposure to iron causes stomatitis, epithelium atrophy, loss of attention, and dyspnea while zinc intake in large quantities is the main cause of oral leukoplakia and parakeratosis (Paithankar et al., 2021). Kidney disease, fragile bones, and lung damage are a result of having over exposure of cadmium while e levated levels of arsenic can lead to cancer of lungs, skin, and liver (Jaishankar et al., 2014). Finally, manganese targets nervous system in human body causing neuropathies when exceeded its concentration limit (Mahurpawar, 2015).

1.2 The Red Sea and the Arabian Gulf

The Red Sea is an elongate marine system running about 1,936 km in length and is surrounded by nine countries with several coastal lagoons and numerous islands. Geographically, this provides a high density of coastal margins throughout the region. The Arabian Sea of the Indian Ocean is connected to the Red Sea by Gulf of Aden to the south, whereas the northern end splits into Gulf of Aqaba and Gulf of Suez. The complete, to the north, and nearly complete, to the south, enclosures produce a basin that is mostly isolated from the worldwide oceanic system. The

Red Sea is often categorized into three zones by depth: shallow shelves (less than 50 m), deep shelves (500 to 1,000 m), and central axis basins (1,000 to 2,900 m). Much of the Red Sea is considered shallow with 25 % falling in the shallow shelf zone and 40% of the area having a depth of under 100m (Rasul et al., 2015). The Red Sea has no permanent fluvial inputs. This paired with its large surface area (approximately 43,970 km^2) yields an unusually high evaporative environment (El-Said & Youssef, 2013). This Red Sea environ, therefore, is shallow, is highly evaporative, and has a high percentage of coastal margins; these conditions provide a large yet ecologically unique marine region. This manifests as an ecosystem with high biodiversity potential. Indeed, the region has long been known to possess such as demonstrated by the residence of more than 1,000 species of fish and 50 types of hermatypic corals (Berumen et al., 2013).

Cities along The Red Sea are expeditiously developing given easy energy accessibility, desalination plants, and strong political interest in economic development which encourages the growth of localized populations (Fine et al., 2019). In the last three decades, human and industrial activities along the Saudi Arabian coast of the Red Sea have noticeably increased and lead to commensurate marine contamination inputs. Despite this, the number of publications that record contaminant levels of the Red Sea region is limited (Ruiz-Compean et al., 2017).

The Arabian Gulf is surrounded by Saudi Arabia, Bahrain, Qatar, United Arab Emirates, Oman, Iran, Iraq, and Kuwait (Lavieren et al., 2011). The Gulf is classified as a shallow, subtropical, semi-enclosed system with little freshwater flowing into it (El-Sorogy et al., 2016: Almahasheer, 2019; Bibak et al., 2018). Therefore, contaminated effluents into the Gulf dilute slower than into other open marine system (Bibak et al., 2018). The climate of the Arabian Gulf is considered extremely tropical in summer and it also has high temperature in winter compared to other latitudinal seas (Almahasheer, 2019).

The Gulf faces anthropogenic pressure from various activities such as oil pollution, dredging and reclamation, desalination plants, and wastewater effluents (Mortazavi et al., 2022a). Also, the coastlines of the countries bordering the Arabian Gulf is experiencing high population growth (around 2.1% per year that is nearly double the world's average of 1.1%), urbanization, and industrialization (Lavieren et al., 2011).

1.3 Mangroves in the environment

Mangrove environments grow in the intertidal area of 70% of subtropical and tropical zones of the world covering 160,000 to 200,000 km^2. These ecosystems contain about 80 species worldwide from roughly 20 families of vascular flora (Marchand et al., 2011). Costal biota is served by mangroves in numerous ways. They provide nutrition, fuel, and medicine as well as decrease the effect of natural catastrophes such as hurricanes. Mangroves can capture significant atmospheric carbon and sequester it to the sediments of shoreline areas (Khalil, 2015; Alongi, 2020). Importantly, they can also act like a sink for heavy metals in marine and adjacent ecosystems due to the chemical and physical properties of the plants, roots, and associated sediments (Marchand et al., 2006). Mangrove sediments have high content of iron and organic matter and have high ability of trapping suspended materials from the water column (Marchand et al., 2011; Yan et al., 2017). Mangrove sediment can, therefore, readily accumulate heavy metals and are considered as effective indicator for heavy metals contamination status of the broader region (Hamed & Emara, 2006). Mangrove forests along the Saudi Arabian Red Sea have experienced growth as they have covered 120, 132, and 135 km of shoreline in 1972, 2000, and 2013, respectively. The mangroves of the Saudi Arabian Red Sea have special characteristics when compared to most locations worldwide since they live and grow under generally unfavorable circumstances for such plants (high salinity, no flowing rivers, and low rainfall) (Eid et al., 2019).

These conditions cause a limited growth of Avicennia marina which is the predominant mangrove species in the Red Sea (Almahasheer, Duarte, et al., 2016). The two other species of mangroves in the region are Rhizophora mucronate and Bruguiera gymnorhiza. Most stands contain a monospecific population optimized to the local conditions. Mangroves of the southern Red Sea have a relatively preferable environment than in north due to a higher surface runoff, nutrition, and lower coast slope (Khalil, 2015; Mandura, 1997). Generally, mangrove environments along the Saudi Arabian Red Sea experience additional stress due to anthropogenic inputs from coastal development, mining, sewage, and industrial waste (Eid et al., 2019). Also, petrochemical industries and their related traffic contribute to polluting the coastal ecosystem of the Red Sea (Alzahrani et al., 2018). Mangrove forests in the area have expanded as mentioned above; however, development, including huge infrastructure projects for harbors and tourism threaten mangrove ecosystem health (Almahasheer et al., 2016).

1.4 Objectives

1.4.1 Chapter 2: Mangrove Sediment Lead Apportionment along the Saudi Arabian Red Sea Coast Using Isotopic Methods.

Studies reporting environmental lead isotopic data for the region are severely lacking. This study provides the first lead isotopic data from Saudi Arabian Red Sea mangrove sediments (Figure 1.1). The aims of this study are to:

A. Measure lead concentrations and isotopic ratios from Red Sea mangrove sediments,
B. Identify and quantify the sources of lead to Red Sea mangrove sediments.

1.4.2 Chapter 3: Assessment of Heavy Metal Distribution, Risk, and Sourcing in Mangrove Sediments from Three Saudi Arabian Red Sea Locations.

Different authors assessed the level of heavy metal contamination of Red Sea mangrove sediments (El-Said and Youssef 2013; Abohassan, 2013; Alzahrani et al., 2018; Usman et al., 2013; Youssef and El-Sorogy 2016); however, there is a lack of studies on mangrove sediments of the Saudi Arabian Red Sea. This study greatly enhances prior work by providing both spatial and temporal trends for the Saudi Red Sea coast (Figure 1.1); such data has yet to be reported for the region. Specifically, the goals of this study are to:

A. Measure the heavy metal loading of V, Cr, Cu, Ni, Zn, Cd, and Pb in the mangrove sediments from the Saudi Arabian Red Sea,
B. Assess the pollution level in the mangrove sediments by applying several risk indices,
C. Compare heavy metal loadings in mangrove sediments between the three latitudinally distinct regions with respect to depth,
D. Identify the heavy metal sources as to whether anthropogenic or natural.

1.4.3 Chapter 4: A Meta-Analysis of Near-Shore Sediment Heavy Metals from the Arabian Gulf.

Different authors have studied heavy metal loadings in sediments from various regions of the Arabian Gulf (T. Alharbi et al., 2017; Al-Kahtany et al., 2018a; Almahasheer, 2019; Rezaei et al., 2021). This study will serve the research community with a meta-analysis of key heavy metals across the Arabian Gulf basin (Figure 1.2). The aims of this work are to:

A. Synthesize the data across all available literature from the region to evaluate the heavy metal loadings Arabian Gulf-wide.
B. Investigate the pollution status across the Arabian Gulf basin by applying different risk indices.
C. Determine the heavy metals sources (anthropogenic or natural).

D. Contrast the heavy metal pollution status between the three sub-regions bordering the Arabian Gulf to assess spatial trends.

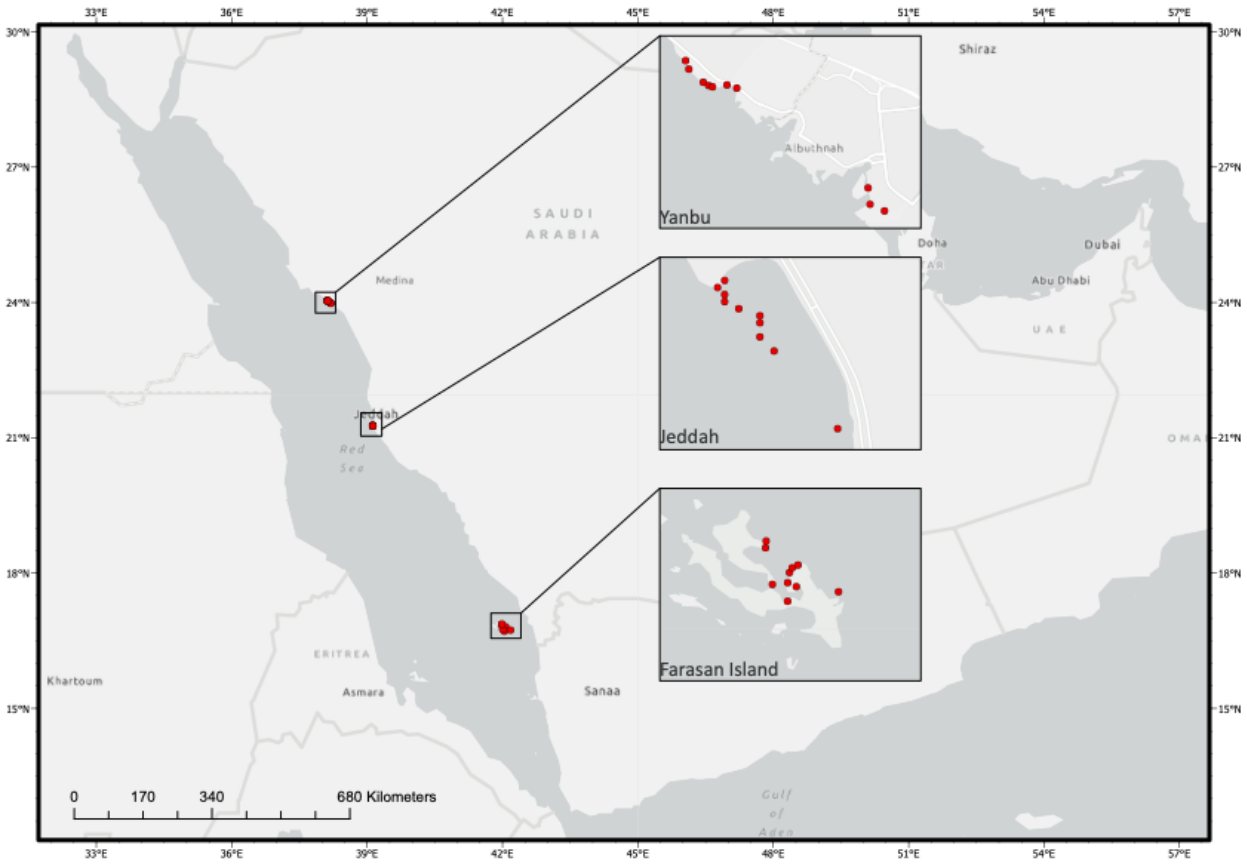

Figure 1.1 Sample locations of the Saudi Arabian Red Sea study area.

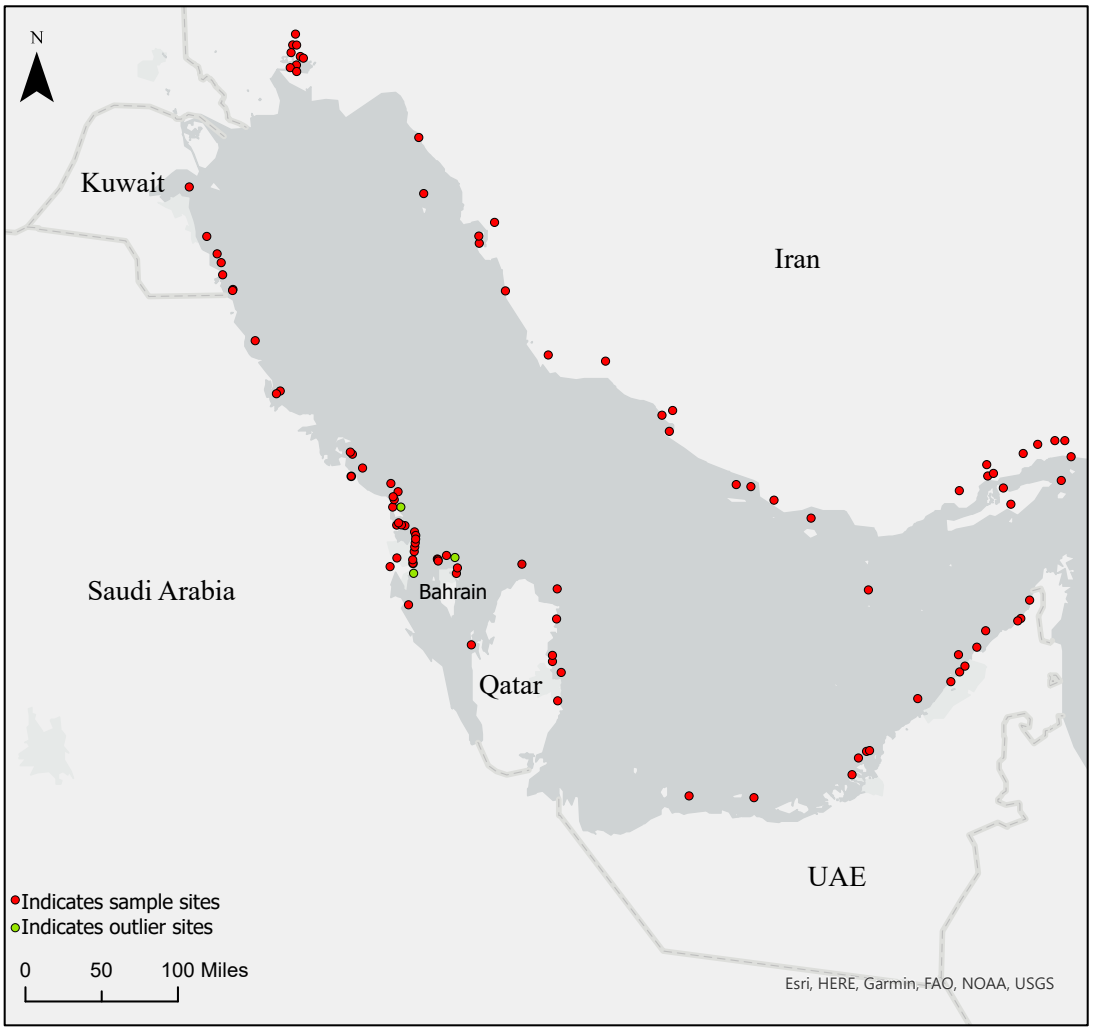

Figure 1.2 Sediment sites surrounding the Arabian Gulf from publications.

1.5 References

Abohassan, R. A. (2013). Heavy metal pollution in Avicennia marina mangrove systems on the Red Sea coast of Saudi Arabia. JKAU: Met., Env. & Arid Land Agric. Sci, 24(1), 35-53.

Ahmad, K., Bhatti, I. A., Muneer, M., Iqbal, M., & Iqbal, Z. (2012). Removal of heavy metals (Zn, Cr, Pb, Cd, Cu and Fe) in aqueous media by calcium carbonate as an adsorbent. International Journal of Chemical and Biochemical Sciences, 2, 48-53.

Alharbi, T., Alfaifi, H., & El-Sorogy, A. (2017). Metal pollution in Al-Khobar seawater, Arabian Gulf, Saudi Arabia. Marine Pollution Bulletin, 119(1), 407–415.

Al-Kahtany, K., El-Sorogy, A., Al-Kahtany, F., & Youssef, M. (2018). Heavy metals in mangrove sediments of the central Arabian Gulf shoreline, Saudi Arabia. Arabian Journal of Geosciences, 11, 1-12.

Almahasheer, H. (2019). High levels of heavy metals in Western Arabian Gulf mangrove soils. Molecular Biology Reports, 46(2), 1585–1592.

Almahasheer, H., Aljowair, A., Duarte, C. M., & Irigoien, X. (2016). Decadal stability of Red Sea mangroves. Estuarine, Coastal and Shelf Science, 169, 164–172.

Almahasheer, H., Duarte, C. M., & Irigoien, X. (2016). Phenology and Growth dynamics of Avicennia marina in the Central Red Sea. Scientific reports, 6(1), 37785.

Alongi, D. M. (2020). Global significance of mangrove blue carbon in climate change mitigation. Sci, 2(3), 67.

Alzahrani, D. A., Selim, E. M. M., & El-Sherbiny, M. M. (2018). Ecological assessment of heavy metals in the grey mangrove (Avicennia marina) and associated sediments along the Red Sea coast of Saudi Arabia. Oceanologia, 60(4), 513–526.

Anbuselvan, N., D., S. N., & Sridharan, M. (2018). Heavy metal assessment in surface sediments off Coromandel Coast of India: Implication on marine pollution. Marine Pollution Bulletin, 131, 712–726.

Berumen, M. L., Hoey, A. S., Bass, W. H., Bouwmeester, J., Catania, D., Cochran, J. E. M., ... & Saenz-Agudelo, P. (2013). The status of coral reef ecology research in the Red Sea. Coral Reefs, 32, 737-748.

Bibak, M., Sattari, M., Agharokh, A., Tahmasebi, S., & Imanpour Namin, J. (2018). Assessing some heavy metals pollutions in sediments of the northern Persian Gulf (Bushehr province). Environmental Health Engineering and Management, 5(3), 175–179.

Bosch, A. C., O'Neill, B., Sigge, G. O., Kerwath, S. E., & Hoffman, L. C. (2016). Heavy metals in marine fish meat and consumer health: a review. Journal of the Science of Food and Agriculture, 96(1), 32-48.

Çevik, F., Göksu, M. Z. L., Derici, O. B., & Findik, Ö. (2009). An assessment of metal pollution in surface sediments of Seyhan dam by using enrichment factor, geoaccumulation index and statistical analyses. Environmental Monitoring and Assessment, 152(1–4), 309–317.

Da'na, E. (2017). Adsorption of heavy metals on functionalized-mesoporous silica: A review. Microporous and Mesoporous Materials, 247, 145-157.

Eid, E. M., Arshad, M., Shaltout, K. H., El-Sheikh, M. A., Alfarhan, A. H., Picó, Y., & Barcelo, D. (2019). Effect of the conversion of mangroves into shrimp farms on carbon stock in the sediment along the southern Red Sea coast, Saudi Arabia. Environmental research, 176, 108536.

Eliseo Ochoa-Valenzuela, L., Gómez-Alvarez, A., García-Rico, L., & Israel Villalba-Atondo, A. (2009). Distribution of heavy metals in surface sediments of the Bacochibampo Bay, Sonora, Mexico. Chemical Speciation & Bioavailability, 21(4), 211-218.

El-Said, G. F., & Youssef, D. H. (2013). Ecotoxicological impact assessment of some heavy metals and their distribution in some fractions of mangrove sediments from Red Sea, Egypt. Environmental monitoring and assessment, 185, 393-404.

Fine, M., Cinar, M., Voolstra, C. R., Safa, A., Rinkevich, B., Laffoley, D., ... & Allemand, D. (2019). Coral reefs of the Red Sea—Challenges and potential solutions. Regional Studies in Marine Science, 25, 100498.

Hamed, M. A., & Emara, A. M. (2006). Marine molluscs as biomonitors for heavy metal levels in the Gulf of Suez, Red Sea. Journal of Marine Systems, 60(3–4), 220–234.

Idris, A. M. (2008). Combining multivariate analysis and geochemical approaches for assessing heavy metal level in sediments from Sudanese harbors along the Red Sea coast. Microchemical Journal, 90(2), 159-163.

Jaishankar, M., Tseten, T., Anbalagan, N., Mathew, B. B., & Beeregowda, K. N. (2014). Toxicity, mechanism and health effects of some heavy metals. Interdisciplinary toxicology, 7(2), 60.

Khalil, A. S. (2015). Mangroves of the red sea. The Red Sea: The formation, morphology, oceanography and environment of a young ocean basin, 585-597.

Lin, J. G., & Chen, S. Y. (1998). The relationship between adsorption of heavy metal and organic matter in river sediments. Environment international, 24(3), 345-352.

Mahurpawar, M. (2015). Effects of heavy metals on human health. Int J Res Granthaalayah, 530(516), 1-7.

Mandura, A. S. (1997). A mangrove stand under sewage pollution stress: Red Sea. Mangroves and Salt marshes, 1, 255-262.

Marchand, C., Allenbach, M., & Lallier-Vergès, E. (2011). Relationships between heavy metals distribution and organic matter cycling in mangrove sediments (Conception Bay, New Caledonia). Geoderma, 160(3-4), 444-456.

Marchand, C., Lallier-Vergès, E., Baltzer, F., Albéric, P., Cossa, D., & Baillif, P. (2006). Heavy metals distribution in mangrove sediments along the mobile coastline of French Guiana. Marine Chemistry, 98(1), 1–17.

Mortazavi, M. S., Sharifian, S., Mohebbi-Nozar, S. L., Saraji, F., & Akbarzadeh, G. A. (2022). The spatial distribution and ecological risks of heavy metals in the north of Persian Gulf. International Journal of Environmental Science and Technology, 19(10), 10143-10156.

Pejman, A., Nabi Bidhendi, G., Ardestani, M., Saeedi, M., & Baghvand, A. (2017). Fractionation of heavy metals in sediments and assessment of their availability risk: A case study in the northwestern of Persian Gulf. Marine Pollution Bulletin, 114(2), 881–887.

Rasul, N. M., Stewart, I. C., & Nawab, Z. A. (2015). Introduction to the Red Sea: its origin, structure, and environment. In The Red Sea: The formation, morphology, oceanography and environment of a young ocean basin (pp. 1-28). Berlin, Heidelberg: Springer Berlin Heidelberg.

Rezaei, M., Kafaei, R., Mahmoodi, M., Sanati, A. M., Vakilabadi, D. R., Arfaeinia, H., ... & Boffito, D. C. (2021). Heavy metals concentration in mangrove tissues and associated sediments and seawater from the north coast of Persian Gulf, Iran: Ecological and health risk assessment. Environmental nanotechnology, monitoring & management, 15, 100456.

Ruiz-Compean, P., Ellis, J., Cúrdia, J., Payumo, R., Langner, U., Jones, B., & Carvalho, S. (2017). Baseline evaluation of sediment contamination in the shallow coastal areas of Saudi Arabian Red Sea. Marine Pollution Bulletin, 123(1–2), 205–218.

Rahman, M. S., Hossain, M. S., Ahmed, M. K., Akther, S., Jolly, Y. N., Akhter, S., ... & Choudhury, T. R. (2019). Assessment of heavy metals contamination in selected tropical marine fish species in Bangladesh and their impact on human health. Environmental Nanotechnology, Monitoring & Management, 11, 100210.

Usman, A. R. A., Alkredaa, R. S., & Al-Wabel, M. I. (2013). Heavy metal contamination in sediments and mangroves from the coast of Red Sea: Avicennia marina as potential metal bioaccumulator. Ecotoxicology and Environmental Safety, 97, 263–270.

Van Lavieren, H., Burt, J., Feary, D. A., Cavalcante, G., Marquis, E., Benedetti, L., ... & Sale, P. F. (2011). Managing the growing impacts of development on fragile coastal and marine ecosystems: Lessons from the Gulf.

Yan, Z., Sun, X., Xu, Y., Zhang, Q., & Li, X. (2017). Accumulation and tolerance of mangroves to heavy metals: a review. Current pollution reports, 3, 302-317.

Yang, D., Wang, M., Lu, H., Ding, Z., Liu, J., & Yan, C. (2019). Magnetic properties and correlation with heavy metals in mangrove sediments, the case study on the coast of Fujian, China. Marine Pollution Bulletin, 146, 865–873.

Yoo, J. C., Lee, C. D., Yang, J. S., & Baek, K. (2013). Extraction characteristics of heavy metals from marine sediments. Chemical Engineering Journal, 228, 688–699.

Youssef, M., & El-Sorogy, A. (2016). Environmental assessment of heavy metal contamination in bottom sediments of Al-Kharrar lagoon, Rabigh, Red Sea, Saudi Arabia. Arabian Journal of Geosciences, 9, 1-10.

CHAPTER 2

MANGROVE SEDIMENT LEAD APPORTIONMENT ALONG THE SAUDI ARABIAN RED SEA COAST USING ISOTOPIC METHODS

Accepted for publication by Taylor & Francis in *Oceanographic and Marine Environmental Studies around the Arabian Peninsula*, Chapter 26.

Authors:
Abdullah S. Alnasser[1,2]
asalnasser@smu.edu, Orcid: 0000-0002-7198-3732
Riyadh F. Halawani[3]
rhalawani@kau.edu.sa, Orcid: 0000-0001-8121-7524
Andrew N. Quicksall[1]
aquicksall@smu.edu, Orcid: 0000-0002-4537-5952

[1]Department of Civil and Environmental Engineering, Southern Methodist University, Dallas, TX 75275, USA
[2]Department of Civil Engineering, College of Engineering, Qassim University, Unaizah, Saudi Arabia
[3]Department of Environmental Science, Faculty of Meteorology, Environment and Arid Land Agriculture, King Abdulaziz University, Jeddah 21589, Saudi Arabia.

2.1 Abstract

Lead concentrations and isotopic ratios were measured in mangrove sediments from three Saudi Arabian Red Sea locations (Yanbu, Jeddah, and the Farasan Islands). Trends of $^{208/206}$Pb vs $^{206/207}$Pb and both ratios vs Pb concentration were examined relative to literature to identify likely sources for each location. A two-end member mixing model was applied to each location to derive fractions of sources. Results show that Jeddah and the Farasan Islands have a blended signature of gasoline-derived and natural lead sources with a greater impact on Jeddah. Despite broad-based lead contamination from gasoline, Jeddah and the Farasan Islands have relatively low, comparable Pb concentrations showing that the gasoline source has a significant impact on isotopic signature while it has little impact on total loading. Conversely, results indicate that Yanbu has an industrial ore isotopic signature besides background Pb sources. This significantly increases Yanbu concentrations relative to the other locations.

Mangrove sediments are known to be sensitive environmental indicators for marine ecosystems. Here, isotopic lead data has shown legacy gasoline-derived contamination is of minimal concern across the region; however, there is an identified lead contamination source impacting Yanbu. Further exploratory study and appropriate management decision making are encouraged given these results.

2.2 Introduction

Mangroves cover about 60%-70% of the worldwide tropical and subtropical shorelines and cover nearly 135 km^2 of the Saudi Arabian Red Sea coastline (Alzubaidy et al. 2016; Almahasheer et al. 2016). Globally, the Red Sea is unusual given the absence of other waterbodies flowing into it (Shukri and Higazy 1944). This limits the diversity of both natural and human-induced sources of lead (Al-Mutairi and Yap 2021). Mangroves benefit the coastal environment in different ways. They can protect the coastal areas from storms, the rise of sea levels, and tsunamis (Alzubaidy et

al. 2016; Khalil 2015). They also offer food, medicine, and habitat for marine organisms and act as a sink for heavy metals in marine ecosystem as they trap sediments in their complicated root structure (Almahasheer et al. 2016; Ramos e Silva et al. 2006; Marchand et al., 2006; Kathiresan 2003). Furthermore, mangroves can capture atmospheric carbon and sequester it in associated sediments (Marchand et al., 2006). However, mangroves forests of the Red Sea live in tough conditions where there is no freshwater input, yielding high salinity and surface water temperatures that exceed 31°C in the summer (Almahasheer et al. 2016). Hence, they are known to be fragmented forests in intertidal areas of the Red Sea of Saudi Arabia. Additionally, Red Sea mangroves environments are under stress due to anthropogenic inputs from mining, coastal growth, petrochemical industries, and industrial waste. Further, infrastructure development for tourism and harbor activities threatens the health of mangrove systems (Almahasheer et al., 2016). Mangrove stands of the Saudi Arabian Red Sea shoreline extend from Jordan to Jizan; however, due to the desert environment, they are not continuous (Shaltout et al. 2020). Further trends in the region show greater densities in the nearshore versus distal areas and greater abundance from southern to northern latitudes. Most of the mangrove forests in the Red Sea consist of a monospecific population capable of thriving in the arid conditions (Mandura 1997).

Lead (Pb) is known as a toxic element that puts both human health and the environment at risk (Wang et al. 2019). Indeed, chronic exposure to Pb can have deleterious effects on the human body by causing problems in the nervous, immune, skeletal, and glandular systems (Lei et al. 2016). Since Pb is persistent in the environment, its concentration may gradually grow in sediments, water, or biological tissues. High Pb concentration in marine systems may negatively impact marine life (Soto-Jiménez et al. 2008). For example, Pb causes behavioral disorders and influences growth of multiple types of fish (Jakimska et al. 2011). Pb can also adversely impact

the growth of plants by causing disturbances in water balance and enzyme activities (Hadi and Aziz 2015). Lead can enter the marine environment naturally through bedrock weathering. It is also introduced via anthropogenic activities such as mining and smelting, coal and leaded gasoline combustion, industrial uses, and sewage sludge applications (Hao et al. 2008; Komárek et al. 2008). Furthermore, Pb can be incorporated into or sorbed to airborne particulate matter yielding the potential for long distance transport before settling (Shetaya et al. 2018).

Pb has four stable isotopes (percent abundance): ^{204}Pb (1%), ^{206}Pb (24%), ^{207}Pb (23%), and ^{208}Pb (52%). ^{206}Pb, ^{207}Pb, and ^{208}Pb are radiogenic isotopes that are generated from the radioactive decay of ^{238}U, ^{235}U, and ^{232}Th, respectively, while ^{204}Pb is the only primordial isotope (Monna et al. 1997; Komárek et al. 2008). The goal of analyzing Pb isotopic ratios is to determine the route of a contaminant transport from its origin to deposition (Charalampides and Manoliadis 2002). Lead isotopes have been used by different researchers. Monna et al. (1997) obtained the Pb isotopic signatures of airborne particulate matter, incinerator ashes, and gasoline samples from France as well as airborne particulate matter and gasoline samples from the southern United Kingdom to determine Pb pollution sources in those regions. Furthermore, Yao et al. (2015) collected gasoline and diesel samples from service stations in Taiwan to determine the Pb isotopic signatures of domestic fuel and then to compare them with other possible sources of atmospheric Pb in Taiwan. Also, Pb isotopic signatures of fly ash from waste incinerators, sewage sludge from a treatment plant, and particulates from auto exhaust from Switzerland were reported by Hansmann and Köppel (2000) and compared to Pb in Swiss soils.

The first goal of this research is to measure the concentration and isotopic ratios of Pb from Red Sea mangrove sediments by analyzing samples from three regions on the Saudi Arabian coast (Figure 2.1). Such values are as yet unreported and will prove a valuable academic resource as a

baseline. The second goal is to identify and, if possible, quantify, the sources of Red Sea mangrove sediment Pb.

2.3 Materials and methods

2.3.1 Study area

Three regions along the Saudi Arabian Red Sea coastline were chosen for the current study ranging from north to south as follows: Yanbu, Jeddah, and the Farasan Islands (Figure 2.1). Yanbu is one of the most industrialized cities on the Saudi Arabian Red Sea coast, having the largest oil shipping center along the Red Sea and is home to various petrochemical and mineral activities (Alharbi et al. 2019). The Jeddah region is an industrial city and a rapidly developing harbor city along the central eastern margin of the Saudi Arabian Red Sea with multiple oil refineries and numerous harbor activities (Mannaa et al. 2021; Mandura 1997; Bantan et al. 2020). The Farasan Islands are a marine sanctuary of the southern part of the Saudi Arabian Red Sea coastline. The nearest industrial activities are about 40 km away in Jizan City, which carries on both industrial and agricultural activities (Bantan and Abu-Zied 2014; Said et al. 2014). The main human activity in the Farasan Islands is fishing although minimal other activities, such as rain fed agriculture, exist (Usman et al. 2013). The Farasan Islands comprise more than a hundred islands and the largest two were selected in the current study, Farasan and Sajid Islands. Seven surficial mangrove sediment samples were taken from Farasan Island and three samples were chosen from Sajid Island.

2.3.2 Sampling preparation and chemical analyses

Ten surficial sediment samples were taken from three mangrove sites of Yanbu, Jeddah, and the Farasan Islands each with a depth from 0 to 10 cm using a stainless-steel scoop and marked by GPS (Figure 2.1). Each sample was then homogenized resulting in thirty samples. Sediments

were oven dried overnight at 105°C, disaggregated via mortar and pestle, then sieved through a 0.074 mm sieve to separate fine particulate matter from coarse debris. Then, an adapted USEPA 3050B method was followed to determine Pb concentrations and isotopic ratios (US Environmental Protection Agency 1996). Briefly, 0.15 to 0.5g of prepared samples were placed into Teflon vessels, based on sample availability after sieving. Next, 6 mL of 5% of nitric acid (HNO_3) was added to remove carbonates. Finally, 20 mL of 70% HNO_3 was added to the Teflon vessels in a fume hood and was brought to and maintained at 85°C in aluminum hot blocks for digestion until the samples were fully dried.

Trace metal grade 70% HNO_3 was diluted to 5% using 18.2 MΩ deionized water. Digested sediment sample salts were redissolved using the prepared 5% nitric acid. Aqueous digestate samples were diluted and analyzed in triplicate using a Thermo Xseries II ICP-MS in collision cell mode with kinetic energy discrimination to determine total Pb concentrations and isotopic abundances (^{206}Pb, ^{207}Pb, and ^{208}Pb). ICP-MS is highly sensitive for this type of analysis since it can provide a count rate of nearly 5.10^5 cps/ppb for lead (Monna et al. 1997). Calibration curves were built using a standard solution from Spex CertiPrep (CLMS-2AN) Claritas PPT. Curves were prepared with 6 calibration points from 0.5 to 20 ppb; all curves had r^2 values greater than 0.999 for each Pb isotope. For quality control purposes, instrumental and experimental blank samples were analyzed every 10 samples. Instrumental blanks were analyzed tubes of 5% HNO_3 used for dilutions and resuspension. Experimental blanks were tubes that underwent all procedures in the experiment and then had 5% HNO_3 added. Using the instrumental and experimental blanks assured ICP-MS run quality against possible problems such as cross contamination. All plasticware used was acid washed for 24 hours and rinsed with 18.2 MΩ water.

2.3.3 Pb Sources

Common approaches used to identify Pb sources include plotting $^{206/207}Pb$ vs $^{208/206}Pb$ and Pb isotopic ratios against Pb concentrations (Komárek et al. 2008; Shetaya et al. 2018). Both techniques were applied here and are discussed below. Once possible sources were identified, a binary mixing model was used to estimate quantitative inputs of two Pb source end members (Komárek et al. 2008). The equation was used to determine the Pb contribution from petrol and natural Pb for Jeddah and the Farasan Islands. An analogous mixing model was used to quantify Pb contribution from ore and natural sources for Yanbu. The rationale for this is discussed below. The two-end-member equations used for both sets of analyses are as follows (Monna et al. 2000; Emmanuel and Erel 2002):

$$Pb_{anthro}\% = 100 * [(^{208/206}Pb_S - ^{208/206}Pb_N)] / [(^{208/206}Pb_{anthro} - ^{208/206}Pb_N)] \quad (2.1)$$

where Pb_{anthro} % is the contribution of the anthropogenic source (gasoline and ores). $^{208/206}Pb_S$ is the measured Pb isotopic ratio in each sample. $^{208/206}Pb_N$ is the averages (2.05) of the natural Pb isotopic ratios from regional literature (Bertrand et al. 2003; Volker et al. 1993; Stuckless et al. 1984; Dupré et al. 1988; Delevaux et al. 1967). $^{208/206}Pb_{anthro}$ is the average (2.15) of isotopic ratios of gasoline-derived sources from worldwide literature since there are no gasoline Pb isotopes studies specific to the region (Erel et al. 1997; Hansmann and Köppel 2000; Monna et al. 1997; Yao et al. 2015). $^{208/206}Pb_{anthro}$ is the average (2.10) of the isotopic ratios of ore sources from local and international literature during the analyses of Yanbu samples, described below (Doe and Delevaux 1972; Doe and Stacey 1974; Bokhari and Kramers 1982; Brevart et al. 1982).

2.3.4 Statistical analyses

Regression analyses were done using a statistical analyses system (SAS JMP 15.1.0).

Regression aided in comparing the Pb isotopic ratios from the current study to previous studies as well as comparing regions with each other.

2.4 Results and Discussion

The average concentrations of Pb (mg/kg) from the study area were highest in Yanbu as follows: 7.39 for Yanbu, 3.82 for Jeddah, and 3.44 for the Farasan Islands. The average background worldwide crustal value used here is 9 mg/kg, as reported by Turekian and Wedepohl (1961) for carbonate sedimentary rocks. The results from Table 2.1 show that three mangrove sediment samples in the Yanbu region, one sample from Jeddah, and two samples from the Farasan Islands exceeded the average crustal background value of Pb (Y1, Y4, Y6, J1, F9, and F10). Yanbu sediments were a few kilometers away from an industrial zone, industrial port, and commercial port. It was expected, therefore, that Yanbu would have more samples exceeding the background average given its closer proximity to potential pollution sources relative to the Jeddah samples and the near absence of such activities near Farasan. The $^{208}Pb/^{206}Pb$ of the area of interest ranged from 2.06 to 2.08 in Yanbu sediments with an average of 2.07. The $^{208}Pb/^{206}Pb$ values of the Jeddah samples varied from 2.07 to 2.12 with an average of 2.09, and from 2.06 to 2.10 for the Farasan Islands with an average of 2.07 (Table 2.1). Yanbu has a range of $^{206}Pb/^{207}Pb$ from 1.18 to 1.20 with an average of 1.19. Jeddah has an average of 1.17 for $^{206}Pb/^{207}Pb$ with a range between 1.15 and 1.20. For the Farasan Islands, the lowest $^{206}Pb/^{207}Pb$ value was 1.15 and the highest was 1.19 with an average of 1.18 (Table 2.1).

Figure 2.2 shows a mixing line with two-end members of gasoline and natural Pb signatures from other studies for comparative value with the current study. Literature used for the comparison is categorized into two groups, natural and anthropogenic. The first represents Pb that may have been transported from regional natural sources including: Arabian plate basalts, Red Sea basalts,

granites from the Arabian Shield of Saudi Arabia, Red Sea Atlantis II deep sediments, and quartz from Saudi Arabia (Bertrand et al. 2003; Volker et al. 1993; Stuckless et al. 1984; Dupré et al. 1988; Delevaux et al. 1967, respectively). The second group provides isotopic Pb signatures that have been derived from gasoline sources from various countries including Israel, Switzerland, France, and Taiwan (Erel et al. 1997; Hansmann and Köppel 2000; Monna et al. 1997; Yao et al. 2015, respectively). Given the lack of lead isotopic studies in the Red Sea region, petrol-Pb signatures were employed from the above mentioned countries. While both potential sources cover a range of ratios, weighted averages of all listed literature for each source were calculated to provide a centroid to be used in modelling and defining the mixing line plotted (Figure 2.2). Figure 2.2 also shows a mixing line of industrial ore sources and natural Pb sources. The industrial ore isotopic ratios employed in the current study were reported by local and international studies and were similarly used in a weighted average calculation to obtain a centroid (Doe and Delevaux 1972; Doe and Stacey 1974; Bokhari and Kramers 1980; Brevart et al. 1982). Measured Pb isotopic ratios of the current study for Yanbu, Jeddah, and the Farasan Islands are also plotted in Figure 2.2 and can, therefore be visually compared to the theoretical mixing lines. The linearity of the data in Figure 2.2 suggests that Jeddah and the Farasan Islands samples are a mix of gasoline and natural Pb sources. In addition, it suggests that Yanbu sediments have a mixture of gasoline and natural sources as well as industrial ore as a third Pb source. Figure 2.3 shows gasoline-derived source contribution and of the Pb concentrations of the three regions. It implies that Jeddah has the highest gasoline Pb load in its sediments compared to Yanbu and the Farasan Islands. It also indicates, however, that despite Yanbu sediments having the highest total Pb concentrations across the study area, they have a lower gasoline loading compared to Jeddah. This leads to an agreement with

Figure 2.2 that Yanbu sediments are affected by an industrial ore Pb source which must be highly elevated in its Pb concentration.

Further evidence is gathered by regression analyses of $^{206/207}$Pb and $^{208/206}$Pb vs Pb concentrations for Yanbu, Jeddah, and the Farasan Islands (Figure 2.4 A and B) in similar fashion to Shetaya et al. (2018). Yanbu sediments have a clear correlation between isotopic signature and concentration which is confirmed by r^2 values reported in Table 2.2. This anthropogenic source elevates Yanbu sediment's concentrations well above the other regions. Its unique signature off axis of the natural-gas mixing line (Figure 2.2) is recorded in the isotopic ratio trends with concentration (Figure 2.4). Meanwhile, the interpretation that Jeddah and the Farasan Islands sediments are solely composed of gasoline and natural Pb sources is supported by the low concentrations (Figure 2.3) and for the poorer correlation between isotopic ratios and concentration (Figure 2.4 A and B). Of note is, in addition to the strong correlation of Yanbu isotopic ratios with concentrations, that Jeddah also has a strong correlation (Table 2.2). Given the relatively low concentrations there, this further supports a background contaminant that alters the isotopic signature with small additions but has little impact on overall loading. This is consistent with the gasoline-derived end member.

Three samples are identified on Figure 2.2 (J1, F9, and F10) from Jeddah and Farasan that are outliers. They have been dropped from analyses and are interpreted to be recording stochastic impact of another source; however, with so few data points of the set of thirty, no further interpretation on that source is possible.

Table 2.3 shows the percentages of gasoline-derived and natural Pb sources for Jeddah and the Farasan Islands. The gasoline-derived average in Jeddah samples is higher (34%) than in Farasan Islands sediments (18%). For Yanbu sediments, Table 2.4 reports the industrial ore and

natural composition percentages with an average of 44% for the industrial ore. Tables 2.3 and 2.4 show that the entire investigated area has more natural Pb than gasoline or ore components which affirms Figure 2.2 since it shows most of the sediment samples, regardless of location, fall closer to the natural end member than the gasoline and the industrial ore sources. Figure 2.5 shows that the higher the concentration the more the industrial ore input to Yanbu sediments confirm that sources control on total lead loading for that location. Also, it shows higher percentages of gasoline Pb are associated with higher Pb concentrations in Jeddah sediments. As suggested above, the Jeddah samples record a strong history of legacy gasoline-derived Pb accumulation; however, they have not yielded significant total Pb contamination. For Jeddah and the Farasan Islands, the outlier samples are most likely from unknown anthropogenic sources since they plot off the mixing line in Figure 2.2 paired with Pb concentrations exceeding the average background crustal value.

2.5 Conclusion

Throughout the study area, Pb concentrations are relatively low when compared to the average preindustrial background, and Jeddah and the Farasan Islands have lower concentrations in general than Yanbu as Table 2.1 indicates. The Farasan Islands and Jeddah have Pb mostly derived from petrol and natural inputs. Jeddah sediments have the highest gasoline-derived Pb loading across the study area although the Pb concentrations are low compared to Yanbu. For Farasan Islands sediments, the dominant Pb source is natural as is expected given the Islands have the least urban activities in the study area as the main industry is fishing with some agricultural activities. Pb isotopic ratios suggest that Yanbu has an unknown industrial ore source of Pb that markedly elevates concentrations proportionally to altering its isotopic signatures.

Mangrove environments are known to be ecosystems that can easily sequester heavy metals when exposed. They, therefore, act as highly sensitive indicators of a region's overall susceptibility

to heavy metal pollution. Here, we find relatively low lead pollution across the region; however, there is clear documentation of what is likely a legacy atmospheric fallout of gasoline-derived lead. While this signature is ubiquitous, it is centered on the urban area of Jeddah. Despite trended gasoline isotopic values with concentrations, this Pb source has little impact on total lead loading. There is a stark contrast with the Yanbu mangrove area. There, an anthropogenic, likely modern and point, source clearly impacts both the isotopic signature and the total Pb loading. While the environmental threat of gasoline-derived Pb is likely stable and only a historical record, the industrial ore sourcing in Yanbu mangrove sediments should be a clear warning. Further work identifying the exact source and the breadth of impact should be prioritized. Additionally, management strategies to mitigate this pollution should be developed and implemented prior to exacerbation.

Table 2.1 Pb concentrations (mg/kg) and isotopic ratios of mangrove sediment samples from the study area. Averages and standard deviations for each region are included.

Sampler ID	Concentration	$^{206/207}$Pb	$^{208/206}$Pb
Yanbu			
Y1	10.10	1.19	2.08
Y2	6.39	1.19	2.07
Y3	5.97	1.19	2.07
Y4	14.50	1.18	2.08
Y5	8.15	1.19	2.07
Y6	9.10	1.18	2.07
Y7	2.87	1.20	2.06
Y8	5.32	1.19	2.07
Y9	8.41	1.20	2.06
Y10	3.07	1.19	2.07
Average	7.39	1.19	2.07
SD	3.48	0.00	0.01
Jeddah			
J1	20.74	1.15	2.12
J2	3.78	1.16	2.10
J3	2.71	1.16	2.09
J4	1.95	1.16	2.08
J5	1.24	1.18	2.08
J6	1.47	1.18	2.08
J7	1.23	1.17	2.08
J8	1.31	1.18	2.07
J9	1.44	1.20	2.07
J10	2.34	1.16	2.09
Average	3.82	1.17	2.09
SD	6.00	0.01	0.02

Table 2.1 (Continued).

Sampler ID	Concentration	$^{206/207}Pb$	$^{208/206}Pb$
Farasan Islands			
F1	3.20	1.18	2.06
F2	2.05	1.18	2.06
F3	1.81	1.19	2.06
F4	1.48	1.18	2.07
F5	1.43	1.19	2.06
F6	1.29	1.19	2.06
F7	2.30	1.18	2.06
F8	1.23	1.18	2.08
F9	9.79	1.16	2.10
F10	9.78	1.15	2.10
Average	3.44	1.18	2.07
SD	3.40	0.01	0.02

Table 2.2 Linear regression r^2 values of $^{208/206}Pb$ and $^{206/207}Pb$ ratios vs Pb concentrations for mangrove sediments from Yanbu, Jeddah, and the Farasan Islands regions represented in Figure 2.4.

Region	r^2 of Figure 2.4 A	r^2 of Figure 2.4 B
Yanbu	0.74	0.36
Jeddah	0.78	0.44
Farasan Islands	0.08	0.01

Table 2.3 Percentages of Gasoline and Natural Pb sources of Jeddah and Farasan Islands sediments.

Sample ID	Gas %	Natural %
J2	56	44
J3	43	57
J4	33	67
J5	29	71
J6	29	71
J7	37	63
J8	22	78
J9	21	79
J10	41	59
Average	34	66
F1	15	85
F2	17	83
F3	16	84
F4	25	75
F5	10	90
F6	13	87
F7	16	84
F8	31	69
Average	18	82

Table 2.4 Percentages of Ore and Natural contributions to total Pb loading of Yanbu samples.

Sample ID	Ore %	Natural %
Y1	58	42
Y2	45	55
Y3	50	50
Y4	71	29
Y5	47	53
Y6	51	49
Y7	20	80
Y8	37	63
Y9	32	68
Y10	34	66
Average	44	56

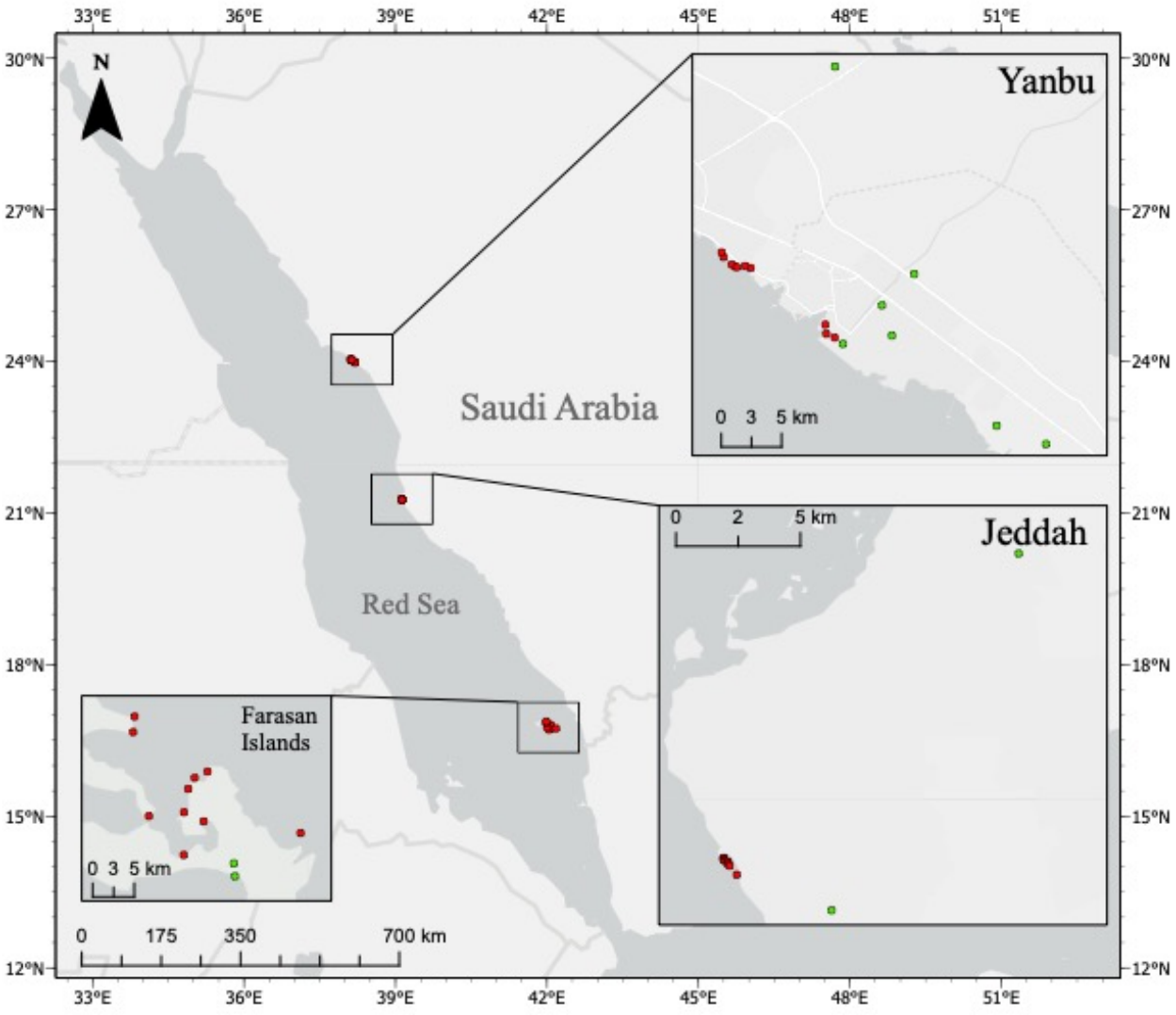

Figure 2.1 Sampling regions on the eastern margin of the Red Sea along the coast of Saudi Arabia. Red markers show specific sample locations for each region. Green markers represent known potential anthropogenic sources.

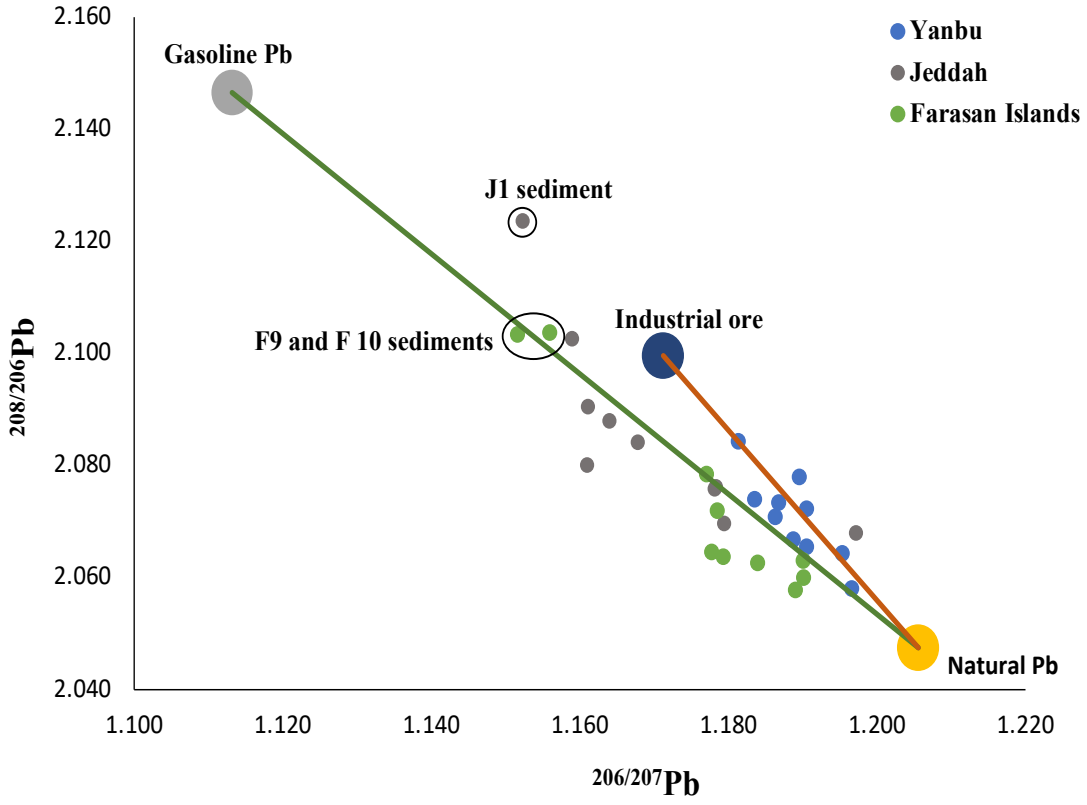

Figure 2.2 $^{208/206}$Pb vs $^{206/207}$Pb values of Yanbu, Jeddah and the Farasan Islands denoted in the legend. Mixing lines of gasoline and natural isotopic ratios (green line) and of industrial ore Pb and natural Pb isotopic ratios (orange line) connect isotopic signatures of known sources. For reference values and method of exact source end member centroid determination, see text.

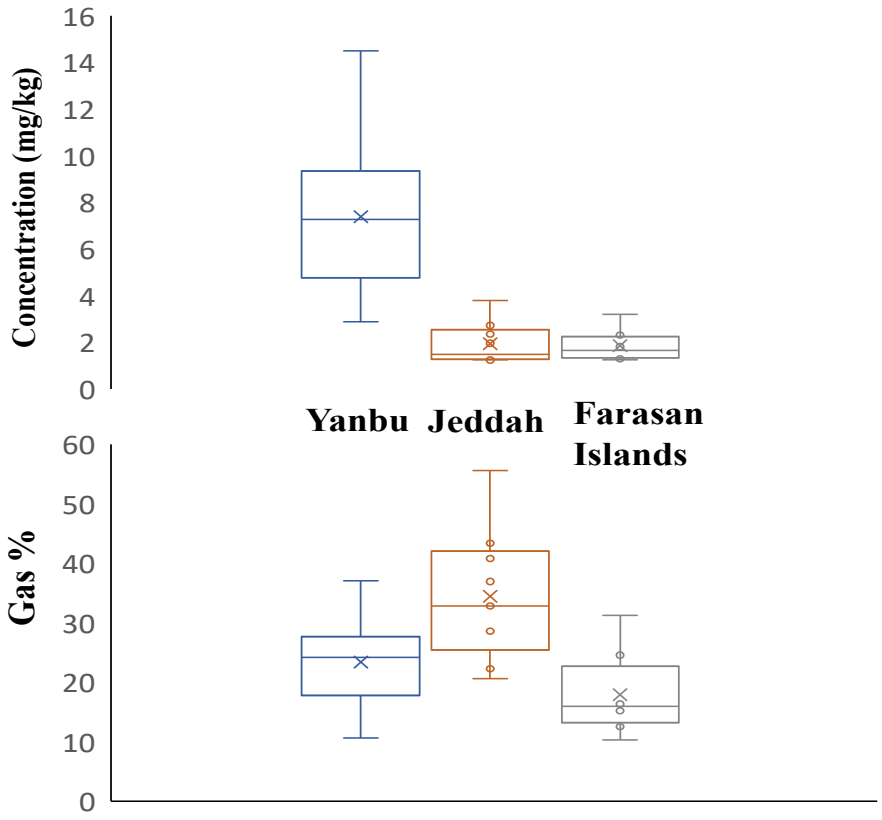

Figure 2.3 Box and whisker plots showing the means designated by x symbol, median, minimum, and maximum values of the distributions of concentrations (top) and percent gas contribution (bottom) for Yanbu, Jeddah, the Farasan Islands.

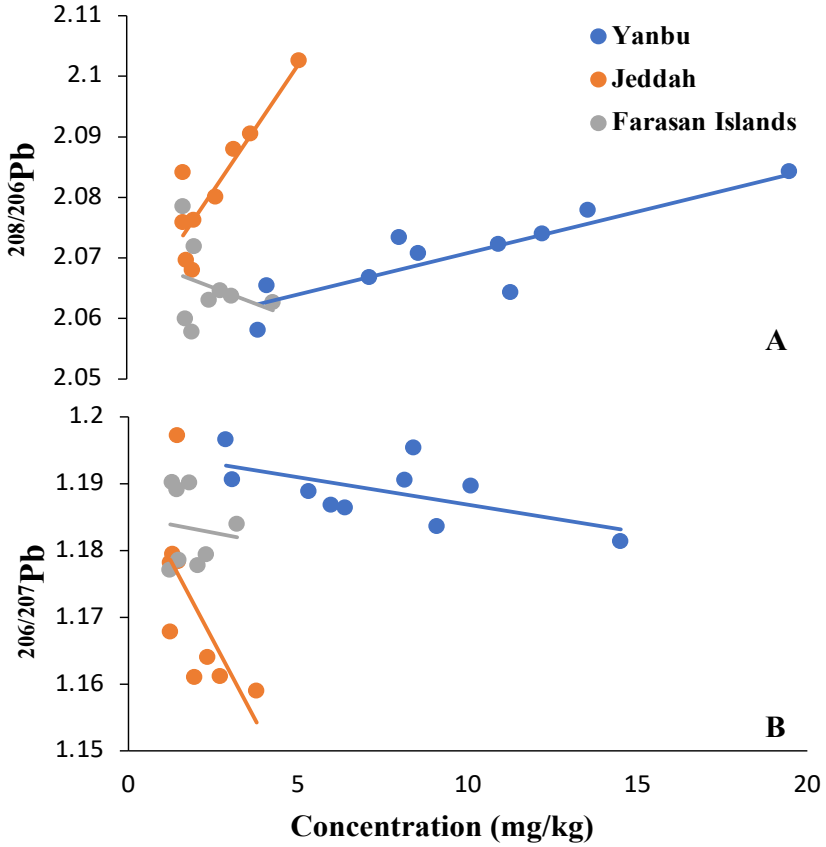

Figure 2.4 $^{208/206}$Pb (A) and $^{206/207}$Pb (B) ratios vs Pb concentrations for Yanbu, Jeddah, and the Farasan Islands. Lines show the least squares regression of best fit. r^2 values for these fits are reported in Table 2.2.

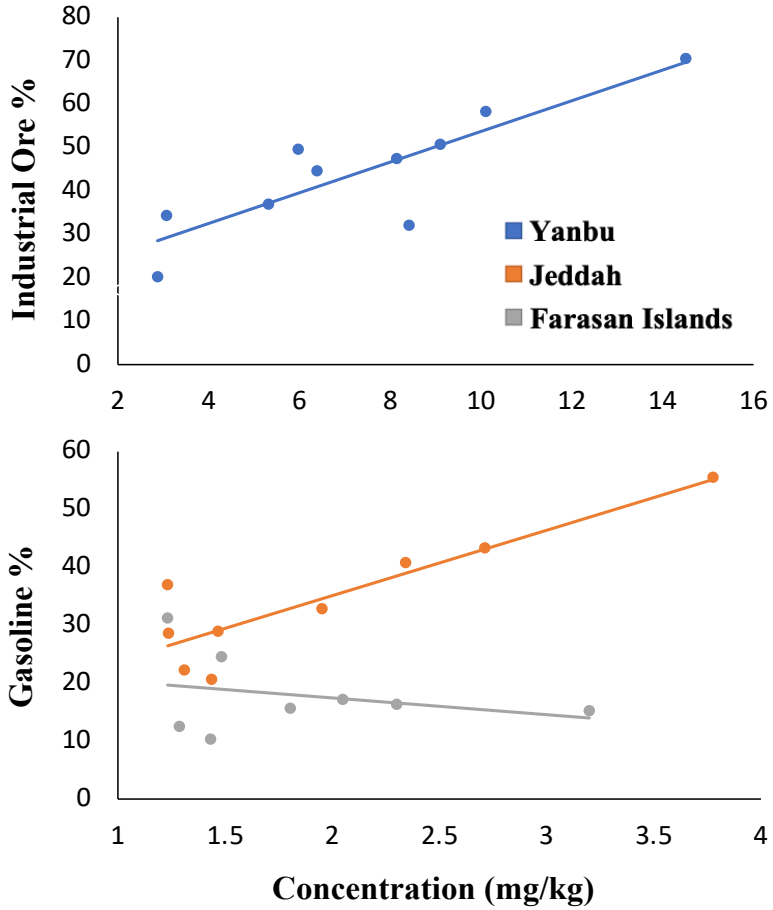

Figure 2.5: Industrial ore percentage contribution vs concentrations for Yanbu (top). Percentage of gasoline-derived sources vs concentrations for Jeddah and Farasan (bottom). Lines show the least squares regression of best fit.

2.6 References

Alharbi, O.M.L., Khattab, R.A., Ali, I., Binnaser, Y.S., and A. Aqeel. 2019. Assessment of heavy metals contamination in the sediments and mangroves (Avicennia marina) at Yanbu coast, Red Sea, Saudi Arabia. Marine Pollution Bull 149: 110669.

Almahasheer, H., Aljowair, A., Duarte, C. M., & Irigoien, X. (2016). Decadal stability of Red Sea mangroves. Estuarine, Coastal and Shelf Science, 169, 164-172.

Al-Mutairi, K.A., and C.K. Yap. 2021. A review of heavy metals in coastal surface sediments from the red sea: Health-ecological risk assessments. Int J Environ Res Public Health 18, no. 6: 2798.

Alzubaidy, H., Essack, M., Malas, T.B., Bokhari, A., Motwalli, O., Kamanu, F.K., Jamhor, S.A., et al. 2016. Rhizosphere microbiome metagenomics of gray mangroves (Avicennia marina) in the Red Sea. Gene 576, no. 2: 626-636.

Bantan, R.A., and R.H. Abu-Zied. 2014. Sediment characteristics and molluscan fossils of the Farasan Islands shorelines, southern Red Sea, Saudi Arabia. Arabian J Geosci 7, no. 2: 773-787.

Bantan, R.A., Al-Dubai, T.A., and A.G. Al-Zubieri. 2020. Geo-environmental assessment of heavy metals in the bottom sediments of the Southern Corniche of Jeddah, Saudi Arabia. Marine Pollution Bull 161: 111721.

Bertrand, H., Chazot, G., Blichert-Toft, J., and S. Thoral. 2003. Implications of widespread high-μ volcanism on the Arabian Plate for Afar mantle plume and lithosphere composition. Chem Geol 198, nos. 1-2: 47-61.

Bokhari, F.Y., and J.D. Kramers. 1982. Lead isotope data from massive sulfide deposits in the Saudi Arabian Shield. Econ Geol 77, no. 7: 1766-1769.

Brevart, O., Dupré, B., and C.J. Allegre. 1982. Metallogenic provinces and the remobilization process studied by lead isotopes; lead-zinc ore deposits from the southern Massif Central, France. Econ Geol 77, no. 3: 564-575.

Charalampides, G., and O. Manoliadis. 2002. Sr and Pb isotopes as environmental indicators in environmental studies. Environ Int 28, no. 3: 147-151.

Delevaux, M.H., Doe, B.R., and Brown, G.F. 1967. Preliminary lead isotope investigations of brine from the Red Sea, galena from the Kingdom of Saudi Arabia, and galena from United Arab Republic (Egypt). Earth Planet Sci Lett 3: 139-144.

Doe, B.R., and J.S. Stacey. 1974. The application of lead isotopes to the problems of ore genesis and ore prospect evaluation: a review. Econ Geol 69, no. 6: 757-776.

Doe, B.R., and M.H. Delevaux. 1972. Source of lead in southeast Missouri galena ores. Econ Geol 67, no. 4: 409-425.

Dupré, B., Blanc, G., Boulègue, J., and C.J. Allègre. 1988. Metal remobilization at a spreading centre studied using lead isotopes. Nature 333, no. 6169: 165-167.

Emmanuel, S., and Y. Erel. 2002. Implications from concentrations and isotopic data for Pb partitioning processes in soils. Geochim Cosmochim Acta 66, no. 14: 2517-2527.

Erel, Y., Veron, A., and L. Halicz. 1997. Tracing the transport of anthropogenic lead in the atmosphere and in soils using isotopic ratios. Geochim Cosmochim Acta 61, no. 21: 4495-4505.al

Hadi, F., and T. Aziz. 2015. A mini review on lead (Pb) toxicity in plants. J Biology Life Sci 6, no. 2: 91-101.

Hansmann, W., and V. Köppel. 2000. Lead-isotopes as tracers of pollutants in soils. Chem Geol 171, no. 1-2: 123-144.

Hao, Y., Guo, Z., Yang, Z., Fan, D., Fang, M., and X. Li. 2008. Tracking historical lead pollution in the coastal area adjacent to the Yangtze River estuary using lead isotopic compositions. Environ Pollution 156, no. 3: 1325-1331.

Jakimska, A., Konieczka, P., Skóra, K., and J. Namieśnik. 2011. Accumulation of metals in tissues and organs of marine organisms. Effect Metals Mar Org 20: 1117-1125.

Kathiresan, K. (2003). How do mangrove forests induce sedimentation?. Revista de biologia tropical, 51(2), 355-360.

Khalil, A. S. (2015). Mangroves of the red sea. The Red Sea: The Formation, Morphology, Oceanography and Environment of a Young Ocean Basin, 585-597.

Komárek, M., Ettler, V., Chrastný, V., and M. Mihaljevič. 2008. Lead isotopes in environmental sciences: a review. Environ Int 34, no. 4: 562-577.

Lei, K., Giubilato, E., Critto, A., Pan, H., and C. Lin. 2016. Contamination and human health risk of lead in soils around lead/zinc smelting areas in China. Environ Sci Pollution Res 23, no. 13: 13128-13136.

Mandura, A.S. 1997. A mangrove stand under sewage pollution stress: Red Sea. Mangroves Salt Marshes 1, no. 4: 255-262.

Mannaa, A.A., Khan, A.A., Haredy, R., and A.G. Al-Zubieri. 2021. Contamination evaluation of heavy metals in a sediment core from the Al-Salam Lagoon, Jeddah coast, Saudi Arabia. J Marine Sci Eng 9, no. 8: 899.

Monna, F., Hamer, K., Lévêque, J., and M. Sauer. 2000. Pb isotopes as a reliable marker of early mining and smelting in the Northern Harz province (Lower Saxony, Germany). J Geochem Exploration 68, no. 3: 201-210.

Monna, F., Lancelot, J., Croudace, I.W., Cundy, A.B., and J.T. Lewis. 1997. Pb isotopic composition of airborne particulate material from France and the southern United Kingdom: implications for Pb pollution sources in urban areas. Environ Sci Technol 31, no. 8: 2277-2286.

Marchand, C., Lallier-Vergès, E., Baltzer, F., Albéric, P., Cossa, D., & Baillif, P. (2006). Heavy metals distribution in mangrove sediments along the mobile coastline of French Guiana. Marine chemistry, 98(1), 1-17.

Ramos e Silva, C.A., Da Silva, A.P., and S.R. De Oliveira. 2006. Concentration, stock and transport rate of heavy metals in a tropical red mangrove, Natal, Brazil. Marine Chem 99, no. 1-4: 2-11.

Said, T.O., Omran, A.A., Fawy, K.F., and A.M. Idris. 2014. Heavy metals in twelve edible marine fish species from Jizan fisheries, Saudi Arabia: monitoring and assessment. Fresenius Environ Bull 23, no. 3: 801-809.

Shaltout, K.H., Ahmed, M.T., Alrumman, S.A., Ahmed, D.A., and E.M. Eid. 2020. Evaluation of the carbon sequestration capacity of arid mangroves along nutrient availability and salinity gradients along the Red Sea coastline of Saudi Arabia. Oceanologia 62, no. 1: 56-69.

Shetaya, W.H., Marzouk, E.R., Mohamed, E.F., Elkassas, M., Bailey, E.H., and S.D. Young. 2018. Lead in Egyptian soils: Origin, reactivity and bioavailability measured by stable isotope dilution. Sci Total Environ 618: 460-468.

Shukri, N.M., and R.A. Higazy. 1944. Mechanical analysis of some bottom deposits of the Northern Red Sea. J Sed Res 14, no. 2: 43-69.

Soto-Jiménez, M.F., Páez-Osuna, F., Scelfo, G., Hibdon, S., Franks, R., Aggarawl, J., and A.R. Flegal. 2008. Lead pollution in subtropical ecosystems on the SE Gulf of California Coast: A study of concentrations and isotopic composition. Marine Environ Res 66, no. 4: 451-458.

Stuckless, J.S., Hedge, C.E., Wenner, D.B., and I.T. Nkomo. 1984. Isotopic studies of postorogenic granites from the northeastern Arabian Shield, Kingdom of Saudi Arabia. Saudi Arabian Deputy Ministry for Mineral Resources. Open-File Report USGS-OF-04-42: 1-40.

Turekian, K.K., and K.H. Wedepohl. 1961. Distribution of the elements in some major units of the earth's crust. Geol Soc Am Bull 72, no. 2: 175-192.

US Environmental Protection Agency (EPA). (1996). Method 3050B: Acid digestion of sediments, sludges, and soils. Test methods for evaluating solid waste, physical/chemical methods.

Usman, A.R.A., Alkredaa, R.S., and M.I. Al-Wabel. 2013. Heavy metal contamination in sediments and mangroves from the coast of Red Sea: Avicennia marina as potential metal bioaccumulator. Ecotoxicol Environ Safety 97: 263-270.

Volker, F., McCulloch, M.T., and R. Altherr. 1993. Submarine basalts from the Red Sea: new Pb, Sr, and Nd isotopic data. Geophys Res Lett 20, no. 10: 927-930.

Wang, Z., Dwyer, G.S., Coleman, D.S., and A. Vengosh. 2019. Lead isotopes as a new tracer for detecting coal fly ash in the environment. Environ Sci Technol Lett 6, no. 12: 714-719.

Yao, P.-H., Shyu, G.-S., Chang, Y.-F., Chou, Y.-C., Shen, C.-C., Chou, C.-S., and T.-K. Chang. 2015. Lead isotope characterization of petroleum fuels in Taipei, Taiwan. Int J Environ Res Public Health 12, no. 5: 4602-4616.

CHAPTER 3

ASSESSMENT OF HEAVY METAL DISTRIBUTION, RISK, AND SOURCING IN MANGROVE SEDIMENTS FROM THREE SAUDI ARABIAN RED SEA LOCATIONS

Accepted for publication by Marine Pollution Bulletin.

Authors:

Abdullah S. Alnasser[1,2]

asalnasser@smu.edu, Orcid: 0000-0002-7198-3732

Riyadh F. Halawani[3]

rhalawani@kau.edu.sa, Orcid: 0000-0001-8121-7524

Andrew N. Quicksall[1]

aquicksall@smu.edu, Orcid: 0000-0002-4537-5952

[1]Department of Civil and Environmental Engineering, Southern Methodist University, Dallas, TX 75275, USA

[2]Department of Civil Engineering, College of Engineering, Qassim University, Unaizah, Saudi Arabia

[3]Department of Environmental Science, Faculty of Meteorology, Environment and Arid Land Agriculture, King Abdulaziz University, Jeddah 21589, Saudi Arabia.

3.1 Abstract

This work measured the concentration of heavy metal cations and associated anionic ligands in mangrove sediments from the Red Sea of Saudi Arabia. Sediments were collected from three regions along the Saudi Arabian coast: Yanbu, Jeddah, and the Farasan Islands. Risk indices and statistical analyses were applied to assess contamination levels and potential sourcing. The results show that Yanbu is at environmental risk as it shows higher concentrations and anthropogenic signatures for most metals compared to the other two regions. Jeddah is also of concern as it shows multiple metals derived from a singular dominant anthropogenic source, likely wastewater discharge. The Farasan Islands environment has the least anthropogenic stress among the three locations. This study provides the research community with an updated record of mangrove sediment contamination in the region. This will prove especially useful given the lack of mangrove sediment data in the Saudi Arabian Red Sea to date.

3.2 Introduction

Mangroves are abundant in tropical saline shoreline environments usually between latitudes 25° N and 25° S. Mangroves can absorb and store carbon from the air then transfer it to the sediments and thus are considered effective carbon sinks (Eid et al. 2019). They also play an important role in providing marine organisms with food and habitat. Furthermore, they can protect coastline areas from both typical erosion and that of catastrophic weather events such as tsunamis and cyclones; the effectiveness of protection depends on mangrove density, average root and stem diameter, forest floor shape and local bathymetry (Blankespoor et al., 2017). Mangrove stands are, indeed, vital to the health of broader marine margin ecosystems.

Mangrove ecosystems can, however, be impacted by heavy metals due to toxicity, possible bioaccumulation in the food chain, and typical non-biodegradability (Usman et al., 2013). Heavy

metal pollution has attracted near universal attention across numerous ecosystems for these same reasons (Hu et al., 2017; Natesan et al., 2014). Heavy metals are released to the environment by anthropogenic processes, such as industrial activities, as well as by natural processes, such as rock weathering (ELTurk et al., 2019). Usually, metals are sorbed to particulates when released into an aquatic environment, then settle and are incorporated into various sediment fractions (Khodami et al., 2017). Mangrove sediments typically have a high capacity to adsorb and retain heavy metals since they are anaerobic and contain high organic matter and sulfide content (Tam & Wong, 2000; Yan et al., 2017). Disruptions such as changes in salinity or long dry periods could drive mangrove sediments to lose sorption capacity. Dry seasons raise salinity by evaporation and, when salinity increases, the concentrations of major cations such as Ca^{2+} and Mg^{2+} increase which can easily exchange with heavy metals on the sediment surface due to their ionic properties (Miranda et al., 2022; Zhang & Huang, 2011). This then causes mobilization of metals yielding a system where mangrove sediments act as a heavy metal source instead of a sink (Yan et al., 2017).

Few mangrove sediment studies have been carried out along the Red Sea of Saudi Arabia with as yet unclear overall trends. From the north to the south of the Red Sea, Abohassan (2013) found that mangrove systems in Yanbu and Shuaiba are unpolluted in comparison with other international mangrove sites. Alternatively, Alharbi et al. (2019) collected surficial sediments with mangrove leaves and roots from the coastline of Yanbu and showed that these sediments were contaminated with heavy metals.

The aim of this work is to clarify contamination trends in mangrove sediments from the Saudi Arabian Red Sea. To do so, the study measured heavy metal (HM) concentrations (V, Cr, Ni, Cu, Zn, Cd, and Pb), as well as soil organic matter (SOM), carbonate, and silicate sediment fractions from latitudinally specific sites described below. Values were then used to evaluate

contamination status by applying the following risk indices: contamination factor (CF), enrichment factor (EF), geoaccumulation index (I_{geo}), and pollution load index (PLI). Finally, anthropogenic versus natural sourcing was assessed by applying statistical analyses to HM, SOM, carbonate, and silicate concentrations for each region.

3.3 Materials and methods

3.3.1 Study area

The study area covers three regions in Saudi Arabia, Yanbu, Jeddah, and the Farasan Islands, from north to south, respectively, along the eastern Red Sea coastline (Figure 3.1). Yanbu is an industrial city that includes the largest oil shipping facility in Saudi Arabia, an industrial harbor, oil refineries, desalination plants, petrochemical factories and various mineral processing activates (Alharbi et al., 2019; Badr et al., 2009). Jeddah is also an industrial city that contains various factories such as power and desalination plants, wastewater treatment facilities, oil refineries as well as commercial harbors (Al-Mur et al., 2017). Lastly, the Farasan Islands were classified as a natural reserve in 1989 and are supervised by the National Commission for Wildlife Conservation and Development (Bantan & Abu-Zied, 2014). The major human activity in the Farasan Islands is fishing as well as light activities of livestock grazing and rain fed crop production (Pavlopoulos et al., 2018).

3.3.2 Sample collection and preparation

Thirty surficial (0-10 cm) mangrove sediment samples were collected as follows: Yanbu (10 stations), Jeddah (10 stations), and Farasan Islands (10 stations). Each sample was then split, as upper sediment (0-5 cm) and lower sediment (5-10 cm) and homogenized yielding a total number of the mangrove sediment aliquots of 60. The upper sediments are as follows: Yanbu Upper (YU), Jeddah Upper (JU), and Farasan Islands Upper (FU). The lower sediments are as

follows: Yanbu Lower (YL), Jeddah Lower (JL), and Farasan Islands Lower (FL). Sample locations were determined using GPS (Figure 3.1).

Mangrove sediments were oven dried overnight at 105 °C, then disaggregated by mortar and pestle. Dried, disaggregated samples were then passed through a 0.074 mm sieve. The retained soil from 0.074 sieve was recorded as the sand fraction and the passed sediment was recorded as the silt-clay fraction. The mass used for sieving ranged from 5.57 g to 8.29 g, due to sample availability.

3.3.3 Instrumental analysis

3.3.3.1 Inductively Coupled Plasma-Mass Spectroscopy (ICP-MS) Analysis

A stock solution of 5% nitric acid (HNO_3) was prepared by mixing trace metal grade 70% concentrated HNO_3 and 18.2 MΩ deionized water to be used for various purposes as described below. The HM concentrations of V, Cr, Ni, Cu, Zn, Cd, and Pb were determined according to an amended USEPA 3050B method (Environmental Protection Agency, 1996). Briefly, from 0.15g to 0.5g of the disaggregated sediments (based on availability) were placed into Teflon vessels. Then, 6 mL of 5% HNO_3 was added for carbonate removal. Next, 20 mL of 70% HNO_3 was added inside a fume hood and left on hot blocks at 85 ºC for digestion until dryness. Digestate salts were quantitatively redissolved in 5% HNO_3. Serial dilutions of the sediment samples' digestates were made using the 5% HNO_3 solution. The samples were introduced to a ThermoFisher Scientific X-Series-II Inductively Coupled Plasma-Mass Spectroscopy to measure the concentrations of V, Cr, Ni, Cu, Zn, Cd, and Pb. The instrument was equipped with collision cell technology employing kinetic energy discrimination. Seven-point calibration curves were made by preparing multi-element standard solutions from Spex CertiPrep (CLMS-2AN) from 0.5 to 25 ppb. To assure quality control, instrumental and experimental blanks were analyzed every 10 samples.

3.3.3.2 Thermogravimetric analysis

The SOM, carbonate, and silicate abundances for each sample were determined by employing thermogravimetric methods (Wang et al., 2011). Sediment samples were oven dried at 105 °C and disaggregated by using a mortar and pestle. Then, they were sieved through 0.074 sieve mm to keep the samples consistent with the ones used for determining the HM concentrations. A thermogravimetric analyzer (Perkin Elmer STA 6000) was set to a heating rate of 10 °C/min from 30 °C to 990 °C under nitrogen gas purge set to a flow rate of 20 ml/min. Approximately 100 mg of dried sample was placed in a corundum (Al_2O_3) crucible then loaded into the thermogravimetric analyzer. The initial dry sample mass (mg) at 105 °C (M_1), the sample mass at 550 °C (M_2), and the sample mass at 950 °C (M_3) were used to calculate the SOM % and carbonate % in equations (1) and equation (2), respectively. The temperatures and equations used were suggested by Heiri et al. (2001) for loss on ignition method. Carbonate, shale, and sandstone are the standard components of sedimentary rocks (Turekian and Wedepohl, 1961). Thus, silicate % was calculated using equation (3).

$$\text{SOM } \% = \left(\frac{M_1 - M_2}{M1}\right) \times 100 \quad (3.1)$$

$$\text{Carbonate } \% = \left(\frac{M_2 - M_3}{M1}\right) \times 100 \times 1.36 \quad (3.2)$$

The 1.36 value in equation (2) is the conversion factor to back calculate from measured CO_2 loss (44 g/mol) to the original solid carbonate (60 g/mol).

Silicate % = 100 - SOM % - Carbonate % (3.3)

3.3.4 Environmental pollution indices

Different authors have used several indices to determine the HM contamination status in sediments (Al-Mur et al., 2017b; Bantan et al., 2020a; Kowalska et al., 2018; Usman et al., 2013). Therefore, to fully evaluate HM contaminations in the study area, various indices were employed:

CF, EF, I_{geo}, and PLI for V, Cr, Ni, Cu, Zn, Cd, and Pb of each sample with respect to location and depth.

CF helps in soil contamination assessment by considering the HM contents of a sediment sample in the area of interest relative to natural background levels. The CF was calculated using equation (4) by Hakanson (1980):

$$\mathrm{CF} = \frac{\mathrm{C_{Sediment}}}{\mathrm{C_{Background}}} \tag{3.4}$$

where, $C_{sediment}$ is the measured concentration of a metal in a sediment sample. $C_{background}$ is the background concentration value of the same metal in the earth's crust as reported by Turekian and Wedepohl (1961) for sedimentary rocks. The interpretations of CF values were introduced by Hakanson (1980) as following: $C_F < 1$ is considered low contamination, $1 < C_F < 3$ is moderate contamination, $3 < C_F < 6$ indicates considerable contamination, and $C_F > 6$ is very high contamination.

EF is utilized to distinguish anthropogenic and natural sources by employing a normalizing technique that uses a conservative element as a reference for both preindustrial background and sample concentrations (Kowalska et al., 2018; Yongming et al., 2006). Typical elements used for normalization are iron, aluminum, rubidium, or manganese (Barbieri, 2016; Sappa et al., 2020); rubidium was used in this study. Further, EF values have been used to show geochemical patterns in mangrove sediments (Haris & Aris, 2013). EF values were computed using equation (5):

$$\mathrm{EF} = \frac{\left(\frac{\mathrm{C_i}}{\mathrm{C_{Rb}}}\right)_{\mathrm{Sediment}}}{\left(\frac{\mathrm{C_i}}{\mathrm{C_{Rb}}}\right)_{\mathrm{Background}}} \tag{3.5}$$

where, C_i represents the measured concentration of an element in a sediment sample and C_{Rb} is the concentration of rubidium in the same sediment. $(C_i/C_{Rb})_{Sediment}$ and $(C_i/C_{Rb})_{Background}$ are, therefore, the normalized concentration of a sediment sample and the background, respectively. When $0.5 \leq$

EF ≤1.5, this indicates a natural source, whereas when EF > 1.5 it implies a significant amount of the metal is derived from anthropogenic sources (J. Zhang & Liu, 2002).

I_{geo} was applied to evaluate the HM contaminations of the study area by contrasting its concentrations to preindustrial values. Several studies on mangrove sediments have employed this index as an efficient way for clarifying sediment quality (Haris & Aris, 2013). I_{geo} was calculated by using equation (6) (Müller, 1979):

$$I_{geo} = \log_2 \left(\frac{C_{Sediment}}{1.5 \times C_{Background}} \right) \quad (3.6)$$

where, C_s is the concentration of an element in a sediment sample, C_b is the concentration of the same element's background value and 1.5 is an empirically derived correction factor for natural processes that affect background values. There are seven classes of interpretation proposed by Müller, (1981): $I_{geo} < 0$ implies uncontaminated, $0 < I_{geo} < 1$ implies uncontaminated to moderately contaminated, $1 < I_{geo} < 2$ implies moderately contaminated, $2 < I_{geo} <$ implies moderately to highly contaminated, $3 < I_{geo} < 4$ implies highly contaminated, $4 < I_{geo} < 5$ highly to extremely contaminated, and $I_{geo} > 5$ implies extremely contaminated.

PLI was used to assess total or combined HM contamination levels in the study area by using equation (7) (Tomlinson et al., 1980):

$$PLI = (C_{F1} \times C_{F2} \times C_{F3} \times C_{Fn})^{\left(\frac{1}{n}\right)} \quad (3.7)$$

where, C_{Fi} is the contamination factor of an element in a sediment sample and n is the number of elements of interest. A PLI < 1 indicates no pollution while a PLI > 1 suggests pollution is present.

3.3.5 Statistical analysis

Bivariant and multivariate analyses were carried out using SAS JMP 15.1.0 to determine relationships between the HM concentrations, soil organic matter, carbonate, and silicate for each location. Linear regression models and principal component analyses (PCA) were applied for this

purpose. Principal components (PCs) with eigenvalues greater than 1.0 were chosen for interpretation.

3.4 Results and discussion

The average HM concentrations (mg/kg) varied by depth and location across the study area. The average concentrations of YU location were Zn > V > Pb > Ni > Cr > Cu > Cd (Table 3.1). YL showed an almost twofold increase relative to YU apart from Cr which was nearly four times the Cr value of YU. Cr, Zn, Cd, and Pb average concentrations in YL sediments and Cu in both YU and YL sediments exceeded their average carbonate sedimentary rock concentrations values by Turekian and Wedepohl (1961) (Table 3.1). For JU, average concentrations yielded the trend of: Zn > V > Cu > Ni > Cr > Pb > Cd (Table 3.1). The JL sediments had similar HM concentrations compared to JU. Cu in JU and JL as well as Zn in JU average concentrations were higher than their world crustal averages by concentrations values by Turekian and Wedepohl (1961). Regarding the Farasan Islands, the average concentrations generally did not differ between the FU and FL sediments. Table 3.1 shows FU average concentrations trended as: Zn > V > Ni > Cu > Cr > Pb > Cd. The average concentrations of Cd in both FU and FL and Zn in FU sediments surpassed their average threshold concentrations values by Turekian and Wedepohl (1961).

The average concentrations of Cr, Ni, Cu, Zn, and Pb of the Yanbu region (YU and YL) in the present study were lower than those in surficial mangrove sediments for the same region found by Alharbi et al. (2019) (Table 3.1). While the average concentrations of Cr (YL), Zn (YU and YL), and Pb (YU and YL) samples in this study were higher than those in mangrove sediments from Yanbu reported by Abohassan (2013) (Table 3.1). The average concentrations of all analytes of interest in the Jeddah sediments (JU and JL) from the current study were lower than those found by Al-Solaimani et al. (2022) for surface mangrove sediments from Jeddah as seen in Table 3.1.

Zn was the only element that was higher in JU and JL sediments than the one obtained by Al-Solaimani et al. (2022). Also, Table 3.1 shows the concentrations of Cr, Ni, Cu, and Cd of mangrove sediments from the Red Sea coast of Saudi Arabia found by Alzahrani et al. (2018) were higher than JU and JL samples with the exception of Pb concentration in JU sediments that was slightly greater than Alzaharani's. Mangrove sediments from the Farasan Islands collected by Usman et al. (2013) were found to have higher concentrations of Cr, Ni, Cu, Zn, Cd and Pb than those of Farasan Islands in the present study (Table 3.1). On the other hand, Table 3.1 illustrates that Zn, Cd, Pb of Farasan islands sediments (FU and FL) were higher in the current study than those presented by Abohassan (2013) for mangrove sediments from Shuaiba, Saudi Arabia, another southern Red Sea site. FU and FL Cu concentrations were lower than Abohassan's Cu concentration with a slight difference of approximately 0.5 mg/kg.

The SOM averages are as follows: YU 4.70%, YL 4.26%, JU 3.07%, JL 3.32%, FU 2.94%, and FL 2.90% as shown in Table 3.2. SOM % decreases from north to south in the study area as Yanbu has the highest SOM and the Farasan Islands has the lowest. Table 3.2 also indicates that carbonate % values throughout the study area are inversely related to SOM as it increases from north to south. The carbonate % values are as follows: YU 28.92%, YL 28.87%, JU 43.54%, JL 44.03%, FU 50.54%, and FL 49.48%. The results from Table 3.2 also show that upper and lower sediments for each region do not significantly differ in SOM % or carbonate %. The average of carbonate and SOM are notably elevated for the whole investigated area relative to those averages obtained by Alzahrani et al. (2018) for surface mangrove sediments along the Red Sea coast of Saudi Arabia (Table 3.2). Given this data, carbonates have been chosen as the sedimentary rock type reference for the study area as reported by Turekian and Wedepohl (1961).

The CF results show that Cu in both YU and YL sediments and Cr, Zn, Cd, and Pb in YL sediments are moderately contaminated (Table 3.3). Jeddah is moderately polluted with Cu in JU and JL and Zn in JU sediments. The Farasan Islands have Zn in the FU sediments and Cd in FU and FL sediments as moderately contaminated. All other CF values of the study area with respect to depth yield low polluted designations (CF values less than 1).

EF averages from Table 3.4 show that Cu is > 1.5 in YU, YL, JU, JL, and FL mangrove sediments for the study area. These results indicate that Cu mostly comes from anthropogenic sources for the region. Table 3.4 further shows that the EF_{Zn} averages suggest anthropogenic Zn sources to JU, JL, and FU sediments. Also, FU and FL sediments have received anthropogenic origins for Cd. All other elements across the study area concerning depth were likely to be generated from natural sources given their EF averages values were < 1.5 as Table 3.4 presents.

I_{geo} values from Table 3.4 show that all the sediments throughout the study area at all depths are uncontaminated except Cd in FU and FL sediments and Cu in YL samples that were rated uncontaminated to moderately polluted. Lastly, PLI averages reveal that YL sediments are the only polluted sediments, while the rest of the sediments of the study area with respect to depth were uncontaminated (Table 3.5).

This study illustrates the opposite by having lower HM concentrations and a higher carbonate content when compared to Alzahrani et al. (2018). The trend suggests that having low HM concentrations in sediments is associated with high carbonate content, as suggested by Pan et al. (2011). HM trends with depth are clear in both Jeddah and Farasan Islands mangrove sediments. Both show little variation in concentrations with depth except for Zn which was higher in the upper sediments of Jeddah and Farasan Islands (22.48 mg/kg, 22.21 mg/kg, respectively) than in lower sediments (17.03 mg/kg, 10.64 mg/kg, respectively) (Table 3.1). The elevated Zn concentrations

in upper sediments might be due to an increase of human activities releasing Zn to the environment which is supported by their EF values as anthropogenic (Table 3.4). The modest change in all other metal concentrations with depth for Jeddah and the Farasan Islands record a degree of homogeneity in the sediments. This affirms the findings of Badr et al. (2009) who found a narrow range of Ni (75 to 95 μg/g) in a core sediment from the Saudi Arabian Red Sea and suggested homogeneity. The temporally homogeneous inputs of the two southern regions are in stark contrast to Yanbu where YL values are almost twice the concentration relative to its upper sediments for most metals. The highest concentrations throughout the study area of V, Cr, Ni, Cu, Zn, and Pb were observed in YL sediments; further, PLI results from Table 3.5 show that YL are the only polluted sediments in the entire investigated area. Also, I_{geo} results indicate that YL sediments were classified as uncontaminated to moderately polluted by Cu (Table 3.4). As well as CF values show YL is moderately contaminated by Cr, Cu, Zn, Cd, and Pb. All analyses combined implies that Yanbu represents the most enriched site with HMs across the study area. While Jeddah and the Farasan Islands receive comparable loading of HMs and show similar risk indices to one another, they are not identical. I_{geo} results, for example, show the Farasan Islands sediments as the second highest contaminated area among the three regions. I_{geo} results classified the Farasan Islands sediments (FU and FL) as uncontaminated to moderately contaminated by Cd while values defined the Jeddah sediments (JU and JL) as uncontaminated.

PCA and bivariant analyses were used to investigate contamination sources (natural or anthropogenic) by showing statistical relationships between the variables. For Yanbu, CF, PLI, and average concentrations of HMs (Table 3.1, 3.3, and 3.5) show, in general, similar trends across depth where YU sediments are dominantly clean and YL sediments are more polluted. Also, PC1 for Yanbu has a loading of V, Cr, Ni, Cu, Zn, Cd, and Pb; all have positive and significant

correlations (≥ 0.54) despite variance in enrichment. Specifically, V and Ni have low CF values and did not exceed their preindustrial concentration average values (Table 3.1) across depths, thus, they mostly have been derived from only natural sources. Cr, Cu, and Zn are positively and significantly correlated with V and Ni (≥ 0.80 on PC1) and ($r \geq 0.62$, $P < 0.01$) for bivariant analysis (Table 3.7); however, the concentrations of Cr, Cu, and Zn surpassed their preindustrial concentrations (Table 3.1) and have high CF values compared to V and Ni in Yanbu sediments (Table 3.3). Combined, this implies that Cr, Cu, and Zn have anthropogenic contribution in addition to natural sources. This all suggests that PC1 of the Yanbu PCA from Table 3.6 may represent a combined anthropogenic and natural source. While this may seem unusual, it is very possible. Given PC1 is also loaded with silicate with a strong correlation (0.70), it is likely that all elements in Yanbu sediments were associated with silicate minerals when sequestered to Yanbu environment. Fine particulate silicates from natural weathering can scavenge metal cations in seawater via surface sorption. Therefore, PC1 acts as a natural source for many metals, given its matrix as a silicate weathering product, but also serves as a depositional conduit for anthropogenic elements that become enriched as sorbed species during marine transport. Cd and Pb have similar expression as Cr, Cu, and Zn where they have been derived from a natural source due to their correlations with V and Ni sources (≥ 0.54 on PC1) and ($r \geq 0.57$, $P < 0.05$) for bivariant analysis. Cd and Pb have also been delivered from anthropogenic sources since they both exceeded their background average concentration values and have CF values as high as Cr, Cu, and Zn. Cd and Pb, however, have a separate anthropogenic contribution via PC3 and since they are solely loaded on PC3 with significant correlations (0.48 and 0.58, respectively). PC3 also has a loading of 0.63 for SOM which indicates that Cd and Pb were likely complexed with organic matter when deposited to the Yanbu ecosystem in addition to silicates as PC1 indicates. PC2 has a loading of

only Cu, SOM, and carbonate with moderate to strong correlations (0.42, -0.68 and 0.73, respectively) which may conclude that Cu has bonded to carbonate when precipitated in addition to silicate as PC1 suggests. Figure 3.2 shows a scatterplot matrix with a fit line for the entire sample set, upper and lower, of V, Cr, Ni, Cu, and Zn from Yanbu sediments with respect to depth and Table 3.7 shows the associated correlations. Figure 3.2 further shows that the data of the YU and YL sediments are clustered in two separate groups, due to concentration variations, while still falling on a strong fit line ($r \geq 0.62$, $P < 0.01$). This agrees with the suggestion that PC1 represents both natural and anthropogenic sources since the trended fit line between those elements regardless the elevated concentrations of Cr, Cu, and Zn. Overall, the statistical analyses of Yanbu sediments show anthropogenic and natural sources for Cr, Cu, Zn, Cd, and Pb. The EF values of Yanbu show an anthropogenic source for only Cu with respect to depth. This might infer that Cr, Zn, Cd, and Pb are not enriched enough to be classified as anthropogenic by EF, however, they still have been partially delivered from an anthropogenic source and could become contaminants of concern in the future. The statistical analyses indicate an HM contamination status of Yanbu as expected given Yanbu is industrial and an urbanizing city.

PCA and bivariant analysis results from Tables 3.6 and 3.7, respectively reveal that Jeddah sediments are different from the other two regions due to the very high positive correlations between its variables and SOM and silicate (≥ 0.80 from PCA, and $r \geq 0.67$ with $P < 0.01$ from the bivariant analyses). Also, the only PC that showed an eigenvalue greater than 1.0 was PC1 (8.86) as seen in Table 3.6. The very high eigenvalue of PC1 and the very significant correlations between all the metals could imply that all the HMs and SOM were delivered to the sediments from the same source. This source is mostly likely a wastewater treatment discharge in south Jeddah due to the proximity of the Jeddah samples to this source. This affirms the findings of Alamri et al. (2021)

who suggested that the elevated metal concentrations in water samples from mangrove areas near Jeddah are likely due to sewage water discharge as their sample locations were close to the sample locations of this study. Dispersion and diffusion phenomena may be the reason for low concentrations in Jeddah sediments by mixing SOM associated HMs and clean sediment. PC1 and the bivariant analyses also show that the HMs in Jeddah samples are highly and negatively correlated with carbonate (-0.99 from PCA and $r > -0.72$ with $P < 0.01$ from the bivariant analyses) (Table 3.6 and 3.7) which suggest that they do not have affinity with carbonate.

For the Farasan Islands, the CF values of V, Cr, Ni, and Cu (Table 3.3) suggest clean sediments and having low concentrations based on their background concentration values (Table 3.1) as they are loaded on PC1. Thus, PC1 represents likely natural sources and accounts for these elements with significant correlations (≥ 0.74). Also, the bivariant analyses indicate similar significant and positive relations between these elements ($r \geq 0.61$, $P < 0.01$) (Table 3.7). PC1 also has a high loading of silicate with a strong correlation (0.93) which suggests that V, Cr, Ni, and Cu were adsorbed by silicate when released to the Farasan Islands ecosystem. PC2 shows positive and strong relations for only Zn, Cd, and SOM (0.73, 0.86, and 0.79, respectively). PC2 is suggested to represent an anthropogenic source for those two elements, as indicated by EF values of Cd and Zn (Table 3.4) and these elements have very weak correlations with other metals loaded on PC1 (natural sources). PC2 also suggests that Cd and Zn have associated to SOM when deposited in the Islands sediments. The bivariant analyses results (Table 3.7) agree with the PCA results by showing Cd and Zn are strongly and positively correlated with each other ($r = 0.65$, $P < 0.01$) and weakly related to the other elements. The statistical analyses agree with EF values for having Zn and Cd delivered from anthropogenic origins. However, they do not indicate Cu as anthropogenic as EF_{Cu} values suggest (Table 3.4) and this could imply that Cu has been delivered

to the sediments of the Farasan Islands by both natural and anthropogenic sources. PC3 of the Farasan Islands is loaded by only Zn and Pb with significant correlations (0.54 and 0.64, respectively). Zn in FL sediments has a low concentration compared to its preindustrial value and has low risk indices, as does Pb across depths. Therefore, PC3 is suggested to represent natural sources in Farasan Island sediments. Zn in Farasan Islands sediments has been delivered by two sources, anthropogenic (PC2) and natural (PC3). While Pb has been derived from two natural sources (PC1 and PC3). PCA and bivariant analysis results also illustrate that carbonate is disassociated with HMs of the Farasan Islands as seen in other locations (Table 3.6 and 3.7).

3.5 Conclusion

Overall, all the three investigated regions in this study have low HM concentrations when compared to other local and worldwide studies (Table 3.1). Notably, the Yanbu site shows higher exposure of HMs among the three locations due to its lower sediment's concentration status. The Yanbu environment receives anthropogenic stress besides natural sources from Cr, Cu, Zn, Cd and Pb. While V and Ni have been delivered from natural sources then have been complexed with the other anthropogenic elements by the silicate sediment fraction. The Farasan Islands region has anthropogenic Cd in its sediments. Cu and Zn in Farasan Islands sediments have natural and anthropogenic sources. The rest of the metals (V, Cr, Ni, and Pb) were likely solely introduced to the Islands environment from natural sources. For the Jeddah location, all HMs and SOM were mostly associated with an anthropogenic source (likely wastewater discharge). Jeddah is at environmental risk due to the anthropogenic source that controls the HMs distribution in its ecosystem. Further studies on mangrove sediments from Yanbu, Jeddah, and Farasan Islands are needed to provide a larger picture of the mangrove health along the Red Sea coast of Saudi Arabia given the number of studies on these regions is still limited. The Yanbu environment is under

industrial and human stress, therefore, continued monitoring of the currently mostly pristine mangrove sediments is recommended for future studies. Also, core mangrove sediments are encouraged for future studies since the concentration variation with respect to depth in this study shows an almost twofold difference. Jeddah is the location that has been controlled by one anthropogenic source, thus, further studies on mangrove sediments from Jeddah are needed to support the findings of this study and more directly identify the source. Core mangrove sediments from the Jeddah site are also suggested for further work to show time-resolved accumulative concentrations from the suggested dominant source. The Farasan Islands are known in the region as a clean area while this study shows that the Islands have anthropogenic inputs for Zn, Cu and Cd, thus, future studies on its mangrove sediments and plants are urged since the number of studies on Farasan Islands mangroves is very limited when compared to the northern part of the Saudi Arabian Red Sea. The overall findings and recommendations of the current work could provide decision makers with an updated picture of mangrove ecosystem health in the region permitting specific HM contamination status monitoring of areas of concern in the region. Finally, the research community could use this study as a baseline record given the limited number of studies on mangrove sediments from the Red Sea coast of Saudi Arabia especially for Jeddah and Farasan Islands sites.

Table 3.1 Average HM concentrations (mg/kg) and standard deviations from mangrove sediments in the present study compared to local and worldwide studies.

Sediment	V	Cr	Ni	Cu	Reference
YU	8.56 ± 1.99	5.13 ± 2.42	5.97 ± 1.85	**4.53** ± 1.71	Present Study
YL	16.27 ± 6.67	**21.99** ± 23.62	12.57 ± 7.00	**9.41** ± 4.98	
Yanbu Average	12.41	13.56	9.27	6.97	
JU	10.44 ± 6.49	4.85 ± 6.17	6.59 ± 5.27	**7.24** ± 9.04	
JL	10.1 ± 4.76	4.36 ± 4.13	5.57 ± 3.35	**7.3** ± 9.18	
Jeddah Average	10.27	4.6	6.08	7.27	
FU	8.89 ± 4.00	3.17 ± 2.48	7.06 ± 3.05	3.65 ± 1.95	
FL	8.88 ± 4.23	3.29 ± 3.27	6.15 ± 2.7	3.74 ± 1.94	
Farasan Average	8.89	3.23	6.61	3.7	
Saudi Arabian Red Sea					
Yanbu	−	86.7	64.7	48.1	Alharbi et al. (2019)
Yanbu	−	11.51	−	13.97	Abohassan (2013)
Shuaiba	−	8.75	−	4.13	Abohassan (2013)
Rabigh	−	20.62	8.69	16	Youssef & El-Sorogy (2016)
Farasan Islands	−	9.61	8.48	112	Usman et al. (2013)
Along the Red Sea	−	46.11	21.11	22.87	Alzahrani et al. (2018)
Jeddah		8.87	34.42	25.99	Al-Solaimani et al. (2022)
Worldwide					
Singapore, S buloh	−	16.61	7.44	7.06	Cuong et al. (2005)
Sungai Puloh, Malaysia	−	−	22.79-55.54	16.45-132.91	Udechukwu et al. (2014)
Punta Mala Bay, Panama	−	23.3	27.3	56.3	Defew et al. (2005)
World crustal average	20	11	20	4	Turekian and Wedepohl (1961)

Bold represents metals that exceeded their background averages by Turekian and Wedepohl (1961).

Table 3.1 (Continued)

Sediment	Zn	Cd	Pb	Reference
YU	14.28 ± 8.33	0.02 ± 0.02	6.66 ± 3.98	Present Study
YL	**26.41** ± 12.71	**0.05** ± 0.04	**10.06** ± 4.91	
Yanbu Average	20.34	0.04	8.36	
JU	**22.48** ± 24.73	0.02 ± 0.02	4.2 ± 6.53	
JL	17.03 ± 19.79	0.02 ± 0.02	3.6 ± 6.11	
Jeddah Average	19.76	0.02	3.9	
FU	**22.21** ± 26.58	**0.08** ± 0.07	2.65 ± 1.1	
FL	10.64 ± 4.66	**0.08** ± 0.08	4.73 ± 7.12	
Farasan Average	16.43	0.08	3.69	
Saudi Arabian Red Sea				
Yanbu	144.7	–	37.9	Alharbi et al. (2019)
Yanbu	13.52	0.2	3.84	Abohassan (2013)
Shuaiba	2.76	0.02	0.53	Abohassan (2013)
Rabigh	49.71	0.26	50.87	Youssef & El-Sorogy (2016)
Farasan Islands	57.2	1.23	45.2	Usman et al. (2013)
Along the Red Sea	–	0.75	3.82	Alzahrani et al. (2018)
Jeddah	16.41	0.25	5.74	Al-Solaimani et al. (2022)
Worldwide				
Singapore, S buloh	51.24	0.18	12.28	Cuong et al. (2005)
Sungai Puloh, Malaysia	291.96-2584.34	0.60-1.55	35.51-167.38	Udechukwu et al. (2014)
Punta Mala Bay, Panama	105	<10	78.2	Defew et al. (2005)
World crustal average	20	0.035	9	Turekian and Wedepohl (1961)

Bold represents metals that exceeded their background averages by Turekian and Wedepohl (1961).

Table 3.2 Chemical and Physical properties of the study area locations.

Sediment	SOM %	Carbonate %	Silicates %
YU	4.7	28.92	66.38
UL	4.26	28.87	66.88
JU	3.07	43.54	53.39
JL	3.32	44.03	52.65
FU	2.94	50.54	46.52
FL	2.90	49.48	47.62
Area Average	3.53	40.90	55.57

Table 3.3 Average Contamination Factors and standard deviations of sediments from study area locations.

Sediment	V	Cr	Ni	Cu	Zn	Cd	Pb
CF							
YU	0.43 ± 0.10	0.47 ± 0.22	0.3 ± 0.09	**1.13** ± 0.43	0.71 ± 0.42	0.71 ± 0.46	0.74 ± 2.15
YL	0.81 ± 0.33	**2.00** ± 2.15	0.63 ± 0.35	**2.35** ± 1.24	**1.32** ± 0.64	**1.44** ± 1.27	**1.12** ± 0.55
JU	0.52 ± 0.32	0.44 ± 0.56	0.33 ± 0.26	**1.81** ± 2.26	**1.12** ± 1.24	0.63 ± 0.57	0.47 ± 0.73
JL	0.50 ± 0.24	0.40 ± 0.38	0.28 ± 0.17	**1.83** ± 2.30	0.85 ± 0.99	0.65 ± 0.56	0.4 ± 0.68
FU	0.44 ± 0.20	0.29 ± 0.23	0.35 ± 0.15	0.91 ± 0.49	**1.11** ± 1.33	**2.2** ± 1.88	0.29 ± 0.12
FL	0.44 ± 0.21	0.30 ± 0.30	0.31 ± 0.14	0.94 ± 0.48	0.53 ± 0.23	**2.18** ± 2.15	0.53 ± 0.79

Bold indicates CF as moderately contaminated.

Table 3.4 Enrichment Factor and Geo-accumulation index averages and standard deviations of sediments from study region locations.

Sediment	V	Cr	Ni	Cu	Zn	Cd	Pb
EF							
YU	0.62 ± 0.18	0.68 ± 0.33	0.42 ± 0.12	**1.64** ± 0.69	1.01 ± 0.52	1.01 ± 0.57	1.03 ± 0.54
YL	0.62 ± 0.13	1.22 ± 0.58	0.46 ± 0.09	**1.82** ± 1.00	1.00 ± 0.35	1.11 ± 0.86	0.90 ± 0.51
JU	1.25 ± 0.35	0.81 ± 0.58	0.8 ± 0.66	**3.47** ± 0.98	**2.67** ± 3.29	1.29 ± 0.51	0.78 ± 0.31
JL	1.36 ± 0.47	0.95 ± 0.46	0.72 ± 0.25	**3.48** ± 1.09	1.67 ± 0.80	1.43 ± 0.60	0.64 ± 0.43
FU	0.72 ± 0.20	0.40 ± 0.13	0.78 ± 1.00	1.44 ± 0.43	**2.11** ± 1.92	**3.88** ± 2.48	0.64 ± 0.55
FL	0.73 ± 0.23	0.39 ± 0.15	0.50 ± 0.12	**1.59** ± 0.7	0.96 ± 0.56	**3.62** ± 2.38	0.82 ± 1.33
Igeo							
YU	-1.85 ± 0.39	-1.9 ± 0.95	-2.41 ± 0.54	-0.5 ± 0.58	-1.3 ± 0.88	-1.24 ± 0.64	-1.22 ± 0.78
YL	-0.98 ± 0.56	-0.12 ± 1.23	-1.41 ± 0.67	**0.48** ± 0.73	-0.32 ± 0.64	-0.38 ± 0.94	-0.61 ± 0.81
JU	-1.68 ± 0.63	-2.31 ± 1.14	-2.51 ± 0.96	-0.21 ± 1.01	-1.25 ± 1.69	-1.69 ± 1.19	-2.41 ± 1.25
JL	-1.68 ± 0.55	-2.24 ± 0.89	-2.59 ± 0.67	-0.29 ± 1.20	-1.47 ± 1.39	-1.68 ± 1.25	-2.86 ± 1.48
FU	-1.91 ± 0.75	-2.81 ± 1.25	-2.22 ± 0.66	-0.91 ± 0.83	-0.99 ± 1.20	**0.28** ± 0.82	-2.47 ± 0.66
FL	-1.89 ± 0.65	-2.82 ± 1.24	-2.41 ± 0.63	-0.83 ± 0.67	-1.63 ± 0.68	**0.19** ± 0.92	-2.71 ± 1.80

Bold shows anthropogenic sources by EF and uncontaminated to moderately polluted by I_{geo} values.

Table 3.5 Pollution load indices throughout the study area.

Sediment	PLI
YU	0.54 ± 0.16
YL	**1.11** ± 0.47
JU	0.63 ± 0.52
JL	0.58 ± 0.46
FU	0.61 ± 0.19
FL	0.58 ± 0.29

Bold represents PLI as polluted.

Table 3.6 Loading matrices, variances, and eigenvalues for major components from PCA for each region.

Variable	PC1	PC2	PC3
Yanbu			
V	0.93	0.25	-0.10
Cr	0.93	-0.02	-0.30
Ni	0.97	0.09	-0.05
Cu	0.80	0.42	0.02
Zn	0.86	0.12	-0.18
Cd	0.54	0.38	0.48
Pb	0.56	0.23	0.58
SOM %	0.20	-0.68	0.63
carbonate %	-0.67	0.73	0.04
Silicates %	0.70	-0.66	-0.19
Variance %	56.26	18.86	11.27
Eigenvalue	5.63	1.89	1.13
Jeddah			
V	0.98		
Cr	0.97		
Ni	0.80		
Cu	0.99		
Zn	0.89		
Cd	0.89		
Pb	0.99		
SOM %	0.93		
carbonate %	-0.99		
Silicates %	0.98		
Variance %	88.86		
Eigenvalue	8.86		

Table 3.6 (Continued)

Farasan Islands	PC1	PC2	PC3
V	0.92	-0.11	-0.14
Cr	0.97	-0.15	0.00
Ni	0.74	-0.08	0.28
Cu	0.90	-0.11	0.13
Zn	0.09	0.71	0.54
Cd	0.17	0.84	0.31
Pb	0.41	-0.46	0.64
SOM %	0.15	0.79	-0.30
carbonate %	-0.92	-0.19	0.29
Silicates %	0.93	0.11	-0.27
Variance %	51.04	21.62	11.56
Eigenvalue	5.1	2.16	1.16

. Table 3.7 Correlation matrices of the HMs, SOM, Carbonate, and Silicate in the investigated area.

Variable	V	Cr	Ni	Cu	Zn	Cd	Pb	SOM %	carbonate %	silicates %
Yanbu										
V	1.00									
Cr	0.92**	1.00								
Ni	0.94**	0.94**	1.00							
Cu	0.86**	0.73**	0.78**	1.00						
Zn	0.79**	0.79**	0.84**	0.62**	1.00					
Cd	0.54*	0.36	0.59**	0.43	0.49*	1.00				
Pb	0.48*	0.28	0.47*	0.67**	0.41	0.42	1.00			
SOM %	0.01	0.07	0.13	-0.11	-0.04	0.16	0.21	1.00		
carbonate %	-0.42	-0.62**	-0.57**	-0.24	-0.49*	-0.06	-0.22	-0.56**	1.00	
Silicates %	0.46*	0.67**	0.60**	0.30	0.55*	0.04	0.20	0.40	-0.98**	1.00
Jeddah										
V	1.00									
Cr	0.98**	1.00								
Ni	0.75**	0.75**	1.00							
Cu	0.97**	0.96**	0.74**	1.00						
Zn	0.83**	0.82**	0.78**	0.86**	1.00					
Cd	0.87**	0.84**	0.67**	0.87**	0.74**	1.00				
Pb	0.97**	0.97**	0.74**	0.99**	0.85**	0.85**	1.00			
SOM %	0.87**	0.85**	0.69**	0.93**	0.81**	0.84**	0.92**	1.00		
carbonate %	-0.96**	-0.96**	-0.73**	-0.98**	-0.87**	-0.86**	-0.98**	-0.94**	1.00	
silicates %	0.97**	0.97**	0.72**	0.97**	0.87**	0.85**	0.98**	0.89**	-0.99**	1.00

*Significant at $P < 0.05$
**Significant at $P < 0.01$

Table 3.7 (Continued)

Variable	V	Cr	Ni	Cu	Zn	Cd	Pb	SOM %	carbonate %	silicates %
Farasan Islands										
V	1.00									
Cr	0.93**	1.00								
Ni	0.61**	0.73**	1.00							
Cu	0.77**	0.88**	0.60**	1.00						
Zn	-0.05	0	0.13	0.07	1.00					
Cd	0.04	0.02	0.13	0.09	0.65**	1.00				
Pb	0.35	0.47*	0.36	0.53*	-0.05	-0.09	1.00			
SOM %	0.07	0.02	-0.06	0.04	0.31	0.56*	-0.32	1.00		
carbonate %	-0.85**	-0.86**	-0.55*	-0.77**	-0.09	-0.22	-0.1	-0.33	1.00	
silicates %	0.87**	0.88**	0.57**	0.79**	0.06	0.17	0.14	0.23	-0.99**	1.00

*Significant at $P < 0.05$
**Significant at $P < 0.01$

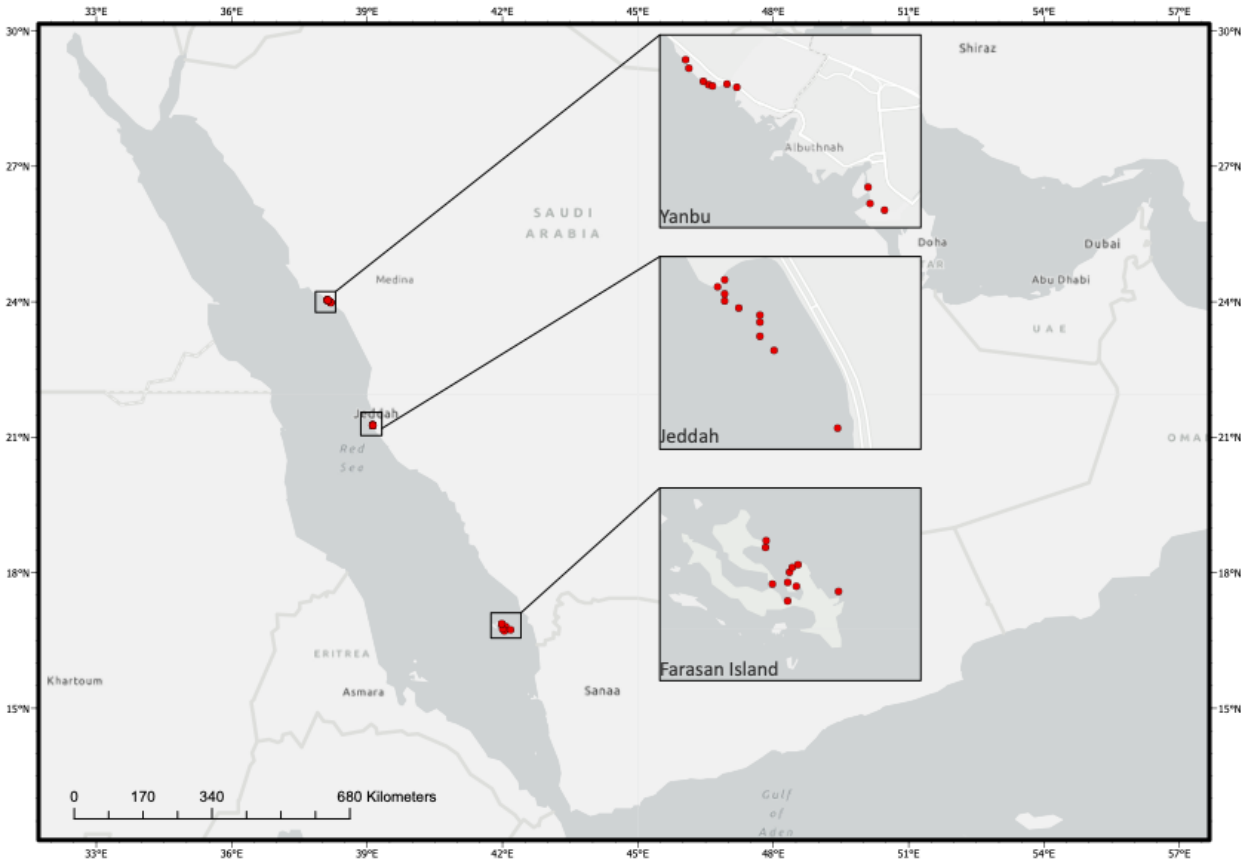

Figure 3.1 Map of the study area showing the three sampling locations: Yanbu to the north, Jeddah along the central coast, and the Farasan Islands to the south. Insets show detailed sampling stations at each of the regional locations.

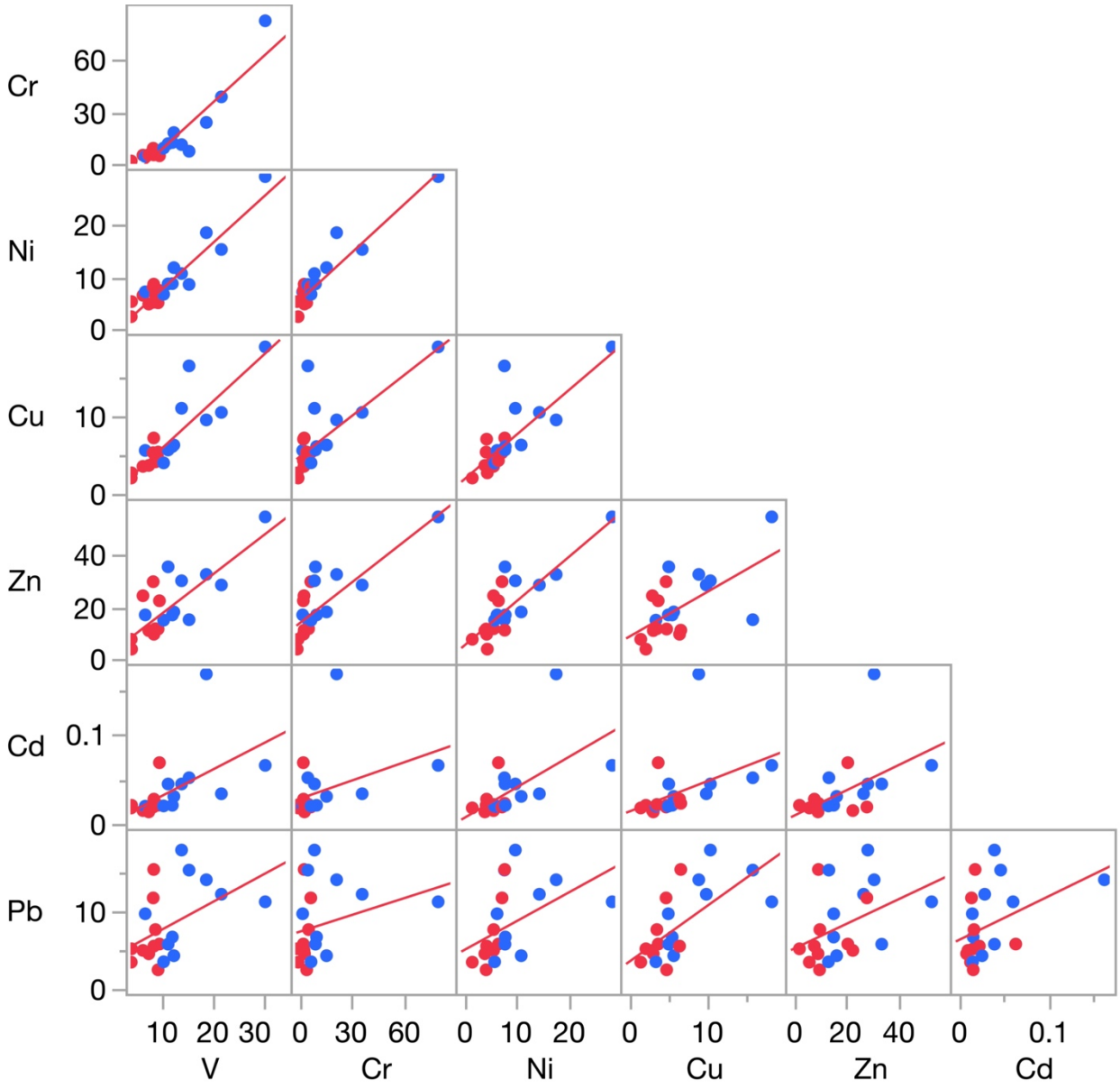

Figure 3.2 Scatterplot matrix for HM concentrations in Yanbu sediments with respect to depth. YU sediments are in red, and blue represents YL samples. The associated correlation coefficients are shown in Table 7. Red lines indicate the linear regression fit of the variables with all data with respect to depth.

3.6 References

Abohassan, R. A. (2013). Heavy metal pollution in Avicennia marina mangrove systems on the Red Sea coast of Saudi Arabia. JKAU: Meteorol. Environ. Arid Land Agric. Sci, 24(1), 35-53

Alamri, D. A., Al-Solaimani, S. G., Abohassan, R. A., Rinklebe, J., & Shaheen, S. M. (2021). Assessment of water contamination by potentially toxic elements in mangrove lagoons of the Red Sea, Saudi Arabia. Environmental geochemistry and health, 43(11), 4819-4830.

Alharbi, B. H., Pasha, M. J., & Al-Shamsi, M. A. S. (2019). Influence of different urban structures on metal contamination in two metropolitan cities. Scientific Reports, 9(1), 1-15.

Alharbi, O. M., Khattab, R. A., Ali, I., Binnaser, Y. S., & Aqeel, A. (2019). Assessment of heavy metals contamination in the sediments and mangroves (Avicennia marina) at Yanbu coast, Red Sea, Saudi Arabia. Marine Pollution Bulletin, 149, 110669.

Al-Mur, B. A., Quicksall, A. N., & Al-Ansari, A. M. A. (2017). Spatial and temporal distribution of heavy metals in coastal core sediments from the Red Sea, Saudi Arabia. Oceanologia, 59(3), 262–270.

Al-Solaimani, S. G., Abohassan, R. A., Alamri, D. A., Yang, X., Rinklebe, J., & Shaheen, S. M. (2022). Assessing the risk of toxic metals contamination and phytoremediation potential of mangrove in three coastal sites along the Red Sea. Marine Pollution Bulletin, 176, 113412.

Alzahrani, D. A., Selim, E. M. M., & El-Sherbiny, M. M. (2018). Ecological assessment of heavy metals in the grey mangrove (Avicennia marina) and associated sediments along the Red Sea coast of Saudi Arabia. Oceanologia, 60(4), 513–526.

Badr, N. B. E., El-Fiky, A. A., Mostafa, A. R., & Al-Mur, B. A. (2009). Metal pollution records in core sediments of some Red Sea coastal areas, Kingdom of Saudi Arabia. Environmental Monitoring and Assessment, 155(1–4), 509–526.

Bantan, R. A., & Abu-Zied, R. H. (2014). Sediment characteristics and molluscan fossils of the Farasan Islands shorelines, southern Red Sea, Saudi Arabia. Arabian Journal of Geosciences, 7(2), 773–787.

Bantan, R. A., Al-Dubai, T. A., & Al-Zubieri, A. G. (2020). Geo-environmental assessment of heavy metals in the bottom sediments of the Southern Corniche of Jeddah, Saudi Arabia. Marine pollution bulletin, 161, 111721.

Barbieri, M. J. J. G. G. (2016). The importance of enrichment factor (EF) and geoaccumulation index (Igeo) to evaluate the soil contamination. J Geol Geophys, 5(1), 1-4.

Blankespoor, B., Dasgupta, S., & Lange, G. M. (2017). Mangroves as a protection from storm surges in a changing climate. Ambio, 46(4), 478–491.

Cuong, D. T., Bayen, S., Wurl, O., Subramanian, K., Wong, K. K. S., Sivasothi, N., & Obbard, J. P. (2005). Heavy metal contamination in mangrove habitats of Singapore. *Marine Pollution Bulletin*, *50*(12), 1732-1738.

Defew, L. H., Mair, J. M., & Guzman, H. M. (2005). An assessment of metal contamination in mangrove sediments and leaves from Punta Mala Bay, Pacific Panama. Marine pollution bulletin, 50(5), 547-552.

Eid, E. M., Arshad, M., Shaltout, K. H., El-Sheikh, M. A., Alfarhan, A. H., Picó, Y., & Barcelo, D. (2019). Effect of the conversion of mangroves into shrimp farms on carbon stock in the sediment along the southern Red Sea coast, Saudi Arabia. Environmental research, 176, 108536.

ELTurk, M., Abdullah, R., Zakaria, R. M., & Bakar, N. K. A. (2019). Heavy metal contamination in mangrove sediments in Klang estuary, Malaysia: Implication of risk assessment. Estuarine, Coastal and Shelf Science, 226, 106266.

Hakanson, L. (1980). An ecological risk index for aquatic pollution control. A sedimentological approach. Water Research, 14(8), 975–1001.

Haris, H., & Aris, A. Z. (2013). The geoaccumulation index and enrichment factor of mercury in mangrove sediment of Port Klang, Selangor, Malaysia. Arabian Journal of Geosciences, 6(11), 4119–4128.

Heiri, O., Lotter, A. F., & Lemcke, G. (2001). Loss on ignition as a method for estimating organic and carbonate content in sediments: reproducibility and comparability of results. Journal of paleolimnology, 25, 101-110.

Hu, B., Wang, J., Jin, B., Li, Y., & Shi, Z. (2017). Assessment of the potential health risks of heavy metals in soils in a coastal industrial region of the Yangtze River Delta. Environmental Science and Pollution Research, 24(24), 19816–19826.

Khodami, S., Surif, M., Wan, W. M., & Daryanabard, R. (2017). Assessment of heavy metal pollution in surface sediments of the Bayan Lepas area, Penang, Malaysia. Marine Pollution Bulletin, 114(1), 615–622.

Kowalska, J. B., Mazurek, R., Gąsiorek, M., & Zaleski, T. (2018). Pollution indices as useful tools for the comprehensive evaluation of the degree of soil contamination–A review. Environmental geochemistry and health, 40, 2395-2420.

Miranda, L. S., Ayoko, G. A., Egodawatta, P., & Goonetilleke, A. (2022). Adsorption-desorption behavior of heavy metals in aquatic environments: Influence of sediment, water and metal ionic properties. Journal of hazardous materials, 421, 126743.

Müller, G. (1979). Schwermetalle in den Sedimenten des Rheins-Veränderungen seit 1971.

Natesan, U., Madan Kumar, M., & Deepthi, K. (2014). Mangrove sediments a sink for heavy metals? An assessment of Muthupet mangroves of Tamil Nadu, southeast coast of India. Environmental Earth Sciences, 72(4), 1255–1270.

Pavlopoulos, K., Koukousioura, O., Triantaphyllou, M., Vandarakis, D., Marion de Procé, S., Chondraki, V., Fouache, E., & Kapsimalis, V. (2018). Geomorphological changes in the coastal area of Farasan Al-Kabir Island (Saudi Arabia) since mid Holocene based on a multi-proxy approach. Quaternary International, 493, 198–211.

Sappa, G., Barbieri, M., & Andrei, F. (2020). Assessment of trace elements natural enrichment in topsoil by some Italian case studies. SN Applied Sciences, 2(8), 1409.

Tam, N. F. Y., & Wong, Y. S. (2000). Spatial variation of heavy metals in surface sediments of Hong Kong mangrove swamps. Environmental Pollution, 110(2), 195–205.

Tomlinson, D. L., Wilson, J. G., Harris, C. R., & Jeffrey, D. W. (1980). Problems in the assessment of heavy-metal levels in estuaries and the formation of a pollution index. Helgoländer meeresuntersuchungen, 33, 566-575.

Turekian, K. K., & Wedepohl, K. H. (1961). Distribution of the elements in some major units of the earth's crust. Geological society of America bulletin, 72(2), 175-192.

Udechukwu, B. E., Ismail, A., Zulkifli, S. Z., & Omar, H. (2015). Distribution, mobility, and pollution assessment of Cd, Cu, Ni, Pb, Zn, and Fe in intertidal surface sediments of Sg. Puloh mangrove estuary, Malaysia. Environmental Science and Pollution Research, 22, 4242-4255.

USEPA. 1996. Method 3050B of acid digestion of sediments, sludges, soils, rev. 2. Washington, DC:US Government Printing Office.

Usman, A. R. A., Alkredaa, R. S., & Al-Wabel, M. I. (2013). Heavy metal contamination in sediments and mangroves from the coast of Red Sea: Avicennia marina as potential metal bioaccumulator. Ecotoxicology and Environmental Safety, 97, 263–270.

Wang, Q., Li, Y., & Wang, Y. (2011). Optimizing the weight loss-on-ignition methodology to quantify organic and carbonate carbon of sediments from diverse sources. Environmental Monitoring and Assessment, 174(1–4), 241–257.

Yan, Z., Sun, X., Xu, Y., Zhang, Q., & Li, X. (2017). Accumulation and tolerance of mangroves to heavy metals: a review. Current pollution reports, 3, 302-317.

Yongming, H., Peixuan, D., Junji, C., & Posmentier, E. S. (2006). Multivariate analysis of heavy metal contamination in urban dusts of Xi'an, Central China. Science of the Total Environment, 355(1–3), 176–186.

Youssef, M., & El-Sorogy, A. (2016). Environmental assessment of heavy metal contamination in bottom sediments of Al-Kharrar lagoon, Rabigh, Red Sea, Saudi Arabia. Arabian Journal of Geosciences, 9, 1-10.

Zhang, C., Yu, Z. G., Zeng, G. M., Jiang, M., Yang, Z. Z., Cui, F., ... & Hu, L. (2014). Effects of sediment geochemical properties on heavy metal bioavailability. Environment international, 73, 270-281. Zhang, J., & Liu, C. L. (2002). Riverine composition and estuarine geochemistry of particulate metals in China - Weathering features, anthropogenic impact and chemical fluxes. Estuarine, Coastal and Shelf Science, 54(6), 1051–1070.

Zhang, J. Z., & Huang, X. L. (2011). Effect of temperature and salinity on phosphate sorption on marine sediments. Environmental science & technology, 45(16), 6831-6837.

CHAPTER 4

A META-ANALYSIS OF NEAR-SHORE SEDIMENTS HEAVY METALS FROM THE ARABIAN GULF BASIN

This chapter is to be submitted to Oceanologia.

Authors:

Abdullah S. Alnasser[1,2]

asalnasser@smu.edu, Orcid: 0000-0002-7198-3732

Andrew N. Quicksall[1]

aquicksall@smu.edu, Orcid: 0000-0002-4537-5952

[1]Department of Civil and Environmental Engineering, Southern Methodist University, Dallas, TX 75275, USA

[2]Department of Civil Engineering, College of Engineering, Qassim University, Unaizah, Saudi Arabia

4.1 Abstract

A meta-analysis (including statistical analysis and risk indices) was applied on heavy metal data that were collected from published work on near-shore surface sediments from the Arabian

Gulf basin. Various studies were carried out; however, no cross-work analysis was published. The collected dataset included 38 publications with near-shore surface sediments of 2086 samples from 106locations bordering the Gulf. The results showed that the Arabian Gulf basin is under high environmental pressure from heavy metal loadings of Cd, Co, Cr, Cu, Ni, Pb, Zn, Fe, V, and As. These metals have been delivered to the Gulf ecosystem from anthropogenic sources from the Gulf nations. Results also indicated that these elements have different degrees of contamination (based on risk indices) where Cd, Co, Cu, Pb, and As have the highest environmental impact. Cr, Ni, and Fe have lower environmental load on the sediments while Zn and V have the lowers environmental risk among the elements. The only element the has been derived from natural sources to the Gulf basin is Mn. According to the current environmental status of the Arabian Gulf, environmental management of the surrounding countries is highly urged to mitigate the current heavy metal contaminations. Also, the environmental regulators are recommended to legislate rules to limit the high release of heavy metals from human activities to the Gulf ecosystem.

4.2 Introduction

4.2.1 Coastal marine sediments

Heavy metal contamination in marine sediments is one of the most serious environmental problems facing the world community. Heavy metals enter marine systems from natural sources through soil erosion and atmospheric deposition and via anthropogenic activities (Almahasheer, 2019). Wastes from smelting ores, sewage sludge, industrial wastewater, and emission from traffic are examples of potential anthropogenic sources (Jahromi et al., 2021). Heavy metals cause a major negative effect on aquatic environments due to their toxicity and persistence in the environment (Almasoud et al., 2015; Delshabet al., 2017). Human health is at risk through the intake of polluted seafood since heavy metals typically bioaccumulate in coastal organisms (Jahromi et al., 2021).

When heavy metals are released into coastal systems, they typically bind to particulate matter and settle to marine sediments. These sediments act as a collection point for both direct solids delivery as well as associated aqueous delivery. Therefore, measuring metal content in sediments is an optimal approach to assess the pollution status of coastal marine areas broadly (Khodami et al., 2017; Mortazavi et al., 2022).

4.2.2 Contamination status of heavy metals in near-shore sediments of the Arabian Gulf

Various authors reported that cadmium is very severely to moderately enriched in sediments from KSA and Iran based on its Enrichment Factor (EF) values (Al-Hashim et al., 2021; Al-Kahtany et al., 2018; El-Sorogy et al., 2016; Jahromi et al., 2021). Also, it was suggested that Cd is moderately to heavily contaminant in samples from KSA, Iran, and Kuwait according to its Contamination Factor (CF) values (Alsamadany et al., 2020; A. S. El-Sorogy et al., 2016; Nour et al., 2022). Others have suggested that Cd is low concentrated in sediments from Iran according to its CF value and within the ranges of US Environmental Protection Agency standards (Samara et al., 2020; Sharifinia et al., 2022).

It was found that sediments from KSA and Iran were moderately to highly enriched with cobalt based on its EF values (El-Sorogy et al., 2016; Jahromi et al., 2021). On the other hand, Co was found to be a low contaminant in sediments from Iran according to its CF value (Vaezi et al., 2015). Also, Co shows little to no pollution in sediments from KSA according to Swedish Environmental Protection Agency (Youssef et al., 2015). Additionally, Co was found within natural background concentration levels in sediments from UAE (El Tokhi et al., 2015).

Different authors reported that chromium in sediments from KSA and Iran is moderately to highly enriched based on its EF values (Al-Hashim et al., 2021; Jahromi et al., 2021; Vaezi et al., 2015). Also, Cr was found to be a non-contaminant to a moderate contaminant in samples from

Iran based on its Geo-accumulation index (I_{geo}) value (Zarezadeh et al., 2017). Conversely, Cr was recorded as a pollutant in sediments from Bahrain due to its pollution index (PI) (Amin & Almahasheer, 2022). In contrast, Cr in sediments from KSA was found to have enrichment factor suggesting no environmental concern (Al-Kahtany et al., 2018b). Also, Cr in samples from UAE was below the UAE standard limits (Samara et al., 2016).

Several authors recorded that copper is low to very highly contaminated in sediments from KSA, Kuwait, and Iran based on its CF values (Alsamadany et al., 2020; Mortazavi et al., 2022; Nour et al., 2022). In addition, Cu was found as moderately enriched in samples from Iran due to its EF value (Vaezi et al., 2015). Conversely, Cu was suggested to be a non-pollutant in samples from Iran and UAE based on its I_{geo} values (Al Rashdi et al., 2015; Zarezadeh et al., 2017). Also, Cu in sediments from UAE was obtained within natural background concentration levels (El Tokhi et al., 2015).

Samples from KSA and Iran were moderately to severely enriched with lead as indicated by its EF values (Al-Hashim et al., 2021; El-Sorogy et al., 2016; Jahromi et al., 2021). Also, Pb in samples from KSA was recorded as a pollutant based on its PI (Amin & Almahasheer, 2022). Contrary, Pb in sediments from Iran was within a natural background level as it was recorded as a low contaminant according to its CF value (Sharifinia et al., 2022; Dadolahi et al., 2013).

It was reported that samples from KSA were severely enriched with vanadium based on its EF value (El-Sorogy et al., 2018). Also, it was higher in sediments from Iran than the V concentration range of the Regional Organization for the Protection of the Marine Environment Sea Area (Pourang et al., 2005). Based on I_{geo} values of sediments from Iran, the sediments were uncontaminated to moderately contaminated by V (Jafarabadi et al., 2017). While it was reported that V concentration in UAE samples was below UAE standard limits (Samara et al., 2016).

It was obtained that sediments from Iran were highly polluted by iron according to its I_{geo} value (Bibak et al., 2018). Also, sediments from KSA were reported as low contaminated by Fe based on its CF value (El-Sorogy et al., 2016). Fe in sediments from Kuwait was reported with lower concentration compared to other worldwide studies (Nour et al., 2022). Additionally, Fe concentrations in samples from UAE were lower than the Fe from natural background levels (El Tokhi et al., 2015).

Nickle was classified as a pollutant in samples from Iran according to its EF values (Delshab et al., 2017; Mehr et al., 2020). Also, Ni concentration in other sediments from Iran was high compared to the secondary standard of the United States EPA (Einollahipeer et al., 2013). Conversely, Ni was classified as a non-pollutant in sediments from Bahrain and KSA based on its PI value (Amin & Almahasheer, 2022). Additionally, Ni was categorized as a non-contaminant in sediments from UAE due to its I_{geo} values (Al Rashdi et al., 2015).

Zinc was reported as moderately enriched in sediments from KSA according to its EF values (Al-Hashim et al., 2021). Likewise, sediments from Iran were moderately to severely enriched in Zn according to EF values (Mehr et al., 2020). However, Zn in sediments from UAE was within the concentration limits of the US Environmental Protection Agency (Samara et al., 2020).

Arsenic in samples from Iran was severely enriched based on its EF values (Vaezi et al., 2015). Similarly, sediments from KSA were remarkably enriched with As according to its EF (Al-Hashim et al., 2021). In addition, sediments from UAE were uncontaminated to moderately contaminated by As as indicated by I_{geo} values (Al Rashdi et al., 2015). While As in sediments from KSA had low concentration according to its PI value (Alharbi et al., 2022).

Manganese concentration was described as elevated in sediments from KSA based on its CF values (Alshahri, 2017). Furthermore, samples from Iran were highly enriched by Mn due to its EF values (Jahromi et al., 2021). However, Mn concentration in sediments from Kuwait was low compared to other locations around the world (Nour et al., 2022). Also, Mn in samples from UAE was within the range of Dubai Municipality Limits (Samara et al., 2020).

4.2.3 Anthropogenic sources of heavy metals surrounding the Arabian Gulf

Various anthropogenic sources were reported from different countries bordering the Arabian Gulf. Oil spills and shipping activities have been routinely implicated as primary sources of metals contamination of near-shore sediments of the adjacent Gulf nations (Bibak et al., 2018; Einollahipeer et al., 2013; El-Sorogy et al., 2018; El-Sorogy et al., 2016; Jafarabadi et al., 2017; Shriadah, 1999). Similarly, different authors have stated that petrochemical industries polluted Gulf sediments (Al-Kahtany et al., 2018; Almasoud et al., 2015; Delshab et al., 2017; Metwally et al., 1997; Mortazavi et al., 2022; Pejman et al., 2017; Jafarabadi et al., 2017). Also, desalination plants are another set of known anthropogenic sources that have contaminated near-shore sediments of the Gulf (Alharbi et al., 2022; Alshahri, 2017; Bibak et al., 2018; Metwally et al., 1997; Mortazavi et al., 2022). It was further reported that sediments from Gulf nations were contaminated by various heavy industrial activities (Al Rashdi et al., 2015; El-Sorogy et al., 2016; Mehr et al., 2020; Samara et al., 2020; Youssef et al., 2015; Zarezadeh et al., 2017). Additionally, sewage and wastewater discharges from the Gulf countries impacted the Gulf coastal sediments (Monikh et al., 2013; Al-Kahtany et al., 2018b; Alsamadany et al., 2020; Nour et al., 2022; Seifi et al., 2019; Shriadah, 1999). Agricultural activities in KSA and Iran have added more environmental pressure on the Gulf environment (Almahasheer, 2019; Alsamadany et al., 2020; Jahromi et al., 2021; Jafarabadi et al., 2017; Zarezadeh et al., 2017). Finally, fishing activities in

countries surrounding the Gulf have contributed to heavy metal loadings in the Gulf near-shore sediments (Al-Hashim et al., 2021; A. El-Sorogy et al., 2018; Pejman et al., 2017; Rezaei et al., 2021; Samara et al., 2016; Youssef et al., 2015).

4.2.4 Aims of the current work

There are various studies on near-shore sediments from the marine environment of the Arabian Gulf with little to no cross-work cohesion. There is a lack of analysis across the Gulf region and no work synthesizing the heavy metal loadings in the near-shore sediments across the Gulf. A meta-analysis is used to comprehensively synthesize a large dataset that has been compiled from different sources (Niu et al., 2020). While metal-analyses were first applied in medical research, recently such techniques been applied to environmental contamination data to achieve broader conclusions(Niu et al., 2020; Yuan et al., 2021). The aims of this work are to analyze the heavy metal loadings in near-shore sediments from the Arabian Gulf basin, to contrast the contamination levels between sub-regions, and to specify contamination sources where possible.

4.3 Methods and material

4.3.1 Data collection and processing

Google scholar, semantic scholar, and worldcat databases were used to compile currently published data into the dataset for this work. Restrictions have been set to define the collected dataset: only publications using one or more heavy acid for digestions were included, all data used is of heavy metal concentrations from near-shore surface sediments of countries surrounding the Arabian Gulf, and publications that presented their concentrations as ranges were excluded. To be clear, other studies that analyzed heavy metals in different samples other than surficial near-shore sediments, such as core sediments, sand samples, and mangrove plants were excluded from the analysis. A total number of 38 studies with sample size of 2086 from 106 locations bordering the Arabian Gulf were included (Figure 1). A meta-analysis was applied on the collected dataset of

heavy metal concentrations (mg/kg) for Cd, Co, Cr, Cu, Mn, Ni, Pb, Zn, Fe, V, and As. For regional comparison purposes, the Gulf area was split into three regions: the Kingdom of Saudi Arabia (KSA), Bahrain, Kuwait, and Qatar labeled as Region 1, generally the south and west of the basin, Iran labeled as Region 2, the north of the basin, and United Arab Emirates (UAE) identified as Region 3, the western portion of the basin.

4.3.2 Study Area

The Gulf is a subtropical area given its location just north of the Tropic of Cancer. Its marine environment has challenging conditions for biological growth given its high temperature and salinity, thus, the diversity of species is low compared to other locations worldwide (Almahasheer 2018; Lavieren et al., 2011). There are eight countries surrounding the Gulf: Iran, Iraq, Saudi Arabia (KSA), Qatar, Kuwait, Bahrain, United Arab Emirates (UAE), and Oman. These countries have a yearly population growth rate of 2.1% which is almost double the world average of 1.1 % (Almahasheer, 2018). The Gulf is a shallow basin with an average depth of 25 m as it is a semi closed water body that is only connected to the Indian Ocean via the strait of Hormuz (Alshemmari & Talebi, 2019). The water temperature ranges from 12 °C to 35 °C while its intertidal areas can experience extreme surface temperatures of 50 °C and higher (Almahasheer, 2018). The dry climate of the Gulf causes high evaporation which leads to high salinity. The southern portions of the Gulf regularly reaches 43 psu compared to a regular oceanic salinity of 37 psu (Lavieren et al., 2011).

4.3.3 Statistical analyses

Principle component analysis (PCA), bivariant analyses, analysis of variance (ANOVA), and Tukey's honesty significant difference test (Tukey's HSD) were applied to the collected dataset to determine the correlations between the heavy metals of interest across the basin and by

sub-region. SAS JMP 15.1.0 was employed for statistical investigations. Quantile range outliers' method was applied on the entire dataset to determine the outlier studies following that any study showed three or more elements with outlier concentrations eliminated from the meta-analysis. Lastly, weighted concentration averages were calculated for the analysis including concentrations, risk indices, and the statistical analysis. The restricted maximum likelihood method was chosen for PCA as an estimation method due to missing individual data from literature. For PCA and bivariant analysis, correlations ≥ 0.70 are suggested to be defined as strong while from 0.50 to < 0.70 would be considered as moderate correlations and less than 0.50 are as weak correlations. Post-analysis, principal components with eigenvalues > 1 were chosen.

4.3.4 Heavy metal pollution assessment

To evaluate the contamination degree level of heavy metals in sediments collected from literature, CF, I_{geo}, and pollution load index (PLI) were calculated for each region separately. These indices have been widely used in previous studies for pollution level evaluation (O. M. L. Alharbi et al., 2019b; Al-Mur et al., 2017a; Al-Solaimani et al., 2022; Gopalakrishnan et al., 2020; Gujre et al., 2021; Rezaei et al., 2021; Usman et al., 2013). CF is the measured concentration of a certain element divided by the same element concentration in background sediments (Varol, 2011). CF values were calculated using equation (4.1) by Hakanson (1980):

$$\mathrm{CF} = \frac{\mathrm{C_{Dataset\ sediment}}}{\mathrm{C_{Background\ sediment}}} \tag{4.1}$$

where, $C_{dataset\ sediment}$ is the concentration of an element from the current dataset. $C_{background}$ is the background concentration of the same element reported by Turekian and Wedepohl (1961). The CF value classifications were suggested by Hakanson (1980) as following: $C_F < 1$ is considered low contamination, $1 < C_F < 3$ is moderate contamination, $3 < C_F < 6$ indicates considerable contamination, and $C_F > 6$ is very high contamination.

I_{geo} is used to evaluate an element pollution in sediments by comparing its concentration with its preindustrial concentration (Bantan et al., 2020b). I_{geo} was calculated using equation (4.2) by Müller (1979):

$$I_{geo} = \log_2 \left(\frac{C_{Dataset\ sediment}}{1.5 \times C_{Background\ sediment}} \right) \quad (4.2)$$

where, $C_{Dataset\ sediments}$ is the concentration of an element in the dataset sediment, $C_{Background\ sediment}$ is the background concentration value of the same element provided by Turekian and Wedepohl (1961). 1.5 is an experimentally derived correction factor for natural processes that impact background values. There are seven categories of defining I_{geo} that were reported by Müller, (1981): $I_{geo} < 0$ implies uncontaminated, $0 < I_{geo} < 1$ implies uncontaminated to moderately contaminated, $1 < I_{geo} < 2$ implies moderately contaminated, $2 < I_{geo} <$ implies moderately to highly contaminated, $3 < I_{geo} < 4$ implies highly contaminated, $4 < I_{geo} < 5$ highly to extremely contaminated, and $I_{geo} > 5$ implies extremely contaminated.

EF is used to differentiate the anthropogenic from natural impacts of the heavy metals in sediments. It normalizes measured heavy metals concentrations to natural background concentrations values by. Al and Fe are elements typically used in this approach as normalization elements (Abrahim & Parker, 2008; Zarezadeh et al., 2017) and, here, Fe was used. EF values were calculated using equation (4.3):

$$EF = \frac{\left(\frac{C_i}{C_{Fe}}\right)_{Dataset\ sediment}}{\left(\frac{C_i}{C_{Fe}}\right)_{Background\ sediment}} \quad (4.3)$$

Where, $C_{i,\ Dataset\ sediments}$ is the concentration of a metal from the collected dataset, $C_{Fe,\ Dataset\ sediment}$ is the concentration of Fe from the collected dataset. $C_{i,\ Background\ sediments}$ is the preindustrial background concentration value reported by Turekian and Wedepohl (1961), $C_{Fe,\ background\ sediments}$ is the concentration of Fe from the natural background value. When $0.5 \leq EF \leq 1.5$, it suggests a

natural source, while EF indicates a significant amount of an element was delivered from anthropogenic sources if the EF > 1.5 (J. Zhang & Liu, 2002).

PLI was employed to evaluate the total heavy metal pollution level and was calculated by using equation (4.4) (Tomlinson et al., 1980):

$$PLI = (C_{F1} \times C_{F2} \times C_{F3} \times C_{Fn})^{\left(\frac{1}{n}\right)} \quad (4.4)$$

where, C_{Fi} is the CF of an element in the dataset sediments and n is the number of CFs in the dataset samples of a region of interest. A PLI < 1 indicates no pollution while a PLI > 1 suggests pollution is present.

4.4 Results and discussion

4.4.1 Heavy metal trends

Based on the quantile range outliers' method (SAS JMP 15.1.0), two studies (Almahasheer, 2019; Alshahri, 2017) including 113 sediment samples from 3 sites in Region 1 were omitted from the entire analysis. The weighted averages of heavy metal concentrations (mg/kg) for Region 1 trended as Fe > V > Mn > Cu > As > Cr > Ni > Zn > Pb > Co > Cd (Table 4.1). For Region 2, the trend was as follows: Fe > Mn > Zn > Cr > Ni > V > Pb > Cu > Co > As > Cd. For Region 3, the weighted averages of heavy metal concentrations followed this order: Fe > Mn > Ni > Pb > Cr > V > Zn > Cu > Co > Cd > As. Table 4.1 also shows that all the metals exceeded their preindustrial background concentrations for Region 1 and 2, except for Mn. Meanwhile, Region 3 has only Mn, Zn, and V not exceeding their background concentrations. Among the three regions, Region 1 has the highest concentrations for Cu, V, and As while Region 2 has the highest concentrations for Cr, Mn, Ni, Pb, Zn, and Fe and Cd and Co have the highest concentrations in Region 3 (Table 4.1). Table 4.2 shows the risk indices results indicating that the PLI of Region 2 has the highest value across all regions (4.85) where the PLI of Region 1 comes after with a value of 3.90, and the lowest

PLI value is for Region 3 (2.23). The concentrations of Cr, Mn, Ni, Pb, Zn, and Fe and PLI value are the highest in Region 2 sediments compared to the other two regions, thus, it can be said that region 2 is the most contaminated area across the Arabian Gulf. Region 1 comes as the second most polluted area whereas Region 3 is the least polluted area recorded.

Table 4.2 also shows the results of CF, I_{geo}, and EF for each region. For Region 1, Cd, Co, Cr, Cu, Ni, Pb V, and As were classified as moderate to very high contaminants based on their CF values. Also, their I_{geo} values indicated that they are non-contaminants to extreme contaminants. In addition, these metals were described as anthropogenic as indicated by their EF values. The Ni EF value (1.43) is a slightly below the anthropogenic threshold value (>1.5). This is likely due to the concentration of Fe in Region 1 slightly exceeding its preindustrial background value which impacted the results of EF as Fe was used as a normalizing element in EF calculations (equation 4.3). Zn has been interpreted by its CF as moderate pollutant while its I_{geo} and EF values suggested it as uncontaminated and natural. Similarly, Fe in the same region is a moderate contaminant based on its CF and it is uncontaminated according to its I_{geo}. Mn is a non-pollutant and has a natural delivery to the sediments as suggested by CF, CF, I_{geo}, and EF.

For Region 2, Cd and Co have the highest risk indices values in the region compared to the other metals. The CF, I_{geo}, and EF values of Cd and Co indicate that these two elements are pollutants, high contaminants, and have been delivered to the Region 2 ecosystem from anthropogenic sources, respectively (Table 4.2). Cr comes after Cd and Co in terms of pollution level where it is a very high pollutant as indicated by CF, a moderate to a high contaminant as I_{geo} shows, and EF suggests it is anthropogenic. Cu, Ni, Pb, Zn, Fe, and As are moderate to considerable pollutants, moderate contaminants, and anthropogenic based on their CF, I_{geo}, and EF values, respectively. EF values of some of these elements are below the 1.5 anthropogenic

threshold of EF according to the very high concentration of Fe in Region 2 sediments (Table 4.1) which greatly exceeded its natural background value and, therefore, skewed the EF values. However, if the Fe concentration was close to its background value, the EF of Cu, Ni, Pb, Zn, and As would be greater than 1.5 implying anthropogenic sources. V has a lower degree of contamination compared to other analytes, except for Mn. Risk indices results showed that V is a moderate pollutant, a non-contaminant to a moderate contaminate, and natural based on CF, I_{geo}, and EF, respectively. Region 2 sediments are low contaminated and not polluted by Mn as indicated by CF and I_{geo}, respectively. Further, Mn was likely naturally delivered to the sediments according to EF results (Table 4.2).

For Region 3, risk indices results from Table 4.2 suggested that the sediments are very highly contaminated, extremely contaminated, and have anthropogenic sources by Cd and Co as suggested by CF, I_{geo}, and EF, respectively. Also, the sediments are contaminated by Cu, Pb, and As, however, with a lower degree of contamination compared to Cd and Co. Cu, Pb, and As were classified as moderate pollutants by CF, non-contaminants to moderate contaminants by I_{geo}, and have entered the Region 3 marine system by anthropogenic sources as EF values suggested. Cr, Ni, and Fe show lower risk indices than Cu, Pb, and As where they are only classified as moderate pollutants based on their CF value. Cr, Ni, and Zn I_{geo} and EF values suggest that they are non-contaminants and have a natural delivery to the ecosystems. The elements that have the lowest risk indices in Region 3 are Mn and V since they are classified as low contaminants, not pollutants, and naturally delivered to the sediments, as indicated by CF, I_{geo}, and EF results, respectively.

4.4.2 Heavy metals sourcing

PCA, bivariant analyses, and ANOVA statistical techniques were applied to each region of this work to determine the sources of heavy metals (anthropogenic or natural). The elemental

correlations were investigated across the Arabian Gulf basin and by sub-regions. For Region 1, PC1 has loading of Cd, Co, Cr, Cu, Mn, Zn, Fe, and V with high correlations (≥ 0.74). Mn is a non-pollutant, and all the other metals are pollutants with different levels of contamination according to the risk indices results (Table 4.2). Thus, PC1 mostly represents combined anthropogenic and natural sources. PC1 also suggests that Cd, Co, Cr, Cu, Mn, Zn, Fe, and V of Region 1 have bonded to Mn and Fe when sequestered to the sediments since Mn and Fe (hydr)oxides can act as ligands in sediment composition. The bivariant analysis show that most of the metals are moderately to strongly correlated with Mn and Fe ($r \geq 0.51$, $P < 0.01$) which supports the PCA suggesting Mn and Fe (hydr)oxides function as sequestering ligands for metals in the sediments (Table 4.4). PC2 is loaded by only Ni, Pb, and As with significant correlations (≥ 0.94). All three of these elements are classified by their risk indices (Table 4.2) as contaminants with different levels of contamination and have been anthropogenically delivered to the region's environment. Hence, PC2 is suggested to represent anthropogenic sources. The bivariant analysis results indicated that Ni is strongly correlated with Pb and As ($r \geq 0.72$, $P < 0.01$) (Table 4.4). The very high correlations of Ni with Pb and As suggested from PCA and the bivariant analysis besides their high risk indices could imply that these metals have been delivered to the marine system from anthropogenic sources.

For Region 2, PC1 is dominated by Cd, Cr, Cu, Ni, and Zn with strong correlations (≥ 0.70) and with moderate correlation for V (0.58) (Table 4.3). The bivariant results also showed most of these elements are highly correlated with each other ($r \geq 0.85$, $P < 0.01$) (Table 4.4). All these metals are pollutants, as indicated by their risk indices (Table 4.2). Hence, PC1 likely represents anthropogenic sources in Region 2. PC2 has a high loading of Co and Mn with correlations of 0.83 and 0.78, respectively. PC2 is also loaded with Pb and V with moderate correlations (0.56 and

0.61, respectively). Mn is a non-contaminant while Co, Pb, and V are pollutants with different levels of contamination based on their risk indices, therefore, PC2 might represent natural and anthropogenic sources of Region 2. PC3 has a loading of Fe with significant correlation (0.90) and a loading of Cd with a moderate correlation (0.67). The risk indices results suggested that Fe and Cd are contaminants, Consequently, PC3 likely represents anthropogenic delivery. In general, the bivariant analysis and PCA (Table 4.3 and 4.4) have a similar trend where Mn has strong correlations with other metals while Fe has weak correlations with other elements. This might suggest the elements have bonded to Mn and Fe (hydr)oxides when precipitated on sediments. The weak correlation between Fe and the other elements could be due to the anthropogenic inputs of Fe.

For Region 3, PC1 is dominated by all metals with high correlations (≥ 0.75), except for Cr and Cu (Table 4.3). The bivariant analyses (Table 4.4) show similar trends as in PCA where most of the heavy metals are highly correlated with each other ($r \geq 0.71$, $P < 0.05$). The metals loaded on PC1 are proposed by the risk indices results (Table 4.2) as pollutants and non-pollutants, hence, PC1 mostly represents combined anthropogenic and natural delivery of the heavy metals to the region. Additionally, PC1 and the bivariant analysis indicate that heavy metals in Region 3 behaved the same way as in Region 1 where Fe and Mn have scavenged the heavy metals when released to the marine system. PC2 is only loaded by Cu with high correlation (0.87) indicating that PC2 represents an anthropogenic source for the region since Cu is noted as a pollutant based on the risk indices. Cu is solely loaded on PC2 with weak correlations to other metals; the bivariant analysis results also showed that the weakest correlations, in general, between the heavy metals across the correlation matrix of Region 2 (Table 4.4) are associated with Cu. This all may suggest that Cu might have been delivered to Region 3 by a singular anthropogenic source. PC3 is

dominated by only Pb with a weak correlation (0.43). Pb is a pollutant and has entered the marine system of Region 2 from anthropogenic sources according to its risk indices (Table 4.2). Thus, PC3 may indicate that Pb has a singular anthropogenic component. However, PC3 accounts for a variance of only 9%, thus, PC3 in Region 3 can be ignored for substantive interpretation.

ANOVA was applied on the heavy metal concentrations of each region to show the statistical differences of each element by region. To achieve this purpose, Tukey's HSD was applied on ANOVA results as a follow-up statistical test. Tukey's HSD results from Table 4.5 and 4.6 indicated that the only elements that are statistically different among the three sub-regions are Cd, Co, Mn, and Fe (Figure 4.1). While the rest of the elements did not reject the null hypothesis where their sub-regional means do not show any statistical differences. Tukey's HSD results showed that Cd in Region 3 is significantly different from Region 1 and 2 which is in agreement with Table 4.1 that shows Cd has the highest concentration in Region 3. Similarly, table 4.1 shows that Mn has notably elevated concentration in Region 2 sediments compared to Mn in the other two regions. Tukey's HSD results support Table 4.1 results indicating that Mn in Region 2 is significantly different from the Mn in the other two regions. Co concentration is the highest in Region 3 sediments (Table 4.1). Tukey's HSD results indicated that Co of Region 3 is significantly different from the Co of Region 1. While Tukey's HSD results also show that there is no statistical difference between Co of Region 3 and Region 2, mostly, due to that both regions have comparable concentrations of Co (8.83 mg/kg for Region 3 and 8.05 mg/kg for Region 2). Likewise, Fe concentration is the highest in Region 2 as Tukey's HSD results show that Fe in region 2 is significantly different from Fe in Region 1, however, it is statistically equal to Fe in Region 3.

4.5 Conclusion

The Arabian Gulf area contamination status was investigated by via a meta-analysis of Cd, Co, Cr, Cu, Mn, Ni, Pb, Zn, Fe, V, and As concentrations in near-shore surficial sediments provided by published work from countries bordering The Arabian Gulf. The Gulf environment suffers from high environmental pressure from Cd, Co, Cu, Pb, and As since these elements surpassed their preindustrial concentration values (Table 4.1) in addition to their moderate to very high risk indices (Table 4.2) across all the three regions. As a result, it can be concluded that the Gulf is at serious environmental risk from the release of these elements into its marine system from the surrounding countries. The risk indices also show that Cr, Ni, and Fe across the Gulf sub-regions have lower contamination level compared to Cd, Co, Cu, Pb, and As. However, they still put the Gulf environment under further contamination pressure in addition to Cd, Co, Cu, Pb, and As. Zn and V cause less concern compared to the other metals as these two elements are non-pollutants in Region 3 while they are in the other two regions. The only metal that has no risk is Mn where it shows low concentrations and low risk indices throughout the three regions of the marine system. PLI values of the three regions suggested that all regions of the Arabian Gulf area are polluted. In general, the environmental pollution status of the Gulf is a high concern, as was expected, due to the heavy and historical oil and gas extraction and transportation as well as other anthropogenic pressures. During the search and investigations through the current work, it was noticed that the number of publications for core sediments is relatively low compared to surficial sediments. Therefore, future work is urged to analyze heavy metals in core samples from different sites around the Gulf showing temporal resolution for contamination. Also, monitoring and remediation to mitigate the current pollution status of heavy metals are highly recommended before further exacerbation. This work provides an updated record for the current spatial

distribution of Cd, Co, Cr, Cu, Mn, Ni, Pb, Zn, Fe, V, and As in the Gulf marine system to the decision makers in environmental pollution management of each country surrounding the Arabian Gulf area.

Table 4.1 The weighted average of the heavy metal concentrations in mg/kg, standard deviation, maximum, minimum, and the background concentration values for each region in the study area. Background values were suggested by Turekian and Wedepohl (1961).

Area	Statistics	Cd	Co	Cr	Cu	Mn	Ni	Pb	Zn	Fe	V	As
	Background values	0.035	0.10	11.00	4.00	1100.00	20.00	9.00	20.00	3800.00	20.00	1.00
Region 1	Weighted average	0.82	0.97	32.73	54.07	82.89	31.21	23.47	23.49	4143.69	389.49	46.08
	SD	0.05	0.07	1.58	3.11	3.45	1.85	1.60	1.15	168.62	59.09	5.68
	Max	0.32	0.21	8.33	17.10	13.42	10.69	8.51	4.84	582.88	170.41	18.56
	Min	0.00	0.00	0.00	0.00	0.01	0.00	0.00	0.00	0.81	0.03	0.00
Region 2	Weighted averages	1.57	8.05	75.61	20.89	207.77	67.41	32.48	76.12	13411.97	33.21	5.26
	SD	0.15	0.44	7.90	1.43	30.31	4.35	2.81	6.16	1530.39	5.60	0.46
	Max	0.74	1.15	29.30	7.28	81.23	22.65	12.74	28.28	6673.25	23.52	1.43
	Min	0.00	0.00	0.01	0.00	0.13	0.01	0.00	0.02	0.00	0.00	0.03
Region 3	Weighted averages	3.92	8.83	15.08	8.57	71.70	23.51	23.23	10.54	4379.22	13.70	2.88
	SD	0.34	0.71	0.77	0.59	4.25	1.48	2.22	0.61	530.76	2.14	0.55
	Max	1.25	2.77	2.84	2.11	13.73	4.37	9.05	2.26	1423.56	6.42	1.72
	Min	0.00	0.00	0.05	0.00	0.08	0.00	0.00	0.05	16.81	0.13	0.01

Table 4.2 CF, I_{geo}, EF, and PLI values for each region across the Arabian Gulf. **Bold** indicates that heavy metals exceeded their risk indices thresholds suggesting a contamination level.

Area	Risk index	Cd	Co	Cr	Cu	Mn	Ni	Pb	Zn	Fe	V	As
Region 1	CF	**23.36**	**9.65**	**2.98**	**13.52**	0.08	**1.56**	**2.61**	**1.17**	**1.09**	**19.47**	**46.08**
	I_{geo}	**3.96**	**2.69**	**0.99**	**3.17**	-4.32	**0.06**	**0.80**	-0.35	-0.46	**3.70**	**4.94**
	EF	**21.42**	**8.85**	**2.73**	**12.40**	0.07	**1.43**	**2.39**	1.08	1.00	**17.86**	**42.26**
	PLI	**3.90**										
Region 2	CF	**44.91**	**80.46**	**6.87**	**5.22**	0.19	**3.37**	**3.61**	**3.81**	**3.53**	**1.66**	**5.26**
	I_{geo}	**4.90**	**5.75**	**2.20**	**1.80**	-2.99	**1.17**	**1.27**	**1.34**	**1.23**	**0.15**	**1.81**
	EF	**12.72**	**22.80**	**1.95**	1.48	0.05	0.95	1.02	1.08	1.00	0.47	**1.49**
	PLI	**4.85**										
Region 3	CF	**111.96**	**88.25**	**1.37**	**2.14**	0.07	**1.18**	**2.58**	0.53	**1.15**	0.69	**2.88**
	I_{geo}	**6.22**	**5.88**	-0.13	**0.51**	-4.52	-0.35	**0.78**	-1.51	-0.38	-1.13	**0.94**
	EF	**97.15**	**76.58**	1.19	**1.86**	0.06	1.02	**2.24**	0.46	1.00	0.59	**2.49**
	PLI	**2.23**										

Table 4.3 Loading matrices, variances, and eigenvalues for major components from PCA for all the three regions.

Area	Element	PC1	PC2	PC3
Region 1	Cd	0.92	-0.25	
	Co	0.74	-0.25	
	Cr	0.98	-0.10	
	Cu	0.74	-0.22	
	Mn	0.87	0.16	
	Ni	0.22	0.94	
	Pb	-0.06	0.98	
	Zn	0.97	-0.04	
	Fe	0.88	0.12	
	V	0.87	0.38	
	As	-0.01	0.98	
	Variance %	56.30	29.01	
	Eigenvalue	6.20	3.19	
Region 2	Cd	0.70	-0.05	0.67
	Co	-0.51	0.83	-0.18
	Cr	0.98	0.13	-0.17
	Cu	0.95	0.20	-0.17
	Mn	-0.52	0.78	-0.29
	Ni	0.96	0.20	-0.14
	Pb	0.61	0.59	0.47
	Zn	0.98	0.15	-0.03
	Fe	-0.26	0.35	0.90
	V	0.58	0.61	-0.26
	As	-0.87	0.46	0.15
	Variance %	57.25	22.48	16.03
	Eigenvalue	6.30	2.47	1.76

Table 4.3 (Continued).

Area	Element	PC1	PC2	PC3
Region 3	Cd	0.93	-0.02	0.10
	Co	0.95	-0.08	0.12
	Cr	0.68	-0.56	0.29
	Cu	0.43	0.87	0.07
	Mn	0.84	-0.19	-0.22
	Ni	0.75	0.04	-0.54
	Pb	0.82	-0.28	0.43
	Zn	0.77	0.36	0.37
	Fe	0.78	-0.12	-0.45
	V	0.86	-0.05	-0.18
	As	0.79	0.40	0.04
	Variance %	63.25	13.62	9.26
	Eigenvalue	6.96	1.50	1.02

Table 4.4 Correlation matrices of heavy metals for each region. * Significant at P < 0.05, ** Significant at P < 0.01.

Region 1	Cd	Co	Cr	Cu	Mn	Ni	Pb	Zn	Fe	V	As
Cd	1.00										
Co	0.14**	1.00									
Cr	0.85**	0.26	1.00								
Cu	0.48**	-0.05	0.48**	1.00							
Mn	0.51**	-0.06	0.72**	0.34*	1.00						
Ni	0.60**	-0.16	0.64**	0.85**	0.68**	1.00					
Pb	0.47**	-0.07	0.46**	0.03	0.43**	0.85**	1.00				
Zn	0.90**	0.57*	0.93**	0.59**	0.78**	0.72**	0.47**	1.00			
Fe	0.66**	-0.11	0.78**	0.53**	0.96**	0.84**	0.40**	0.87**	1.00		
V	0.96**	0.37	0.95**	0.95**	0.95**	0.50	0.02	0.83*	0.95**	1.00	
As	0.51*	0.35	0.18	-0.03	0.39	0.73**	0.99**	0.38	0.36	0.96**	1.00
Region 2											
Cd	1.00										
Co	0.19	1.00									
Cr	0.96**	0.92**	1.00								
Cu	0.12	0.41	0.85**	1.00							
Mn	-0.16	0.90**	0.99**	0.85**	1.00						
Ni	0.43*	0.66**	0.91**	0.97**	0.95**	1.00					
Pb	0.53**	0.56*	0.74**	0.51**	0.98**	0.79**	1.00				
Zn	0.43*	0.08	0.88**	0.99**	0.82**	0.85**	0.54**	1.00			
Fe	0.20	0.60*	0.04	0.42	0.44	0.10	0.88**	0.50*	1.00		
V	0.97**	0.99**	0.17	0.46	0.89**	0.95**	0.98**	0.17	-0.35	1.00	
As	-0.32	0.64*	0.88**	0.89**	0.90**	0.82**	0.96**	0.94**	0.18	0.81**	1.00

Table 4.4 (Continued). * Significant at P < 0.05, ** Significant at P < 0.01.

Region 3	Cd	Co	Cr	Cu	Mn	Ni	Pb	Zn	Fe	V	As
Cd	1.00										
Co	0.98**	1.00									
Cr	0.69**	0.73**	1.00								
Cu	0.57*	0.58*	0.52*	1.00							
Mn	0.72**	0.74**	0.84**	0.46	1.00						
Ni	0.69**	0.75**	0.68**	0.42	0.80**	1.00					
Pb	0.98**	0.98**	0.75**	0.59*	0.71**	0.69**	1.00				
Zn	0.89**	0.94**	0.70*	0.91**	0.77**	0.77**	0.90**	1.00			
Fe	0.96**	0.97**	0.86**	0.69*	0.89**	0.83**	0.84**	0.30	1.00		
V	0.98**	0.99**	0.98**	0.68	1.00**	0.97**	0.97**	0.94	1.00**	1.00	
As	0.99**	0.99**	0.97**	0.97**	0.99**	1.00**	0.98**	1.00**	0.99**	0.98**	1.00

Table 4.5 Tukey's HSD results for each element. A and B letters distinguish statistical differences where elements that have same letter indicate no significant difference.

Element	Region 1	Region 2	Region 3
Cd	B	B	A
Co	B	AB	A
Cr	A	A	A
Cu	A	A	A
Mn	B	A	B
Ni	A	A	A
Pb	A	A	A
Zn	A	A	A
Fe	B	A	AB
V	A	A	A
As	A	A	A

Table 4.6 The associated P-values of the elements that are statistically different from Table 4.5

Element	Region 1 vs Region2	Region 1 vs Region3	Region 2 vs Region 3
Cd	0.66	< 0.01	< 0.01
Co	0.051	<0.05	0.75
Mn	< 0.01	0.8	< 0.05
Fe	< 0.05	0.44	0.59

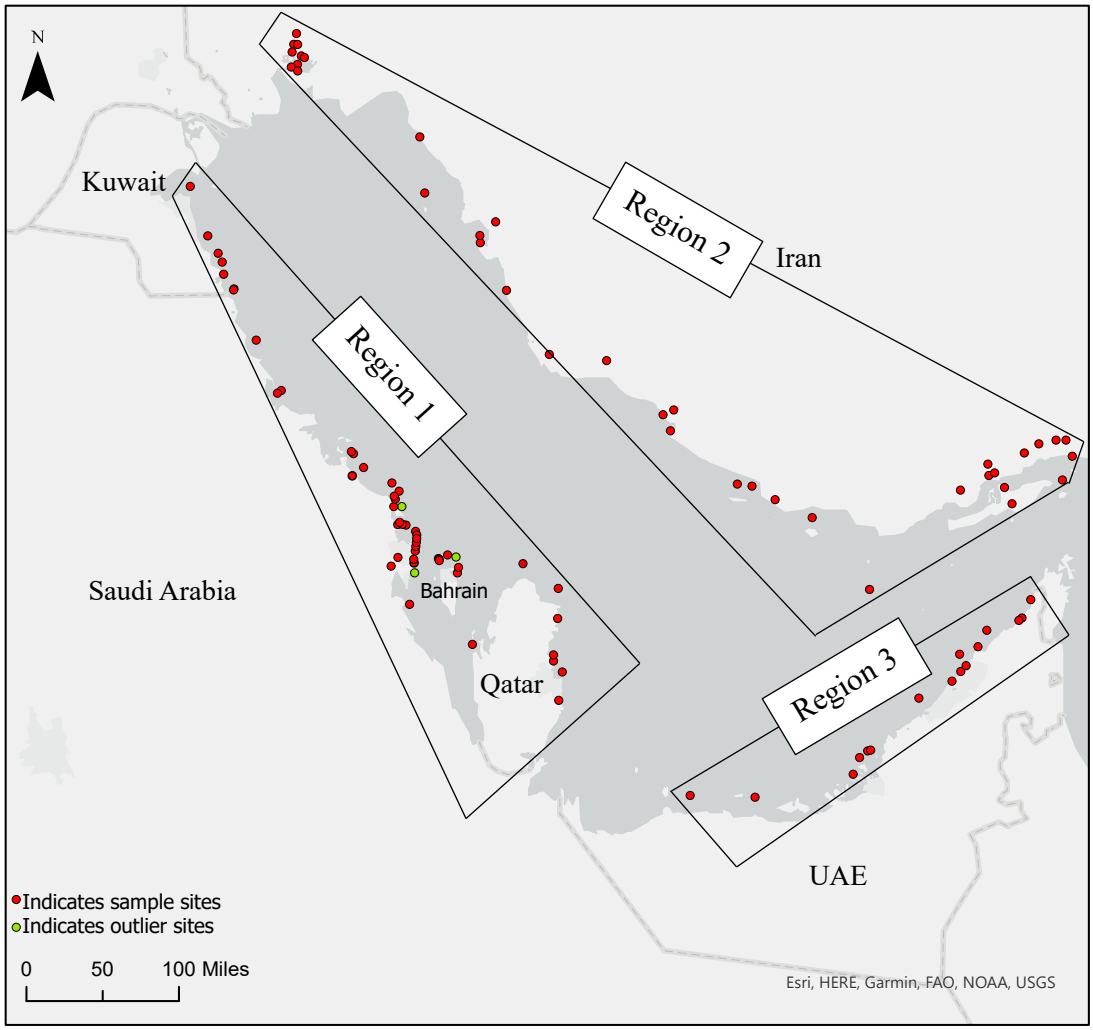

Figure 4.1 near-shore sediment sites from literature for Region 1, 2, and 3.

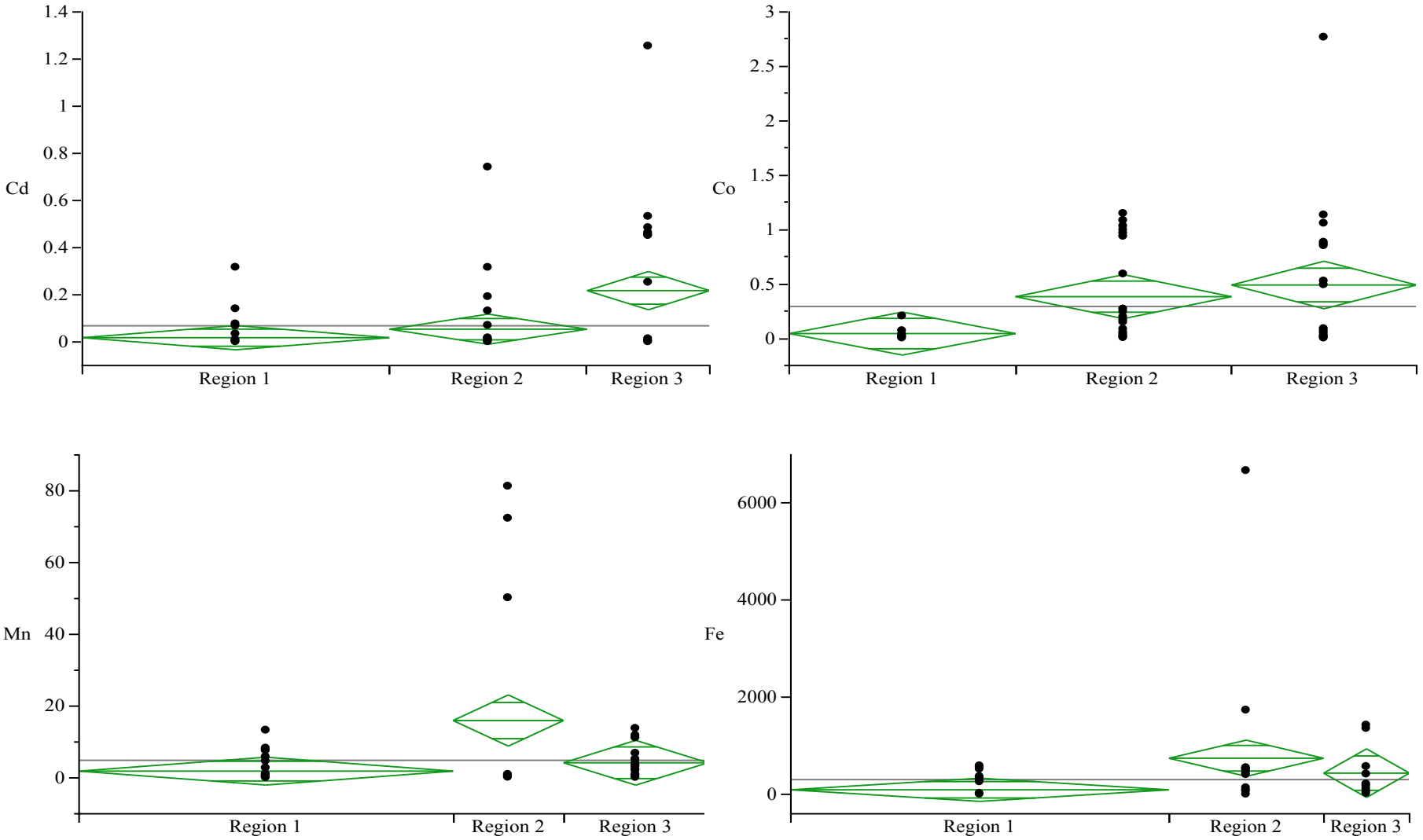

Figure 4.2 ANOVA plots of Cd, Co, Mn, and Fe throughout the study area. Green diamonds show the variance means as the upper and lower edges of the diamonds represent 95 % of confidence intervals. Width of diamonds is proportional to sample size. Gray lines indicate the mean of the means of each metal. Black dots are the concentration distribution of each element for each region.

4.6 References

Abdolahpur Monikh, F., Safahieh, A., Savari, A., & Doraghi, A. (2013). Heavy metal concentration in sediment, benthic, benthopelagic, and pelagic fish species from Musa Estuary (Persian Gulf). Environmental monitoring and assessment, 185(1), 215-222.

Abrahim, G. M. S., & Parker, R. J. (2008). Assessment of heavy metal enrichment factors and the degree of contamination in marine sediments from Tamaki Estuary, Auckland, New Zealand. Environmental monitoring and assessment, 136, 227-238.

Al Rashdi, S., Arabi, A. A., Howari, F. M., & Siad, A. (2015). Distribution of heavy metals in the coastal area of Abu Dhabi in the United Arab Emirates. Marine pollution bulletin, 97(1-2), 494-498.

Alharbi, O. M., Khattab, R. A., Ali, I., Binnaser, Y. S., & Aqeel, A. (2019). Assessment of heavy metals contamination in the sediments and mangroves (Avicennia marina) at Yanbu coast, Red Sea, Saudi Arabia. Marine Pollution Bulletin, 149, 110669.

Alharbi, T., Al-Kahtany, K., Nour, H. E., Giacobbe, S., & El-Sorogy, A. S. (2022). Contamination and health risk assessment of arsenic and chromium in coastal sediments of Al-Khobar area, Arabian Gulf, Saudi Arabia. Marine Pollution Bulletin, 185, 114255.

Al-Hashim, M. H., El-Sorogy, A. S., Al Qaisi, S., & Alharbi, T. (2021). Contamination and ecological risk of heavy metals in Al-Uqair coastal sediments, Saudi Arabia. Marine Pollution Bulletin, 171, 112748.

Al-Kahtany, K., El-Sorogy, A., Al-Kahtany, F., & Youssef, M. (2018). Heavy metals in mangrove sediments of the central Arabian Gulf shoreline, Saudi Arabia. Arabian Journal of Geosciences, 11, 1-12.

Almahasheer, H. (2018). Spatial coverage of mangrove communities in the Arabian Gulf. Environmental monitoring and assessment, 190(2), 85.

Almahasheer, H. (2019). High levels of heavy metals in Western Arabian Gulf mangrove soils. Molecular biology reports, 46(2), 1585-1592.

Almasoud, F. I., Usman, A. R., & Al-Farraj, A. S. (2015). Heavy metals in the soils of the Arabian Gulf coast affected by industrial activities: analysis and assessment using enrichment factor and multivariate analysis. Arabian Journal of Geosciences, 8, 1691-1703.

Al-Mur, B. A., Quicksall, A. N., & Al-Ansari, A. M. (2017). Spatial and temporal distribution of heavy metals in coastal core sediments from the Red Sea, Saudi Arabia. Oceanologia, 59(3), 262-270.

Alsamadany, H., Al-Zahrani, H. S., Selim, E. M. M., & El-Sherbiny, M. M. (2020). Spatial distribution and potential ecological risk assessment of some trace elements in sediments and grey mangrove (Avicennia marina) along the Arabian Gulf coast, Saudi Arabia. Open Chemistry, 18(1), 77-96.

Alshahri, F. (2017). Heavy metal contamination in sand and sediments near to disposal site of reject brine from desalination plant, Arabian Gulf: Assessment of environmental pollution. Environmental Science and Pollution Research, 24(2), 1821-1831.

Alshemmari, H., & Talebi, L. (2019). Heavy metal concentrations in the surface sediments of the northwestern Arabian Gulf, Kuwait. Arabian Journal of Geosciences, 12, 1-9.

Al-Solaimani, S. G., Abohassan, R. A., Alamri, D. A., Yang, X., Rinklebe, J., & Shaheen, S. M. (2022). Assessing the risk of toxic metals contamination and phytoremediation potential of mangrove in three coastal sites along the Red Sea. Marine Pollution Bulletin, 176, 113412.

Amin, S. A., & Almahasheer, H. (2022). Pollution indices of heavy metals in the Western Arabian Gulf coastal area. The Egyptian Journal of Aquatic Research, 48(1), 21-27.

Bantan, R. A., Al-Dubai, T. A., & Al-Zubieri, A. G. (2020). Geo-environmental assessment of heavy metals in the bottom sediments of the Southern Corniche of Jeddah, Saudi Arabia. Marine pollution bulletin, 161, 111721.

Bastami, K. D., Afkhami, M., Mohammadizadeh, M., Ehsanpour, M., Chambari, S., Aghaei, S., ... & Baniamam, M. (2015). Bioaccumulation and ecological risk assessment of heavy metals in the sediments and mullet Liza klunzingeri in the northern part of the Persian Gulf. Marine pollution bulletin, 94(1-2), 329-334.

Bibak, M., Sattari, M., Agharokh, A., Tahmasebi, S., & Imanpour Namin, J. (2018). Assessing some heavy metals pollutions in sediments of the northern Persian Gulf (Bushehr province). Environmental Health Engineering and Management, 5(3), 175–179.

Dadolahi Sohrab, A., & Nazarizadeh Dehkordi, M. (2013). Heavy metals contamination in sediments from the north of the Strait of Hormuz. Journal of the Persian Gulf, 4(11), 39-46.

De Mora, S., Fowler, S. W., Wyse, E., & Azemard, S. (2004). Distribution of heavy metals in marine bivalves, fish and coastal sediments in the Gulf and Gulf of Oman. Marine pollution bulletin, 49(5-6), 410-424.

Delshab, H., Farshchi, P., & Keshavarzi, B. (2017). Geochemical distribution, fractionation and contamination assessment of heavy metals in marine sediments of the Asaluyeh port, Persian Gulf. Marine Pollution Bulletin, 115(1–2), 401–411.

Einollahipeer, F., Khammar, S., & Sabaghzadeh, A. (2013). A study on heavy metal concentration in sediment and mangrove (Avicenia marina) tissues in Qeshm island, Persian Gulf. Journal of Novel Applied Sciences, 2(10), 498-504.

El Tokhi, M., Mahmoud, B., & Alaabed, S. (2015). Distribution of heavy metals in the bottom sediments of the Arabian Gulf, United Arab Emirates. Acta Physica Polonica A, 128(2B).

El-Sorogy, A., Al-Kahtany, K., Youssef, M., Al-Kahtany, F., & Al-Malky, M. (2018). Distribution and metal contamination in the coastal sediments of Dammam Al-Jubail area, Arabian Gulf, Saudi Arabia. Marine Pollution Bulletin, 128, 8–16.

El-Sorogy, A. S., Youssef, M., & Al-Kahtany, K. (2016). Integrated assessment of the Tarut Island coast, Arabian Gulf, Saudi Arabia. Environmental Earth Sciences, 75, 1-14.

Gopalakrishnan, G., Wang, S., Mo, L., Zou, J., & Zhou, Y. (2020). Distribution determination, risk assessment, and source identification of heavy metals in mangrove wetland sediments from Qi'ao Island, South China. Regional Studies in Marine Science, 33, 100961.

Gujre, N., Rangan, L., & Mitra, S. (2021). Occurrence, geochemical fraction, ecological and health risk assessment of cadmium, copper and nickel in soils contaminated with municipal solid wastes. Chemosphere, 271, 129573.

Hakanson, L. (1980). An ecological risk index for aquatic pollution control. A sedimentological approach. Water research, 14(8), 975-1001.

Jafarabadi, A. R., Bakhtiyari, A. R., Toosi, A. S., & Jadot, C. (2017). Spatial distribution, ecological and health risk assessment of heavy metals in marine surface sediments and coastal seawaters of fringing coral reefs of the Persian Gulf, Iran. Chemosphere, 185, 1090-1111.

Jahromi, F. A., Keshavarzi, B., Moore, F., Abbasi, S., Busquets, R., Hooda, P. S., & Jaafarzadeh, N. (2021). Source and risk assessment of heavy metals and microplastics in bivalves and coastal sediments of the Northern Persian Gulf, Hormogzan Province. Environmental Research, 196, 110963.

Khodami, S., Surif, M., WO, W. M., & Daryanabard, R. (2017). Assessment of heavy metal pollution in surface sediments of the Bayan Lepas area, Penang, Malaysia. Marine Pollution Bulletin, 114(1), 615-622.

Mehr, M. R., Keshavarzi, B., Moore, F., Fooladivanda, S., Sorooshian, A., & Biester, H. (2020). Spatial distribution, environmental risk and sources of heavy metals and polycyclic aromatic hydrocarbons (PAHs) in surface sediments-northwest of Persian Gulf. Continental Shelf Research, 193, 104036.

Metwally, M. S., Al-Muzaini, S., Jacob, P. G., Bahloul, M., Urushigawa, Y., Sato, S., & Matsmura, A. (1997). Petroleum hydrocarbons and related heavy metals in the near-shore marine sediments of Kuwait. Environment international, 23(1), 115-121.

Mortazavi, M. S., Sharifian, S., Mohebbi-Nozar, S. L., Saraji, F., & Akbarzadeh, G. A. (2022). The spatial distribution and ecological risks of heavy metals in the north of Persian Gulf. International Journal of Environmental Science and Technology, 19(10), 10143-10156.

Niu, Y., Jiang, X., Wang, K., Xia, J., Jiao, W., Niu, Y., & Yu, H. (2020). Meta analysis of heavy metal pollution and sources in surface sediments of Lake Taihu, China. Science of the Total Environment, 700, 134509.

Nour, H. E., Ramadan, F., El Shammari, N., & Tawfik, M. (2022). Status and contamination assessment of heavy metals pollution in coastal sediments, southern Kuwait. AIMS Environmental Science, 9(4), 538–552.

Pejman, A., Nabi Bidhendi, G., Ardestani, M., Saeedi, M., & Baghvand, A. (2017). Fractionation of heavy metals in sediments and assessment of their availability risk: A case study in the northwestern of Persian Gulf. Marine Pollution Bulletin, 114(2), 881–887.

Pourang, N., Nikouyan, A., & Dennis, J. H. (2005). Trace element concentrations in fish, surficial sediments and water from northern part of the Persian Gulf. Environmental Monitoring and Assessment, 109(1–3), 293–316.

Rezaei, M., Kafaei, R., Mahmoodi, M., Sanati, A. M., Vakilabadi, D. R., Arfaeinia, H., ... & Boffito, D. C. (2021). Heavy metals concentration in mangrove tissues and associated sediments and seawater from the north coast of Persian Gulf, Iran: Ecological and health risk assessment. Environmental nanotechnology, monitoring & management, 15, 100456.

Samara, F., Elsayed, Y., Soghomonian, B., & Knuteson, S. L. (2016). Chemical and biological assessment of sediments and water of Khalid Khor, Sharjah, United Arab Emirates. Marine Pollution Bulletin, 111(1–2), 268–276.

Samara, F., Solovieva, N., Ghalayini, T., Nasrallah, Z. A., & Saburova, M. (2020). Assessment of the environmental status of the mangrove ecosystem in the United Arab Emirates. Water, 12(6), 1623.

Seifi, M., Mahvi, A. H., Hashemi, S. Y., Arfaeinia, H., Pasalari, H., Zarei, A., & Changani, F. (2019). Spatial distribution, enrichment and geo-accumulation of heavy metals in surface sediments near urban and industrial areas in the Persian Gulf. Desalination and Water Treatment, 158, 130–139.

Sharifinia, M., Keshavarzifard, M., Hosseinkhezri, P., Khanjani, M. H., Yap, C. K., Smith Jr, W. O., ... & Haghshenas, A. (2022). The impact assessment of desalination plant discharges on heavy metal pollution in the coastal sediments of the Persian Gulf. Marine Pollution Bulletin, 178, 113599.

Shriadah, M. M. A. (1999). Heavy metals in mangrove sediments of the United Arab Emirates shoreline (Arabian Gulf). Water, Air, and Soil Pollution, 116, 523-534.

Tomlinson, D. L., Wilson, J. G., Harris, C. R., & Jeffrey, D. W. (1980). Problems in the assessment of heavy-metal levels in estuaries and the formation of a pollution index. Helgoländer meeresuntersuchungen, 33, 566-575.

Turekian, K. K., & Wedepohl, K. H. (1961). Distribution of the elements in some major units of the earth's crust. Geological society of America bulletin, 72(2), 175-192.

Usman, A. R. A., Alkredaa, R. S., & Al-Wabel, M. I. (2013). Heavy metal contamination in sediments and mangroves from the coast of Red Sea: Avicennia marina as potential metal bioaccumulator. Ecotoxicology and Environmental Safety, 97, 263–270.

Vaezi, A. R., Karbassi, A. R., & Fakhraee, M. (2015). Assessing the trace metal pollution in the sediments of Mahshahr Bay, Persian Gulf, via a novel pollution index. Environmental monitoring and assessment, 187, 1-12.

Van Lavieren, H., Burt, J., Feary, D. A., Cavalcante, G., Marquis, E., Benedetti, L., Trick, C., Kjerfve, B., & Sale, P. F. (2011). Managing the growing impacts of development on fragile coastal and marine ecosystems: Lessons from the Gulf.

Varol, M. (2011). Assessment of heavy metal contamination in sediments of the Tigris River (Turkey) using pollution indices and multivariate statistical techniques. Journal of Hazardous Materials, 195, 355–364.

Youssef, M., El-Sorogy, A., Al Kahtany, K., & Al Otiaby, N. (2015). Environmental assessment of coastal surface sediments at Tarut Island, Arabian Gulf (Saudi Arabia). Marine Pollution Bulletin, 96(1-2), 424-433.

Yuan, X., Xue, N., & Han, Z. (2021). A meta-analysis of heavy metals pollution in farmland and urban soils in China over the past 20 years. Journal of Environmental Sciences, 101, 217-226.

Zarezadeh, R., Rezaee, P., Lak, R., Masoodi, M., & Ghorbani, M. (2017). Distribution and accumulation of heavy metals in sediments of the northern part of mangrove in Hara Biosphere Reserve, Qeshm Island (Persian Gulf). Soil and Water Research, 12(2), 86-95.

Zhang, J., & Liu, C. L. (2002). Riverine composition and estuarine geochemistry of particulate metals in China—weathering features, anthropogenic impact and chemical fluxes. Estuarine, coastal and shelf science, 54(6), 1051-1070.

CHAPTER 5

SUMMARY AND IMPLICATIONS

The Saudi Arabian Red Sea and the Arabian Gulf basins experience pollution inputs from human and industrial activities due to the growth of costal populations in the broader region. This dissertation assessed the current contamination status and sourcing of heavy metals in surface sediments in the two major marine basins in the region, the Red Sea and the Arabian Gulf. Specifically, mangrove sediments from three locations (Yanbu, Jeddah, and Farasan Islands) on the east coast of Saudi Arabian Red Sea were collected and analyzed for broad metals contamination as well as a detailed look at Pb (both as a contaminant and as a potential tracer of contamination). Furthermore, a meta-analysis was employed using 2086 near-shore surface sediments from 106 sites from around the Arabian Gulf basin to evaluate the spatial distribution of heavy metals and their environmental effects.

Chapter two measured Pb isotopes (^{206}Pb, ^{207}Pb, and ^{208}Pb) and the Pb concentrations in thirty surface mangrove sediments from Yanbu, Jeddah, and Farasan Islands. Two-end member mixing lines were generated and used to analyze component contribution. Mixing of gasoline and natural Pb signatures as well as industrial ore and natural end members were investigated. The data show that Jeddah and Farasan Islands have, in general, comparable Pb concentrations and both

regions have Pb derived from petrol and natural. However, Jeddah has the highest Pb petrol impact across the three regions and the Farasan Islands have most of the Pb in its sediments delivered from natural sources. Yanbu, in addition to the petrol and natural Pb inputs, has a third component from industry that altered its isotopic ratios and elevated its total Pb concentrations relative to the other two regions. This third Pb source in Yanbu most likely has been derived from ore use from the industrial city in Yanbu.

Chapter three analyzed sixty surface mangrove samples from Yanbu, Jeddah, and Farasan Islands. Ten samples from each location were collected then were split as upper sediments (0-5 cm) and lower sediments (5-10 cm) making a total of twenty samples for each site. The heavy metals in samples were measured in addition to, SOM, carbonate, and silicate concentrations . Also, risk indices and statistical analyses were applied to establish contamination levels and heavy metal sources (anthropogenic, natural, or both vectors) for each site. The results indicated that Yanbu has the highest heavy metals exposure due to its lower sediments metal concentrations which is elevated compared to its upper sediments and to the other two regions with respect to depth. Further, Yanbu lower sediments had the highest PLI compared to Jeddah and Farasan Islands with respect to depth. Cr, Cu, Zn, Cd, and Pb have derived from anthropogenic and natural sources to the Yanbu marine system while V and Ni have solely natural delivery. Jeddah and the Farasan Islands have, in general, comparable heavy metals concentrations as well as PLI values with respect to depth. However, all heavy metals in Jeddah sediments were mostly derived from one controlling anthropogenic source (likely wastewater discharge). The Farasan Islands has Cd from an anthropogenic source. Cu and Zn from natural and anthropogenic sources, and V, Cr, Ni, and Pb from only natural sources.

The heavy metal concentrations in Yanbu, Jeddah, and Farasan Islands are, in general, relatively low compared to other regional and worldwide locations (Table 3.1). However, chapter three clearly shows that Yanbu is the most contaminated region in the study area due to its elevated metal concentrations in its lower sediments as well as its PLI value. Jeddah comes as the next most polluted region across the study area, although, it has generally comparable heavy metals concentrations with the Islands. The controlling anthropogenic source of all the heavy metals in Jeddah sets it apart from the Islands. The Farasan Islands has the lowest environmental concern across the regions, as expected, given that the Islands have fewer human activities compared to Jeddah and Yanbu. However, the results indicated that Cd in the Farasan Islands sediments have the highest Cd concentration across the three regions and its associated risk indices are high as well as it has an anthropogenic delivery to the Islands marine system.

Chapter two and three act like indicators that support each other showing the current environmental risk status across the Saudi Arabian Red Sea. Both chapters have different fundamental methods and techniques; however, they have very similar trends. The results showed that Yanbu is the most contaminated area across the study area due to its elevated Pb concentrations that have been delivered from industrial ore, gasoline, and natural sources. Chapter two is also in agreement with chapter three since it illustrated that Jeddah is the second most polluted area given its highest petrol Pb signatures compared to Yanbu and the Islands. The Farasan Islands receive most of its Pb from natural sources; therefore, the Islands are at little environmental risk. This trend in overall conclusions shows that Yanbu is at environmental risk and Jeddah comes as the second contaminated area after Yanbu that also at environmental stress while the Farasan Islands are at low risk, except for Cd. Future work on the contamination status in mangrove sediments is needed since there is a lack on the number of studies on mangrove sediments in the region. Studies

on core sediments are also recommended for Yanbu and Jeddah locations since chapter three shows that the metal concentrations vary in lower Yanbu sediments than in its upper given that the samples are surficial. Core sediments would provide more information on the accumulation of heavy metals over time and how changing region activities with time correlate with concentration changes. The Farasan Islands have the least number of studies compared to the northern and central areas of the Saudi Arabian Red Sea, thus, more studies on mangrove sediments and surface coastal sediments are highly urged. This work showed that even though the Farasan Islands do not have heavy land development pressure compared to the other two regions on the east coast of Saudi Arabia, Cd is elevated and coming from anthropogenic sources. The number of studies of Pb isotopic ratios is very limited in the Red Sea region, not only Saudi Arabian Red Sea, but also all other countries bordering the Red Sea. Therefore, further studies are highly recommended and needed to provide a better picture of Pb contamination status and sourcing.

Chapter four applied a meta-analysis approach to near-shore sediments from the Arabian Gulf where data were collected from literature to investigate heavy metals loadings across the basin. Further, the analysis compared the heavy metal contamination status between countries bordering the Gulf in addition to distinguishing sourcing. The results showed that the Arabian Gulf is at serious environmental risk from the anthropogenic release of Cd, Co, Cu, Pb, and As into its marine system from the surrounding countries. Also, Cr, Ni, and Fe add more environmental pressure to the Arabian Gulf environment from anthropogenic sources, however, these metals are less stressful. Moreover, Zn and V have mild anthropogenic inputs compared to the other metals . The only metal that has been delivered from solely natural sources from all the countries into the Arabian Gulf is Mn. This all suggests that the Arabian Gulf marine system, in general, suffers from anthropogenic stress from the surrounding countries releasing Cd, Co, Cr, Cu, Ni, Pb, Zn, Fe, V,

and As to its environment. These elements have different contamination levels based on their risk indices; however, they are all considered pollutants. Across all countries, UAE has the least environmental impact on the Arabian Gulf where Zn, and V in its sediments have been naturally delivered in addition to Mn. Also, Cr and Ni have low contamination levels in UAE sediments compared to the other countries. Fe and Zn have notably higher stress from Iran to the Gulf ecosystem than from the other countries.

Based on the current overall contamination status, the consideration of decision makers to new more stringent management decisions from all surrounding countries is extremely urged and needed to mitigate the pollution level of heavy metals. Also, remediation actions should be considered. Projects to plant mangroves are suggested since mangrove stands act as natural filters. For the research community, more studies on mangrove sediments for heavy metal contamination are highly recommended given the limited number of mangrove sediments studies in the Arabian Gulf area.

This dissertation provides an updated record of the contamination status of the east coast of Saudi Arabian Red Sea in addition to the status of heavy metals loadings on the Arabian Gulf and their environmental impacts. This record could serve both the research community and environmental management agencies for further investigations and mitigation. The Saudi Arabian Res Sea, in general, has a healthier marine system than the Arabian Gulf coast, thus, mitigation plans from management are recommended to take a place first for the Gulf marine system.